3 Projections of Future Anthropogenic Climate Change

L. Phil Graham, Deliang Chen, Ole Bøssing Christensen, Erik Kjellström, Valentina Krysanova, H. E. Markus Meier, Maciej Radziejewski, Jouni Räisänen, Burkhardt Rockel, Kimmo Ruosteenoja

3.1 Introduction to Future Anthropogenic Climate Change Projections

This chapter focuses on summarising projections of future anthropogenic climate change for the Baltic Sea Basin. This includes the science of climate change and how future projections are made, taking into account anthropogenic influence on greenhouse gases (GHG). Looking forward toward future climates requires using state-of-the-art modelling tools to represent climate processes.

The chapter begins with an overview of the current understanding of global anthropogenic climate change and how this is applied for projections into the 21st century. Important processes for the global climate and their representation in global climate models (GCMs) are introduced. Projected global changes are summarised and then put into specific context for the Baltic Sea Basin. This includes discussion of the performance of such models for the present climate. A range of future climate outcomes is presented, originating from using several GCMs and from using a set of different projected GHG emissions scenarios.

Due to the coarse scales of GCMs, downscaling techniques are used to produce detailed results on regional to local scales. Methods for both statistical downscaling and dynamical downscaling using regional climate models (RCMs) are described. Results for the key climate variables of precipitation and temperature, and others, are summarised for the Baltic Sea Basin. Projections of anthropogenic climate change are further coupled to hydrological and oceanographic processes via models to assess basinwide climate change impacts. Hydrological modelling shows how climate-driven changes impact on the distribution and timing of runoff into the Baltic Sea. Oceanographic modelling shows corresponding changes in water temperature, sea ice, salinity and sea levels.

3.2 Global Anthropogenic Climate Change

Before presenting anthropogenic climate change projections for the Baltic Sea Basin, it is necessary to give a brief overview of the current understanding of global anthropogenic climate change during and after the 21st century. In our discussion, we draw heavily on the IPCC Third Assessment Report (IPCC 2001a), particularly its chapter on projections of future anthropogenic climate change (Cubasch et al. 2001).

Changes in the global climate can occur both as a result of natural variability and as a response to anthropogenic forcing. Part of the natural variability is forced, that is, caused by external factors such as solar variability and volcanic eruptions; part is unforced, that is, associated with the internal dynamics of the climate system. The most important source of anthropogenic climate forcing is changes in the atmospheric composition. Increases in CO_2 and other greenhouse gases make the atmosphere less transparent for thermal radiation and therefore tend to warm up the surface and the troposphere.

However, human activities have also increased the concentrations of several aerosol types. The net effect of anthropogenic aerosols is thought to be to cool the global climate, although this effect is quantitatively much less well known than the impact of increasing greenhouse gases. The relative importance of aerosol-induced cooling, as opposed to greenhouse-gas-induced warming, is likely to decrease in the future.

External factors that may cause changes in the global climate are commonly compared in terms of globally averaged *radiative forcing*. Radiative forcing measures, in approximate terms, the change in the energy balance of the Earth–atmosphere system that a given change in external conditions would induce with no compensating changes in climate (for the exact definition, see IPCC 2001a, p. 795). Positive radiative forcing tends to increase and negative forcing decrease the global mean temperature. The magnitude of the temperature response depends on several feedback processes acting in the climate system and needs to be estimated with climate models. Model simulations suggest that the ratio of the response to the magnitude of the forcing is approximately the

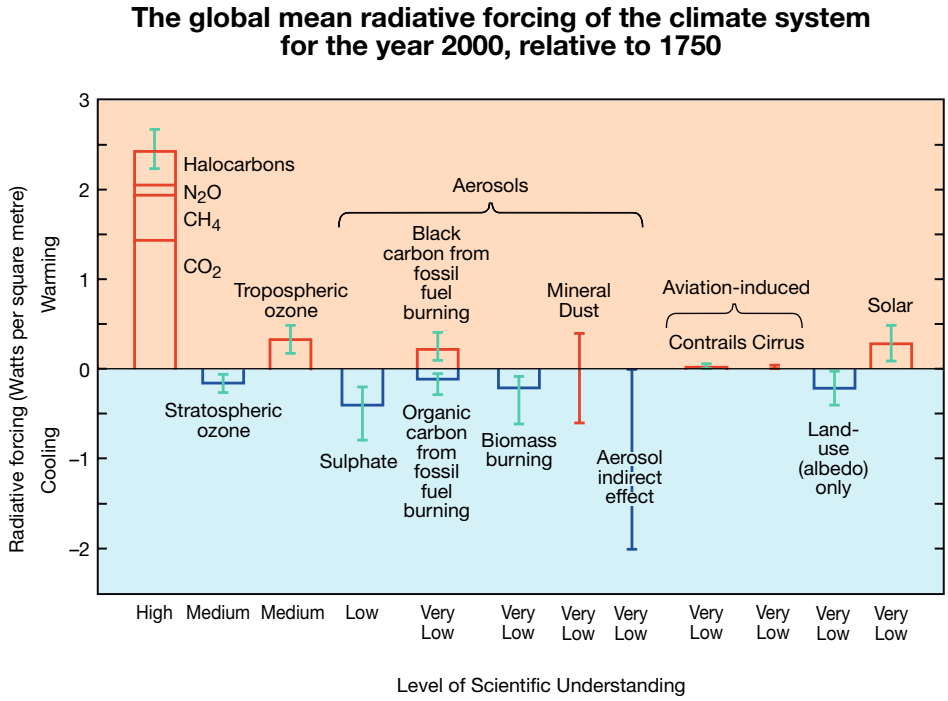

Fig. 3.1. Estimates of globally averaged radiative forcing resulting from various changes in external conditions from the year 1750 to the year 2000 (IPCC 2001a, Summary for Policymakers, Fig. 3). For each forcing agent, the bar shows the best estimate of the forcing and the vertical line the uncertainty range mainly based on the variation among published studies. See IPCC (2001a) for further details

same for different forcing agents (e.g. Forster et al. 2000; Joshi et al. 2003).

Estimates of the present-day radiative forcing from IPCC (2001a) are shown in Fig. 3.1. Increases in CO_2, CH_4, N_2O and other long-lived greenhouse gases since the preindustrial time are estimated to have caused a positive forcing of about $2.5\,\mathrm{Wm}^{-2}$. This value is associated with only a relatively small uncertainty, unlike the effects of many other forcing agents. Stratospheric ozone depletion has caused a slight negative and increases in tropospheric ozone probably a slightly larger positive forcing. The direct effect of anthropogenic aerosols, associated with the scattering and absorption of solar radiation by aerosol particles, varies in sign between different aerosol types but the net forcing is probably negative. The indirect aerosol forcing associated with aerosol-induced increases in cloud albedo and lifetime is most probably negative. However, as the estimated uncertainty range 0 to $-2\,\mathrm{Wm}^{-2}$ indicates, the magnitude of this effect is poorly known. Among the other forcing agents included in the figure, changes in land use are estimated to have caused a slight negative forcing. The forcing associated with changes in solar irradiance is thought to be positive, mainly because of increases in solar irradiance in the first half of the 20$^{\mathrm{th}}$ century.

Many of the forcing agents that are thought to have affected the global climate in recent decades and centuries are poorly known in quantitative terms. Nevertheless, the forcing estimates shown in Fig. 3.1 clearly suggest that the largest contribution to the observed global warming in the industrial era has come from increased greenhouse gas concentrations. This is the case especially for the last few decades when the increase in greenhouse gas concentrations has been most rapid. Estimates of greenhouse gas emissions and concentrations for the rest of the 21$^{\mathrm{st}}$ century (discussed below) suggest that positive greenhouse gas forcing will become increasingly dominant in the future.

3.2.1 Global Warming in the 21$^{\mathrm{st}}$ Century

In their projections of global climate change in the 21$^{\mathrm{st}}$ century, Cubasch et al. (2001) focused on climate changes resulting from anthropogenic

changes in the atmospheric composition. They estimated that changes in greenhouse gas and aerosol concentrations would raise the global mean temperature[1] by 1.4–5.8 °C between the years 1990 and 2100. The lower limit of this uncertainty interval is approximately twice the global mean warming observed in the 20th century. The upper limit is similar to the difference between present-day and ice-age conditions (e.g. Weaver et al. 1998). The wide uncertainty interval takes into account two sources of uncertainty: that due to the future emissions of greenhouse gases and aerosol precursors, and that associated with the response of the global mean temperature to a given change in the atmospheric composition. These two factors are discussed in more detail below. It is important to note that there are additional sources of uncertainty that may not be adequately accounted for by this range of projected changes, such as the conversion of emissions to atmospheric concentrations of GHGs and aerosols. Such issues are also further discussed below.

Projections of future anthropogenic climate change require estimates of future greenhouse gas and aerosol concentrations. Such estimates are dependent on information about future emissions. Because the emissions depend on factors such as population growth, economic growth, structure of economy, methods for producing energy and so on, precise prediction of them is impossible. Instead, several emissions scenarios are used. Such scenarios are based on alternative but plausible and internally consistent sets of assumptions about the demographic, socioeconomic and technological changes that together determine the evolution of emissions in the future.

A comprehensive set of emissions scenarios, the so-called SRES (Special Report on Emissions Scenarios) scenarios were developed and described by Nakićenović et al. (2000). The SRES scenarios were built around four narrative storylines that describe the evolution of the world in the 21st century. Altogether, 40 different emissions scenarios were constructed, 35 of which were detailed enough to be used in anthropogenic climate change projections. Six of these (A1B, A1T, A1FI, A2, B1 and B2) were chosen by the IPCC as illustrative marker scenarios. The main underlying assumptions behind these scenarios are described in Annex 6.

[1]The temperature discussed here and in the following refers to the two-meter level air temperature, if not otherwise stated.

The various SRES emissions scenarios remain relatively similar during the early parts of the 21st century. In particular, they all indicate an increase in global CO_2 emissions in the next few decades (Fig. 3.2a), as a result of increasing energy consumption required by increasing population and world economy. Towards the late 21st century, the scenarios tend to diverge. Some of them (e.g. A1FI and A2) project a strong increase in CO_2 emissions throughout the century, leading by the year 2100 to emissions several times larger than today. In some other scenarios (e.g. A1T and B1), however, the CO_2 emissions peak by the mid-21st century and fall below the present level by the year 2100. These differences are reflected in the CO_2 concentrations derived from the emissions (Fig. 3.2b). In the year 2100, the B1 emission scenario is calculated to lead to a CO_2 level of about 550 parts per million (ppm), as compared to a present-day level of about 375 ppm. The corresponding value for the highest scenario (A1FI) is about 970 ppm. However, even for the B1 scenario with the largest decrease in CO_2 emissions after 2050, the CO_2 concentration still continues to rise slowly in the end of the 21st century.

The SRES scenarios also describe the emissions of several other greenhouse gases, including methane (CH_4) and nitrous oxide (N_2O). The resulting concentrations are quite variable across the scenarios, particularly for CH_4 which has a relatively short lifetime and therefore responds rapidly to changes in emissions. The A2 scenario is calculated to lead to a CH_4 concentration of about 3700 parts per billion (ppb) in the year 2100 (as compared to 1760 ppb in the year 2000), while the corresponding value for the B1 scenario is below 1600 ppb. For N_2O, all the SRES scenarios indicate an increase in the atmospheric concentration, although the rate of the increase depends on the projected emissions that vary substantially among the scenarios. Many of the scenarios also indicate an increase in average tropospheric ozone (O_3) concentration, as a result of increases in pollutants that participate in the formation of O_3. Most of the SRES scenarios suggest that the net effect from changes in non-CO_2 greenhouse gases will strengthen the global warming during this century; this effect is likely to be smaller than that of increasing CO_2, but it is not negligible.

Anthropogenic increases in atmospheric aerosol concentrations, which are thought to have suppressed the greenhouse-induced warming during the 20th century (Mitchell et al. 2001), will not

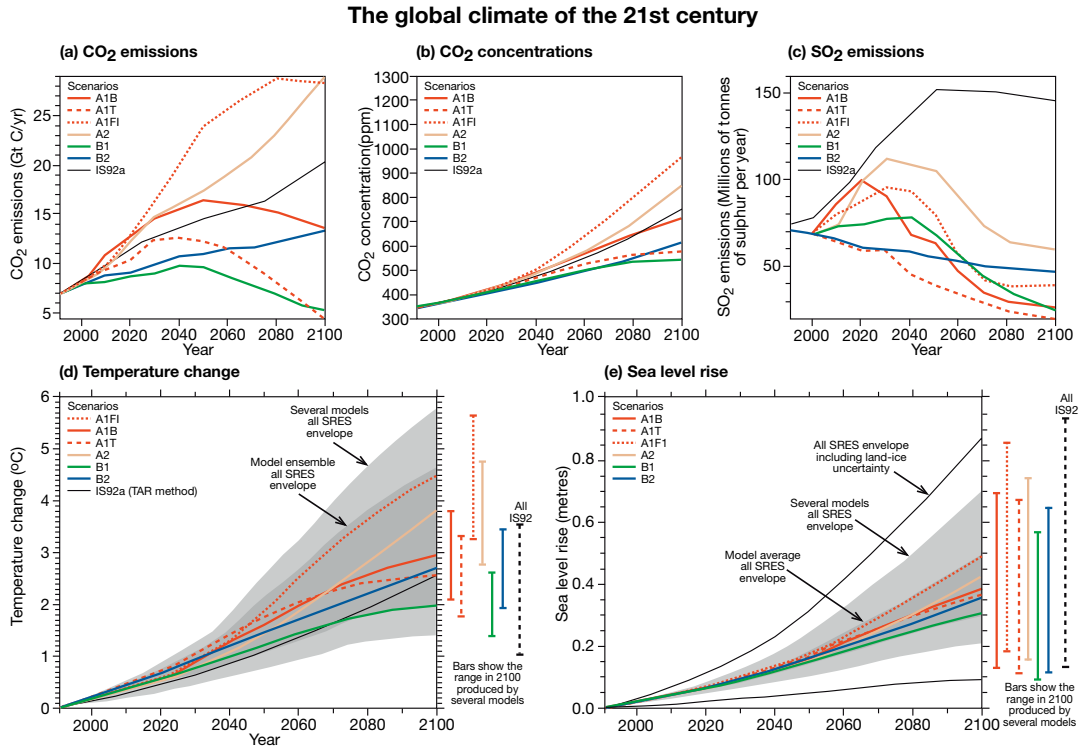

Fig. 3.2. Summary of some key factors related to global anthropogenic climate change in the 21st century, as presented in the IPCC Third Assessment Report (IPCC 2001a, Summary for Policymakers, Fig. 5). (**a**) shows the CO_2 emissions of the six illustrative SRES scenarios along with an older scenario (IS92a) used in the IPCC Second Assessment Report. (**b**) shows projected CO_2 concentrations. (**c**) shows anthropogenic SO_2 emissions. Note that the older IS92a scenario, with very large SO_2 emissions in the late 21st century, is now believed to be unrealistic. (**d**) and (**e**) show the projected global mean temperature and sea level responses, respectively. The "several models all SRES envelope" in (**d**) and (**e**) shows the temperature and sea level rise, respectively, for a simple climate model forced with all 35 SRES scenarios and tuned separately to mimic the behaviour of seven complex climate models. The "model average all SRES envelope" shows the average from these models for the range of scenarios. Note that the diagrams do not include all sources of uncertainty

necessarily continue to do so in the future. The main contributor to anthropogenic aerosol-induced cooling, SO_2 emissions, are still projected to increase in a global mean sense during the first decades of the 21st century in most SRES scenarios, which would suppress the warming during this period. By the end of the century, however, the world-wide introduction of cleaner technologies is projected to reduce the global SO_2 emissions distinctly below present-day levels (Fig. 3.2c). Due to the very short lifetime of tropospheric aerosols, this would result in an immediate decrease in sulphate aerosol concentrations. The large projected increases in greenhouse gas concentrations, in combination with small or negative changes in aerosol concentrations, would imply a large increase in the total anthropogenic radiative forcing (Fig. 3.3).

The second source of uncertainty included in the quoted 1.4–5.8 °C range is the imprecisely known response of the climate system to changes in atmospheric composition. To account for this uncertainty, Cubasch et al. (2001) used the results of seven different general circulation models (GCMs) to calibrate a simple climate model, which was run separately for all 35 SRES scenarios and with parameters corresponding to each of the seven GCMs. The GCMs were not used directly to simulate the climate evolution under all the SRES scenarios, because this would have been extremely demanding in terms of computing resources. However, the differences in simulated global mean warming between the GCMs and the calibrated simple model are likely to be small. Various types of climate models are described in more detail in Annex 6.

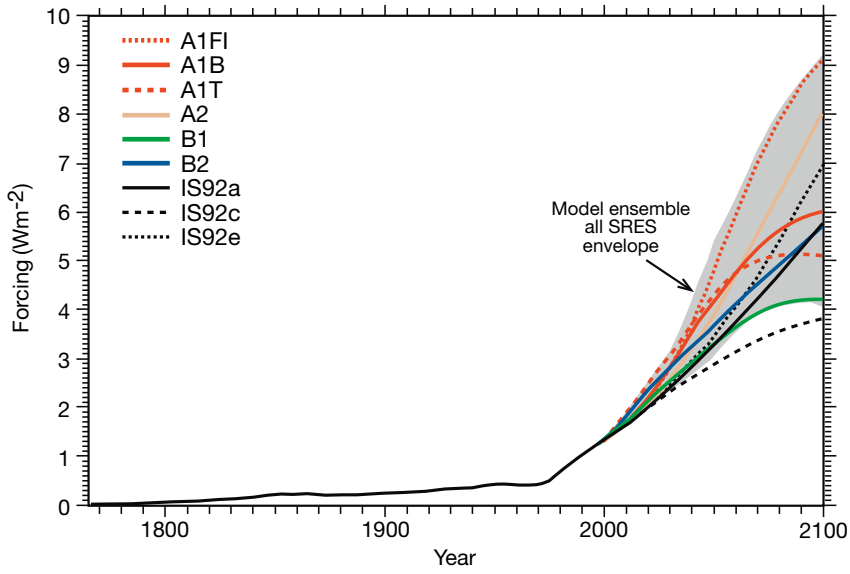

Fig. 3.3. Best-estimate historical anthropogenic radiative forcing up to the year 2000 followed by radiative forcing for the six illustrative SRES scenarios. The shading shows the envelope of the forcing that encompasses the full set of 35 SRES scenarios. Forcing estimates for three earlier scenarios (IS92a, IS92c and IS92e) are also shown (IPCC 2001a, Technical Summary, Fig. 19)

The computed evolution of the global mean temperature, presented as differences from 1990, is shown in Fig. 3.2d. The differences among the SRES scenarios remain relatively modest during the first decades of the century but grow rapidly thereafter, when the different emission and concentration projections diverge. Averaging the results of the seven models, the estimate of warming from the year 1990 to the year 2100 is 2.0 ˚C for the lowest and 4.6 ˚C for the highest SRES scenario. A direct comparison of these numbers with the full range of 1.4–5.8 ˚C would suggest that differences between emission scenarios are a larger source of uncertainty in century-scale global warming than differences among climate models. However, because the set of seven models used for generating these temperature projections did not include the least and most sensitive of all climate models, Cubasch et al. (2001) concluded that the uncertainties related to emission scenarios and climate models are of comparable importance.

The 1.4–5.8 ˚C range should not be interpreted as giving the absolutely lowest and highest possible global mean temperature changes by the year 2100. In fact, several sources of uncertainty are excluded or included only partially. One factor that is excluded is the uncertainty related to deriving the concentrations of CO_2 and other greenhouse gases from emissions. Due to uncertainties in modelling the carbon cycle and particularly its response to anthropogenic climate changes, the actual CO_2 concentration resulting from the high A1FI emissions scenario in the year 2100 might be as low as 820 ppm or as high as 1250 ppm, as compared to the estimate used of 970 ppm (Prentice et al. 2001). The full uncertainty in estimating the radiative effects of atmospheric aerosols is also excluded, although the relative importance of this uncertainty will decrease when the greenhouse-gas-induced warming becomes increasingly dominant over the aerosol-induced cooling (Wigley and Raper 2001). Moreover, as noted above, the range does not necessarily capture the total uncertainty associated with climate models. Similarly, although a wide range of different emission scenarios are used, it is not inconceivable that the real emissions would fall outside this range. For example, because the SRES scenarios exclude new policy measures to control greenhouse gas emissions, success in international climate policy could in principle allow the emissions to fall below the SRES interval, or become less for some certain world development alternative.

The 1.4–5.8 ˚C range also excludes natural climate variability which could either amplify or counteract the anthropogenic warming. Model simulations (e.g. Bertrand et al. 2002) and recent estimates of past climate variability (Moberg

et al. 2005) suggest that the natural variations of global mean temperature may amount to a few tenths of °C per century. This is not negligible, but considering the wide uncertainty interval in anthropogenic warming it only represents a relatively small additional uncertainty. On the other hand, natural climate variability increases towards smaller spatial scales. It may therefore have a substantial effect on regional climate changes, particularly in the near future when the anthropogenic forcing is still relatively weak (e.g. Hulme et al. 1999).

Despite the excluded uncertainties, temperature changes that fall somewhere in the middle of the 1.4–5.8 °C range seem to be more likely than changes that fall at the extremes or outside of this range. Wigley and Raper (2001) estimated probability distributions of future global warming by assuming equal likelihood for all 35 SRES scenarios and a log-normal probability distribution for climate sensitivity approximately representing the models used by Cubasch et al. (2001). Unlike Cubasch et al. (2001), they also allowed for uncertainty in the carbon cycle and aerosol forcing, but they found these additional sources of uncertainty to be of only secondary importance. They estimated the 5–95% uncertainty range of global warming from 1990–2100 as 1.7–4.9 °C, with a median of 3.1 °C. The corresponding 5–95% range for the warming in 1990–2070 was 1.3–3.3 °C and that for 1990–2030 0.5–1.2 °C. However, their analysis makes several simplifying assumptions, so that the actual uncertainty ranges may be wider.

3.2.2 Geographical Distribution of Anthropogenic Climate Changes

Global warming is expected to vary both geographically and seasonally (Cubasch et al. 2001). Continents are generally expected to warm more rapidly than the oceans, so that nearly all land areas are likely to warm faster than the global average (Fig. 3.4a). Particularly strong warming is projected for Northern Hemisphere high-latitude areas in winter, not only over land but even more over the Arctic Ocean, where the warming is greatly amplified by reduced sea ice. Most other ocean areas are likely to warm less rapidly than the global average. The simulated warming tends to be particularly modest over the Southern Ocean and in the northern North Atlantic. In these areas, the ocean is well-mixed to great depths, and surface warming is therefore retarded by the slow warming of the deep ocean. In addition, most models simulate a decrease in the North Atlantic thermohaline circulation. This also acts to reduce the warming in the northern North Atlantic and actually leads in some models to local cooling in this area. Although the large-scale patterns of temperature change are reasonably similar between various models (e.g. Harvey 2004), there are substantial variations at smaller horizontal scales. These variations are caused mostly by differences in the models themselves, but also by unforced variability ("noise") superimposed on the forced anthropogenic climate change signal (e.g. Räisänen 2001a). The variation between different GCM simulations within the Baltic Sea Basin is addressed in more detail in Sect. 3.3.

There will likely be a slight increase in the globally averaged precipitation during this century. Most models suggest a 1–2% increase in global precipitation for each 1 °C increase in global mean temperature (Cubasch et al. 2001; Räisänen 2001a). However, more so than with temperature, precipitation changes will vary geographically (Cubasch et al. 2001; Räisänen 2001a; Harvey 2004; see also Fig. 3.4b). High-latitude areas are expected to experience a general increase in precipitation, particularly in winter, when increases are also likely in many mid-latitude areas. Increases are also expected in most tropical regions, although there is less consistency in precipitation change between different models at low latitudes than at high latitudes (Cubasch et al. 2001; Giorgio et al. 2001; Räisänen 2001a). By contrast, most subtropical regions and many regions in the lower midlatitudes are likely to suffer a decrease in mean precipitation. Simulated precipitation changes have a lower signal-to-noise ratio than temperature changes. Precipitation changes will therefore be more difficult to discern from natural variability than temperature changes, at least during the early stages of anthropogenic climate change. Partly for the same reason, precipitation changes are generally less consistent among the models than temperature changes, although the agreement tends to be better at high latitudes than at low latitudes (Räisänen 2001a).

The patterns of anthropogenic climate change shown in Fig. 3.4b were generated by averaging the results of 20 climate models. These are given in a normalized form as the ratio of the local temperature or precipitation change to the change in the global mean temperature. This way of presentation is justified by the model-based evidence

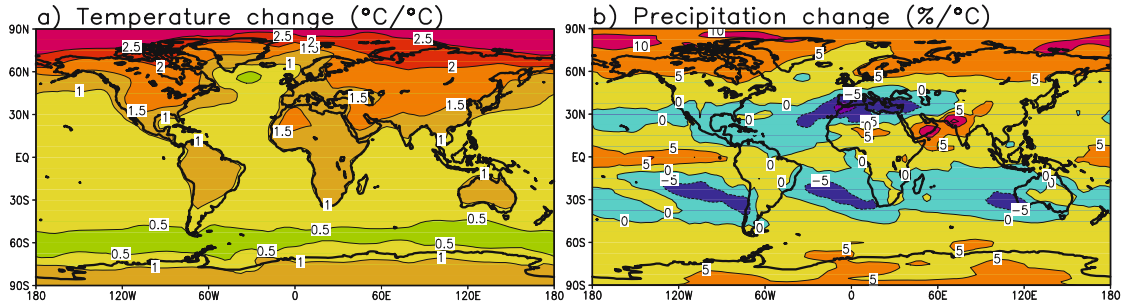

Fig. 3.4. Typical patterns of annual mean temperature and precipitation change in global climate models, both scaled for a 1 °C increase in global mean temperature. These maps are based on the idealised CMIP2 simulations in which CO_2 gradually doubles in 70 years (see Sect. 3.3.1). The temperature and precipitation changes in the 20-year period surrounding the doubling of CO_2 were first evaluated for 20 models and then averaged over all of them. Finally, the changes were divided by the global 20-model mean warming in these simulations (1.7 °C). Note that the geographical distribution of the changes differs between the models

that local anthropogenic climate changes tend to scale approximately linearly with the change in the global mean temperature (Mitchell et al. 1999; Huntingford and Cox 2000; Mitchell 2003; Harvey 2004). However, this pattern scaling principle only holds for the deterministic climate change signal associated with external forcing such as increased greenhouse gas concentrations, not for the noise associated with internally generated natural variability. For some climate variables, such as precipitation and windiness, it might take a long time before the anthropogenic climate change signal grows large enough that it can be easily discerned from the noise.

The detailed geographical patterns of change are model-dependent. They also depend to some extent on the forcing agents included in the simulation. Simulations that include changes in aerosol concentrations may give somewhat different patterns of anthropogenic climate change from simulations that only include increasing greenhouse gas concentrations, even for the same global mean warming.

A warmer atmosphere will be able to contain more water vapour. As a result, the high extreme values of daily precipitation are likely to increase even in many of those areas where the average precipitation remains unchanged or decreases (e.g. Zwiers and Kharin 1998; Hegerl et al. 2004). On the other hand, the number of precipitation days is likely to decrease in many regions of the world, including some regions with a slight increase in the average precipitation (Hennessy et al. 1997; Räisänen and Joelsson 2001; Räisänen et al. 2003).

3.2.3 Global Sea Level Rise

The thermal expansion of sea water, together with melting of glaciers, is computed to increase the globally averaged sea level by 9–88 cm from the year 1990 to the year 2100 (Fig. 3.2e). The uncertainty range is mostly associated with uncertainties in modelling anthropogenic climate change, ocean heat uptake and glacier behaviour. Because globally averaged sea level responds to anthropogenic climate changes with a substantial time lag, differences between emissions scenarios have only a limited effect on the projected sea level changes during this century.

3.2.4 Global Warming and Sea Level Rise After the Year 2100

The changes in global climate are expected to continue after the year 2100. Even if the atmospheric greenhouse gas concentrations were stabilised, the global mean temperature would still continue to rise for several centuries, although at a reduced rate. The additional global warming following the stabilisation of the atmospheric composition might exceed 1 °C (Cubasch et al. 2001, Fig. 9.19). The thermal expansion of sea water will continue for several centuries even after the surface temperature has stabilised, as the warming gradually penetrates deeper into the ocean. The total increase in global sea level due to thermal expansion alone might reach 1–3 m by the year 3000, assuming that atmospheric greenhouse concentrations were stabilised at a level equivalent to a quadrupling of the pre-industrial CO_2 concentration (Church et al. 2001). In addition to this, a gradual melting of

the Greenland ice sheet appears likely if the local warming in Greenland exceeds 3 °C (Huybrechts and De Wolde 1999). This would increase the global sea level by about 7 m. For a mid-range scenario with a warming of 5.5 °C in Greenland, about 3 m of this increase would be realized by the year 3000 (Church et al. 2001, Fig. 11.16). A decrease in the mass of the West Antarctic Ice Sheet could also potentially increase the global sea level, by up to 6 m for a complete melting of the ice sheet. Whether changes in this ice sheet are likely to make a significant contribution to global sea level rise during the next millennium is, however, still debated (Church et al. 2001).

3.3 Anthropogenic Climate Change in the Baltic Sea Basin: Projections from Global Climate Models

Global climate models, also known as general circulation models (the acronyme GCM is used in both meanings and the two terms are used interchangeably in this text) are used for numerical simulations of the global climate. These models aim to represent all the physical processes of the atmosphere, land surface and oceans which are thought to be important for determining the evolution of climate on time scales extending up to several centuries. Modelling over climatological time scales on a global basis is computationally demanding, and this constrains the resolution that can be used in the models. The horizontal resolution of GCMs tends to be some 300 km in the atmosphere and often about 150 km in the oceans. This is sufficient for the models to reproduce the major atmospheric and oceanic circulation patterns and trends for climatological variables over continental scales.

3.3.1 Global Climate Model Experiments

This section addresses projections of 21st century anthropogenic climate change in the Baltic Sea Basin using simulations made with global atmosphere–ocean general circulation models (GCMs). The focus is on changes in time mean temperature and precipitation. However, to help the interpretation of the temperature and precipitation changes, changes in the atmospheric circulation and in the North Atlantic thermohaline circulation are also discussed briefly.

Before proceeding to specific aspects for the Baltic Sea Basin, some general issues related to anthropogenic climate change simulations are discussed. Three main questions are addressed in this introductory subsection: (i) what kind of anthropogenic climate change experiments have been made with GCMs, (ii) which sets of model experiments are used in this assessment, and (iii) how anthropogenic climate changes are estimated from the simulations.

Anthropogenic climate change experiments can be broadly divided into two classes: scenario experiments and sensitivity experiments. Scenario experiments are conducted to provide plausible projections of future climate. A prerequisite for this is that the external forcing used in the simulations – changes in the concentrations of different atmospheric greenhouse gases and aerosols – is consistent with a plausible and internally consistent emissions scenario, such as one of the SRES scenarios. By contrast, sensitivity experiments are mainly motivated by the need to study model behaviour. The forcing in these experiments is usually simple, such as an increase in atmospheric CO_2 with no other changes.

In this section, results from both sensitivity experiments and scenario experiments on anthropogenic climate changes in the Baltic Sea Basin are discussed. In addition to results extracted from published literature, some updates of earlier calculations are presented. These updates are based on two sets of model simulations: the so-called CMIP2 experiments (Meehl et al. 2000), and experiments based on the SRES forcing scenarios available from the IPCC Data Distribution Centre (http://ipcc-ddc.cru.uea.ac.uk/).

CMIP2, the second phase of the Coupled Model Intercomparison Project, is an intercomparison of standard idealised anthropogenic climate change experiments made with many climate models. For this assessment, CMIP2 results for 20 models were available. Each model has been used to make two 80-year simulations: a control simulation with constant (approximately present-day) CO_2 concentration and an increased greenhouse gas simulation with gradually (1% per year compound) increasing CO_2.

The increase in CO_2 concentration in the CMIP2 greenhouse runs, with a doubling over 70 years, is faster than that projected to occur under any of the SRES scenarios. On the other hand, the concentrations of other greenhouse gases such as CH_4 and N_2O are kept constant in CMIP2, although increases in these gases are actually likely to amplify the global warming in the real world.

As a result, the rate of global warming in the CMIP2 greenhouse runs compares well with simulations based on mid-range SRES forcing scenarios. The same conclusion holds for the main geographic patterns of anthropogenic climate change. This is both because the increase in CO_2 is projected to be the main cause of anthropogenic climate change during this century and because the geographic patterns of simulated anthropogenic climate change tend to be reasonably insensitive to the exact nature of the forcing (Boer and Yu 2003; Harvey 2004). Anthropogenic climate changes in the CMIP2 simulations are reported in Sect. 3.3.3.

The main limitation of the CMIP2 data set in the context of projecting anthropogenic climate changes is the fact that the experiments are based on a single forcing scenario and lack aerosol effects. As a result, this set of simulations will tend to underestimate the uncertainty of anthropogenic climate changes in the real world.

An analysis of the temperature and precipitation changes in the Baltic Sea Basin in the SRES simulations is given in Sect. 3.3.4. This analysis is based on a smaller number of models than are available in CMIP2, but it allows us to explore how the simulated anthropogenic climate changes depend on the assumed evolution of greenhouse gas and aerosol emissions. Readers interested in quantitative, internally consistent projections of anthropogenic climate change in the Baltic Sea Basin should primarily use the SRES-based information in Sect. 3.3.4, rather than the CMIP2-based results in Sect. 3.3.3. In addition, the SRES-based GCM simulations are more directly comparable with the regional climate model results reported in Sect. 3.5 than the CMIP2 simulations.

The models used in this section are listed in Table 3.1. CMIP2 simulations are available for 20 models and SRES simulations for seven models. One of the SRES models (CCSR/NIES2) is, however, excluded for most of the analysis as explained below. Most of the models in the SRES data set also participated in CMIP2. However, the SRES data set includes a more recent version of the Canadian Centre for Climate Modelling and Analysis model (CGCM2) than CMIP2 (CGCM1).

Model-based estimates of anthropogenic climate change are usually computed from the difference in climate between two simulated periods, a scenario period and a control period. In transient scenario simulations, which typically span the whole time range from some time in the 19$^{\text{th}}$ or 20$^{\text{th}}$ century to the late 21$^{\text{st}}$ century, the control period is often chosen as 1961–1990, corresponding to the presently used WMO normal period. One or more scenario periods are chosen from later times in the same continuous simulation, as demonstrated in Fig. 3.5. In sensitivity experiments, a separate control run with no anthropogenic forcing is often made to estimate the control period climate, as already mentioned for the CMIP2 simulations. In neither case are anthropogenic climate changes estimated by comparing simulated future climate directly with observed present-day climate, due to systematic errors in the models. Differences between simulated and observed present-day climate are often comparable to, or in some cases even larger than, differences between simulated future and present-day climates. However, if model errors are assumed to have similar effects on the simulated present-day and future climates, their net effect approximately vanishes when taking the difference.

The performance of models in simulating present-day climate provides one means for estimating their reliability. Prior to presenting model-based projections of future anthropogenic climate change, the simulation of present-day climate in the Baltic Sea Basin is therefore discussed (Sect. 3.3.2). It is difficult to compress the evaluation of model-simulated climate into a single figure of merit, and it is even more difficult to convert this information to a quantitative estimate of model credibility in simulating anthropogenic climate changes. This is partly because the models are complex, but also because good performance in simulating the present climate in some area might hide compensating errors between different parts of the model. In fact, models that simulate the present climate with similar skill may simulate widely different changes in climate when forced with increased greenhouse gas concentrations (e.g. Murphy et al. 2004; Stainforth et al. 2005). Thus, when anthropogenic climate change simulations are available for several models, a comparison between the simulated changes probably gives a more direct measure of uncertainty than an evaluation of the control climates. However, it is important to remember the caveat that anthropogenic climate changes in the real world may in principle fall outside the range of model results.

In what follows, the ability of global climate models to simulate the present climate in the Baltic Sea area (Sect. 3.3.2) is first addressed. After this, model-simulated anthropogenic climate

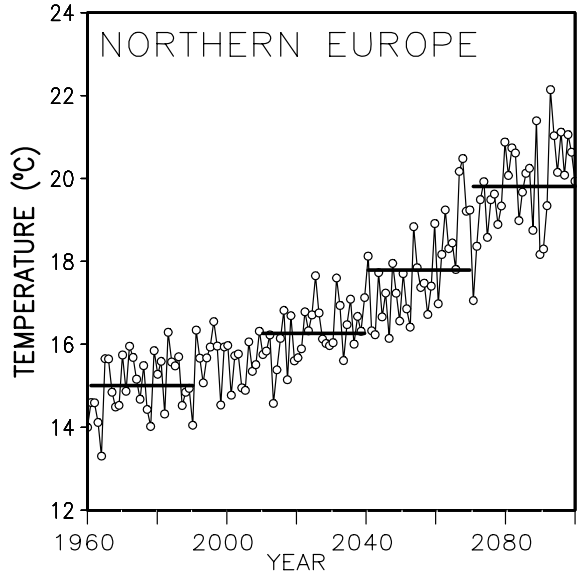

Fig. 3.5. Estimation of anthropogenic climate changes from a model-simulated time series (in this case, the summer mean temperature in northern Europe in the HadCM3 simulation forced by the SRES-A2 scenario). The first horizontal line shows the mean of the time series for years 1961–1990, and the remaining three lines the means for periods 2010–2039, 2040–2069 and 2070–2099. Temperature changes for the latter 30-year periods are calculated by subtracting the mean for 1961–1990 from the mean in the corresponding period

changes in the region are addressed (Sects. 3.3.3–3.3.4). The aims in Sect. 3.3.3 are more qualitative than quantitative. The purpose is to give an overview of the typical features of anthropogenic climate change in the Baltic Sea Basin in greenhouse gas experiments and of the intermodel differences, but the results are not intended to be interpreted as quantitative anthropogenic climate change projections for the real world. Examples of such quantitative projections are given in Sect. 3.3.4 for different SRES emission scenarios.

3.3.2 Simulation of Present-day Climate from Global Climate Models

Although the global geographic distributions of present-day temperature and precipitation climates are generally well simulated by GCMs, biases on the regional scale may be substantial (McAvaney et al. 2001; Giorgi et al. 2001). Model performance in simulating the climate in northern Europe has been the subject of several studies, including multi-model intercomparisons by Räisänen (1994, 2000) and Jylhä et al. (2004). In this subsection, these earlier studies are complemented and updated by presenting some results specifically tailored for the Baltic Sea Basin. Area means of simulated temperature and precipitation were then calculated over the land area in the Baltic Sea Basin, indicated by shading in Fig. 3.9. The model results were compared with observational estimates derived from the University of East Anglia Climate Research Unit (CRU) climatology (New et al. 1999) representing the period 1961–1990.

Figure 3.6 compares the seasonal cycles of temperature and precipitation, as averaged over the land area in the Baltic Sea Basin, between the CMIP2 control simulations and the CRU analysis. The variation between the models is large. In a few extreme cases, simulated monthly temperatures differ by about 8–10 °C from the observational estimate. The largest cold and warm biases tend to occur in the winter half-year, from November to April, but in one model there is also a very large warm bias in summer. However, because the simulated temperatures are distributed on both sides of the observed values, the 20-model mean temperatures are mostly close to those observed. A slight average cold bias is present in most months of the year, but this bias is generally small compared with the differences among the models. The only exception is spring, when the cold bias is about 2 °C.

Table 3.1. Models used in Sect. 3.3. The columns labeled as CMIP2 and SRES indicate the model runs included in the analysis of the CMIP2 and the SRES simulations in Sects. 3.3.2–3.3.4. The atmospheric resolution includes both the horizontal and the vertical resolution. The former is expressed either as degrees latitude × degrees longitude or as a spectral truncation and the approximate equivalent grid size (in parentheses). In the IPSL-CM2 model, the meridional grid has 50 points evenly distributed in the sine of latitude and the actual resolution is therefore coarser than 3.6° in high latitudes. The vertical resolution is given as "Lmm", where mm is the number of levels. The last column indicates whether flux adjustments are used for the heat (H), freshwater (W) and momentum (M) fluxes, respectively

MODEL NAME	COUNTRY OF ORIGIN	REFERENCE	CMIP2	SRES	ATMOSPHERIC RESOLUTION	FLUX ADJ.
ARPEGE/OPA2	France	Barthelet et al. (1998)	X		T31 (3.9° × 3.9°) L19	–
BMRCb	Australia	Power et al. (1993)	X		R21 (3.2° × 5.6°) L17	HW
CCSR/NIES1	Japan	Emori et al. (1999)	X		T21 (5.6° × 5.6°) L20	HW
CCSR/NIES2	Japan	Nozawa et al. (2000)	X	(A1FI, A2 , B1, B2)	T21 (5.6° × 5.6°) L20	HW
CGCM1	Canada	Flato et al. (2000)	X		T32 (3.8° × 3.8°) L10	HW
CGCM2	Canada	Flato and Boer (2001)		A2, B2	T32 (3.8° × 3.8°) L10	HW
CSIRO Mk2	Australia	Hirst et al. (2000)	X	A2, B1, B2	R21 (3.2° × 5.6°) L9	HWM
CSM 1.0	USA	Boville and Gent (1998)	X		T42 (2.8° × 2.8°) L18	–
ECHAM3/LSG	Germany	Voss et al. (1998)	X		T21 (5.6° × 5.6°) L19	HWM
ECHAM4/OPYC3	Germany	Roeckner et al. (1999)	X	A2, B2	T42 (2.8° × 2.8°) L19	HW
GFDL_R15_a	USA	Manabe et al. (1991)	X		R15 (4.5° × 7.5°) L9	HW
GFDL_R30_a	USA	Knutson et al. (1999)	X	A2, B2	R30 (2.25° × 3.75°) L14	HW
GISS2	USA	Russell and Rind (1999)	X		4.0° × 5.0° L9	–
GOALS	China	Zhang et al. (2000)	X		R15 (4.5° × 7.5°) L9	HWM
HadCM2	UK	Johns et al. (1997)	X		2.5° × 3.75° L19	HW
HadCM3	UK	Gordon et al. (2000)	X	A1FI, A2, B1, B2	2.5° × 3.8° L19	–
INM	Russia	Diansky and Volodin (2002)	X		4.0° × 5.0° L21	–
IPSL-CM2	France	Braconnot et al. (1997)	X		3.6°s × 5.6° L15	–
MRI1	Japan	Tokioka et al. (1995)	X		4.0° × 5.0° L15	HW
MRI2	Japan	Yukimoto et al. (2000)	X		T42 (2.8° × 2.8°) L30	HWM
PCM	USA	Washington et al. (2000)	X	A2, B2	T42 (2.8° × 2.8°) L18	–

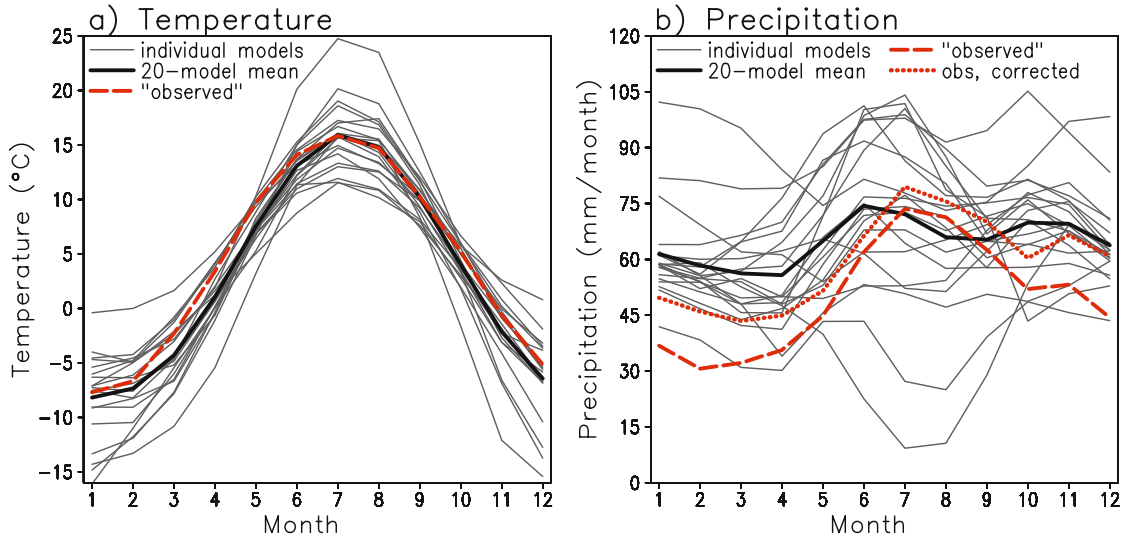

Fig. 3.6. Average seasonal cycles of (**a**) temperature and (**b**) precipitation over the total land area of the Baltic Sea Basin. The thin solid lines represent the control run climates of the 20 individual CMIP2 models and the thick solid line the 20-model mean. The dashed lines give observational estimates derived directly from the CRU climatology (New et al. 1999). For precipitation, a corrected observational estimate is also given (*dotted, see text for details*)

A more detailed look at different parts of the Baltic Sea Basin reveals that temperature biases vary across the region. In winter, in particular, there is a marked contrast between the eastern parts (Finland and western Russia) and the north-western parts (particularly central and northern Sweden) of the basin. In the former area, average simulated winter temperatures are 1–4 ˚C below the observed values, in the latter several ˚C above them (see Fig. 2 in Räisänen 2000). Räisänen (2000) attributed the warm bias in north-western Scandinavia to the relatively coarse resolution of the models, which allows the influence of the Atlantic Ocean to extend further inland in the simulations than in reality. He likewise noted that the smoothening and lowering of the Scandinavian mountains associated with the coarse resolution might also contribute to the warm bias in this area.

The seasonal cycle of precipitation is simulated less well by the models than that of temperature (Fig. 3.6b). The scatter among the models is large in all seasons, but it is particularly pronounced in late summer (July–August). A few of the models simulate an annual minimum of precipitation in this time of the year, in contrast to the maximum shown by observations, but there are also a few models with an over-pronounced summer maximum in precipitation.

Verification of model-simulated precipitation is complicated by the tendency of gauge measurements to underestimate the actual precipitation, particularly in winter when much of the precipitation falls as snow. The CRU analysis is based in most regions on uncorrected measurements (New et al. 1999) and it thus also suffers from this problem. Figure 3.6b therefore also shows a corrected precipitation estimate, which was obtained by multiplying the uncorrected CRU values with coefficients based on the work of Rubel and Hantel (2001), as detailed in Jones and Ullerstig (2002) and Räisänen et al. (2003) (see also Sect. 2.1.3). The correction is relatively small in summer but it amounts to about 40% in winter and 19% in the annual mean (Räisänen et al. 2003). The 20-model mean simulated annual precipitation is 30% above the uncorrected observational estimate, but only 9% above the corrected estimate. If the correction is not too small, a large majority of the models simulate too much precipitation in winter and in spring (Fig. 3.6b).

The ability of GCMs to simulate small-scale regional variations in precipitation is severely limited by the coarse resolution of these models. This is particularly evident in the vicinity of high orography, such as the Scandinavian mountains. Observations show a very steep contrast between abundant precipitation on the western slopes of

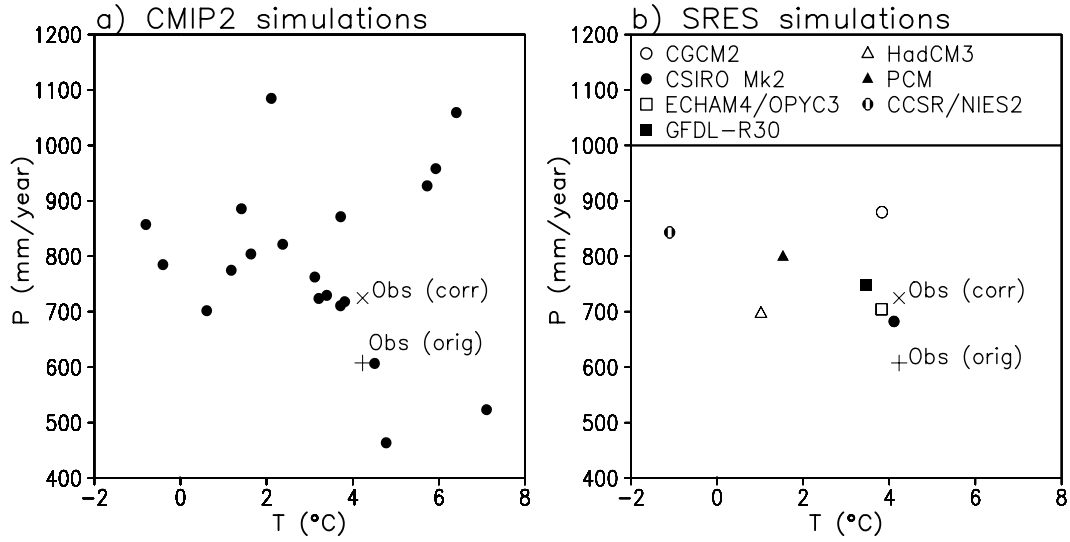

Fig. 3.7. Annual area means of temperature (*horizontal axis*) and precipitation (*vertical axis*) over the Baltic Sea Basin land area (**a**) in the CMIP2 control simulations and (**b**) in the SRES simulations for the years 1961–1990. The plus sign (+) represents the observational estimate derived directly from the CRU climatology and the cross (×) the estimate including the precipitation correction mentioned in the text

the mountain range and much less precipitation on the eastern side, but in GCMs this contrast is much less pronounced (Rummukainen et al. 1998; Räisänen and Döscher 1999; Räisänen 2000). Thus, some of the precipitation that should fall down in Norway spills in the models over to the Baltic Sea Basin, particularly to central and northern Sweden.

Simulated annual area means of temperature in the Baltic Sea Basin land area vary from −0.8 °C to 7.1 °C, 14 of the 20 models being colder than the CRU observational estimate of 4.2 °C (Fig. 3.7a). The 20-model range in annual area mean precipitation is from 460 to 1080 mm, to be compared with uncorrected and corrected observational estimates of 610 and 720 mm. For comparison, Fig. 3.7b shows the control period (1961–1990) annual area means of temperature and precipitation for the set of models that will be used in Sect. 3.3.4 for deriving projections of anthropogenic climate change under the SRES forcing scenarios. Among these models, the annual area mean precipitation is between 680 and 880 mm, being thus reasonably close to the corrected observational estimate. The simulated annual area mean temperature is within 1 °C of the observed value in four of the seven models but clearly too low in the remaining three models.

One of the factors that affect the simulated temperature and precipitation climate is the simulation of atmospheric circulation. The observed (National Centres for Environmental Prediction reanalysis; Kistler et al. 2001) and average CMIP2 control run distributions of winter and summer mean sea level pressure are compared in Fig. 3.8. The general features of the observed and simulated pressure distributions are very similar, although this similarity hides substantial variations among the individual models (Räisänen 2000). However, the wintertime extension of the Icelandic low towards the Barents Sea is not simulated well. The average simulated pressure in winter is slightly too high over the northernmost North Atlantic and the Barents Sea, and slightly too low over Europe approximately at 50°–65° N. A similar pattern of pressure biases occurs in spring (not shown). These biases in the average pressure field suggest that in most models the eastern end of the North Atlantic cyclone track is too zonally oriented, with too little cyclone activity over the European sector of the Arctic Ocean and too much activity over the European mainland. Räisänen (2000) speculated that this may contribute to the mentioned excess of winter and spring precipitation over at least some parts of northern and central Europe.

A few studies have compared model-simulated interannual variability with observations. Jylhä et al. (2004) note that the interannual standard deviation of Finland area mean temperature in 1961–1990 was 1.1 °C, whereas the six models stud-

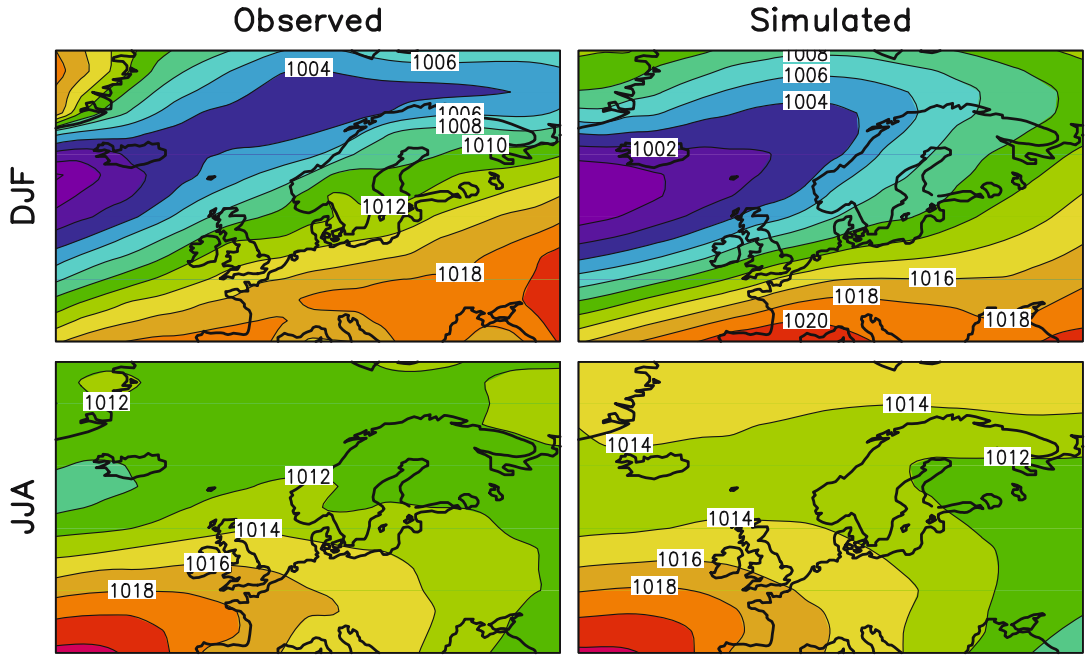

Fig. 3.8. Distribution of mean sea level pressure in winter (*top*) and summer (*bottom*) as observed in 1961–1990 (Kistler et al. 2001) and as averaged over the CMIP2 simulations. Contours are drawn at every 2 hPa

ied by them simulated values between 0.9 °C and 1.3 °C. The coefficient of variation of observed annual area mean precipitation was 12%, whereas model-simulated values ranged from 8% to 13%. Räisänen (2001b) averaged the local interannual standard deviation of monthly temperature and precipitation over 19 models and over all land grid boxes within Finland, Sweden, Norway and Denmark. He found the models to reproduce the observed seasonal cycle of temperature variability, with much larger variability in winter than in summer. The magnitude of the simulated variability was also in agreement with observations except in April and November, when the simulated variability was too large. The average standard deviation of monthly precipitation was close to that observed in winter and spring but below the observed values in summer and autumn. However, because the simulated mean precipitation was too high in winter and spring, the relative variability of monthly precipitation was too small in all months.

This is qualitatively as expected, because the resolution of the models is not sufficient to capture the details of individual precipitating weather systems. However, the simulated relative variability still remained below the observational estimate when the latter was derived from observations first aggregated to model grid boxes.

The atmospheric circulation over Europe (see also Annex 1.2) varies substantially from year to year, which leads to variations in temperature, precipitation, windiness and other aspects of the surface climate. A large part of this variation is associated with the North Atlantic Oscillation (NAO; Hurrell and van Loon 1997; Hurrell et al. 2003; Annex 7), particularly in winter. A positive (negative) NAO index indicates stronger (weaker) than average westerly flow over the North Atlantic at about 50–60° N. Global climate models simulate NAO variability with many properties in agreement with observations, including its spatial signature in the pressure (Osborn et al. 1999) and temperature fields (Stephenson and Pavan 2003), and the temporal autocorrelation structure (Stephenson and Pavan 2003). However, as pointed out by Stephenson and Pavan (2003) and Osborn (2004), different models simulate NAO variability with different skill, the amplitude of the variability also varying between models.

The causes of the observed strong positive trend in the NAO index from the early 1960's to the early 1990's are still poorly understood. In the light of model simulations, the trend appears to be at the outer limits of what could be expected from internal variability alone, although this conclusion may be sensitive to the exact definition of the NAO

index and to the magnitude of the simulated internal variability (Osborn 2004; Selten et al. 2004). This suggests that the trend might have been at least in part externally forced. However, it is not clear whether the trend can be attributed to increased greenhouse gas concentrations, since most models simulate only modest changes in NAO in response to greenhouse gas forcing (Räisänen and Alexandersson 2003; Osborn 2004). Stratospheric ozone depletion might also have affected the trend in the NAO index (Volodin and Galin 1999), but recent model results do not support the idea that it would have made a major contribution (Shindell et al. 2001; Gillett et al. 2003). Scaife et al. (2005) show that the observed NAO trend is reproduced well in a climate model simulation with a prescribed increasing trend in stratospheric westerlies resembling that observed from 1965 to 1995. However, their study does not explain why the stratospheric winds changed. Similarly, although studies by Hurrell et al. (2004), Hoerling et al. (2004) and Selten et al. (2004) suggest that the observed trend in the NAO index has been partly triggered by changes in the distribution of sea surface temperature in the tropical Indian Ocean, the cause of these changes (internal variability or anthropogenic forcing) is still unclear.

3.3.3 Projections of Future Climate from Global Climate Models

In this and the following subsection, we assess GCM-simulated anthropogenic climate changes in northern and central Europe in general and within the Baltic Sea Basin in particular. The aim of this subsection is to give an overview of the temperature and precipitation changes typically simulated by GCMs when forced by increasing greenhouse gas concentrations, of the differences in the model projections and of the factors that may affect the simulated temperature and precipitation changes and the intermodel differences. Most of this subsection is based on the idealised CMIP2 simulations, which are available for a significantly larger number of models than simulations based on the more detailed SRES forcing scenarios.

3.3.3.1 *Temperature and Precipitation*

The globally and annually averaged warming at the time of the doubling of CO_2 in the CMIP2 simulations varies from 1.0 to 3.1 °C, with a 20-model mean of 1.7 °C. The 20-model mean in northern Europe is about 2.5 °C, or 50% larger than the global mean warming, with somewhat greater warming in winter than in summer (left column of Fig. 3.9). The warming in winter typically increases from southwest to northeast, from the Atlantic Ocean towards the inner parts of Eurasia and the Arctic Ocean. The warming in summer has a slight tendency to increase towards southeast, but the gradient in this season is weaker than in winter. The changes in spring and autumn are generally between those in winter and summer (e.g. Räisänen 2000). The simulated annual precipitation increases, on the average, by about 10% in northern Europe (middle column of Fig. 3.9). In Central Europe, including the southernmost parts of the Baltic Sea Basin, the average model results suggest an increase in precipitation in winter but a decrease in summer. In northern Europe, precipitation increases in most models throughout the year, but less in summer than in the other seasons (Räisänen 2000, 2001b).

All the CMIP2 models simulate an increase in both the annual area mean temperature and the annual area mean precipitation in the Baltic Sea Basin land area. However, the magnitude of the changes varies substantially among the models (Fig. 3.10a). The range in annual temperature change is from 0.7 °C to 6.9 °C with a mean of 2.6 °C, and that in precipitation change from 3% to 22% with a mean of 8%. One of the models (CCSR/NIES2) simulates much larger increases in both temperature and precipitation than any of the others. This model also stands out as the one with the largest global mean warming in the CMIP2 data set (3.1 °C, to be compared with the second largest value of 2.1 °C).

Some variation between the anthropogenic climate changes simulated by the various models would be expected simply as a result of the internal variability that accompanies the forced anthropogenic climate change in the simulations (Cubasch et al. 2001; Räisänen 2000, 2001a). However, the differences in change between the models are too large to be explained by this factor alone. An estimation of internal variability in the CMIP2 simulations using the method of Räisänen (2001a) suggests that only about 7% of the intermodel variance in Baltic Sea Basin land area annual mean temperature change is due to internal variability. For annual precipitation change, the corresponding fraction is 17%. This implies that most of the differences in precipitation change and, particularly, temperature change are directly caused by the differences between the models. The

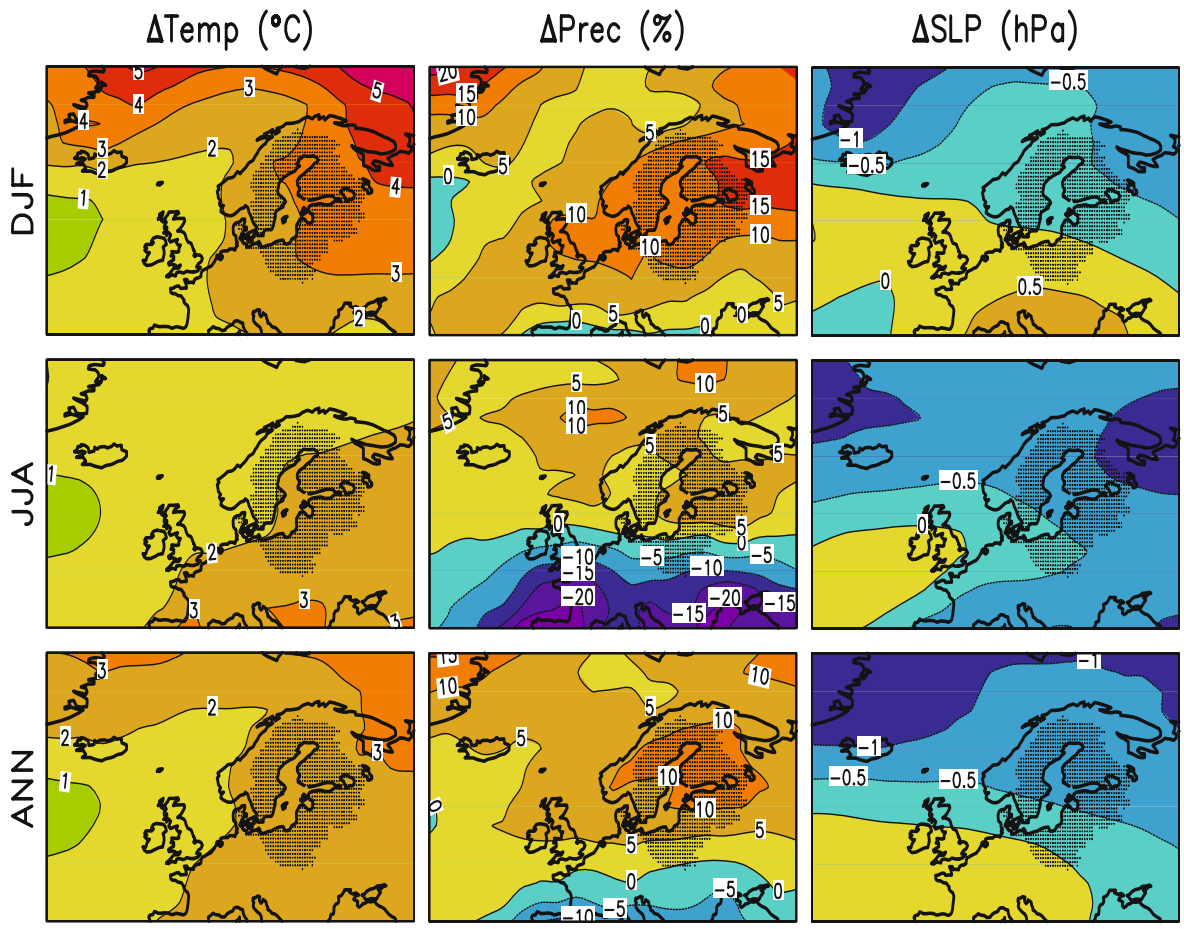

Fig. 3.9. Changes in temperature (*left*), precipitation (*middle*) and sea level pressure (*right*) around the time of the doubling of CO_2 (model years 61–80) as averaged over the CMIP2 models. Results are shown for winter (DJF = December–January–February), summer (JJA = June–July–August) and the annual mean (ANN). The contour interval is 1 °C for changes in temperature, 5% for changes in precipitation and 0.5 hPa for changes in sea level pressure. The shading indicates the Baltic Sea Basin land area

same conclusion also generally holds for seasonal temperature and precipitation changes, although the relative importance of internal variability is larger on the seasonal than on the annual time scale.

The changes in temperature and precipitation tend to be positively correlated (Fig. 3.10a). This is the case in winter, spring and autumn, but not in summer. As argued by Räisänen (2000), the positive correlation in winter and in the transitional seasons is consistent with the Clausius–Clayperon relationship. The larger the increase in temperature, the larger the increase in the capability of air to bring moisture from lower latitudes and the Atlantic Ocean to northern Europe. The lack of positive correlation in summer is consistent with the smaller relative importance of atmospheric moisture transport, as opposed to the local evaporation, in providing the precipitating water in this season (Numaguti 1999). In addition, feedbacks associated with soil moisture and/or cloudiness may play a role. When evaporation becomes restricted by a drying out of the soil, this tends to induce both a decrease in precipitation and an increase in temperature due to increased sensible heat flux and increased solar radiation allowed by reduced cloudiness (Wetherald and Manabe 1995; Gregory et al. 1997).

The simulated annual mean warming in the Baltic Sea Basin is strongly correlated ($r = 0.8$, although this is reduced to $r = 0.6$ if CCSR/NIES2 is excluded) with the global mean warming as

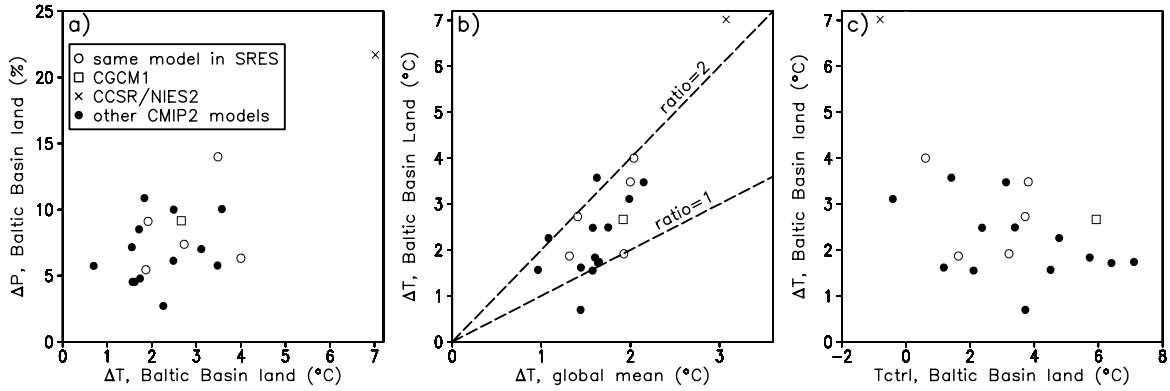

Fig. 3.10. (**a**) Changes in annual area mean temperature (*horizontal axis*) and precipitation (*vertical axis*) in the Baltic Sea Basin land area in the CMIP2 simulations, (**b**) Changes in global mean temperature (*horizontal axis*) and Baltic Sea Basin land area mean temperature (*vertical axis*; note the difference in scale), (**c**) Control run mean temperature (*horizontal axis*) and temperature change in the Baltic Sea Basin land area (*vertical axis*). The models for which SRES simulation data are also available are shown with special symbols, as detailed in the first panel

shown in Fig. 3.10b. Despite this correlation, the ratio between the warming in the Baltic Sea Basin and the global mean warming varies considerably between the models. In three of the 20 models, the warming in the Baltic Sea Basin is more than twice the global mean warming, and in another three models the Baltic Sea Basin warms less than the world on the average. In the remaining 14 models, the warming in the Baltic Sea Basin exceeds the global mean warming but less than by a factor of two.

There is a slight tendency of the Baltic Sea Basin annual mean temperature to increase more in those models in which the simulated control run temperatures are low (Fig. 3.10c). This tendency, which is strongest in winter, is consistent with the idea that feedbacks associated with changes in snow and ice cover should be stronger in a colder climate with more extensive snow and ice cover (Rind et al. 1995). In addition, models with low wintertime near-surface temperatures are more likely to have a stable boundary layer characterized by a surface inversion (e.g. Räisänen 1994). Strong stability suppresses vertical mixing in the atmosphere and may therefore allow strong greenhouse-gas-induced warming in the lowest troposphere even if the warming at higher levels is modest (Mitchell et al. 1990).

3.3.3.2 *Atmospheric and Oceanic Circulation*

Temperature and precipitation changes in the Baltic Sea Basin may also be affected by changes in atmospheric and oceanic circulation. To characterise the changes in atmospheric circulation in the CMIP2 simulations, the average changes in time mean sea level pressure are shown in the right column of Fig. 3.9 (because of incomplete data availability, only 17 models are included in the average in this case). The maps suggest a slight decrease in sea level pressure over the northernmost North Atlantic and the Arctic Ocean throughout the year, and smaller decreases or slight increases further south over the Atlantic Ocean and in central Europe. This pattern of change implies a slight increase in westerly winds over the northern North Atlantic and northern Europe, qualitatively similar to the recent wintertime changes. However, the amplitude of the 17-model mean pressure changes is very small, although partly as a result of opposing changes in different models (e.g. Räisänen 2000).

Some studies have addressed how simulated circulation changes impact on changes in temperature and precipitation. Regression-based calculations of Rauthe and Paeth (2004) suggest that, in winter, average model-simulated changes in atmospheric circulation would warm northern Europe by 0.2–0.6 °C by the year 2050 from the period 1900–1980, as compared with a total warming of about 3 °C for the forcing scenario used in their calculations. They also found a circulation-induced increase in winter precipitation in northern Europe, particularly Norway, but little contribution to either the changes in temperature or precipitation in central Europe. Their results indicate that,

although circulation changes may make some contribution to European temperature and precipitation changes, they are not likely to be the dominant agent of change. Similarly, Stephenson et al. (2006) found that changes in the NAO index only have a minor effect on the changes in winter temperature and precipitation in the CMIP2 simulations. In another study, Jylhä et al. (2004) compared the simulated temperature changes in Finland under the SRES A2 and B2 forcing scenarios with the changes in the westerly component of the geostrophic wind. In all seasons except for summer, they found a positive correlation between the two parameters, with models with a larger increase in westerly flow simulating larger warming. However, they only studied results from five models.

In summary, results from global climate models would suggest that changes in the atmospheric circulation are likely to have only a secondary impact on future changes in temperature and precipitation in the Baltic Sea Basin. On the other hand, simulations with regional climate models (see Sect. 3.5) indicate that circulation changes may nevertheless be very important for some aspects of anthropogenic climate change, such as changes in average and extreme wind speeds and the regional details of precipitation change in mountainous areas.

The relatively modest role that circulation changes appear to play in most anthropogenic climate change simulations is in apparent contrast with recently observed interdecadal variations in climate. In particular, a persistently positive phase of the NAO has been pointed out as the main cause of the series of mild winters that has characterised the climate in northern Europe since the late 1980's (Tuomenvirta and Heino 1996; Räisänen and Alexandersson 2003; Sect. 2.1.2.1). If the model results are realistic, they imply that the recent circulation changes, particularly the strong positive trend in NAO from the 1960's to the 1990's, cannot be necessarily extrapolated to the future. At least in some climate models, NAO trends comparable to that recently observed occur purely as a result of internal climate variability (e.g. Selten et al. 2004). On the other hand, some studies (Shindell et al. 1999; Gillett et al. 2003) have suggested that current climate models may underestimate the sensitivity of the atmospheric circulation to greenhouse gas forcing.

Another significant source of uncertainty for future anthropogenic climate change in Europe is the behaviour of the North Atlantic Ocean circulation. At present, the Atlantic Ocean transports about 1.2 PW of heat poleward of 25° N, or 20–30% of the total heat flux carried by the atmosphere–ocean system at this latitude (Hall and Bryden 1982). The large northward heat transport in the Atlantic Ocean is one of the reasons for the relatively mild climate in northern and central Europe, as compared with other regions in the same latitude zone. Much of the oceanic heat transport is due to the so-called thermohaline circulation (THC). This circulation includes the Gulf Stream and the North Atlantic Drift at the surface, and a southward return flow in the deep ocean. The surface and deep currents are connected by convective sinking of water that is thought to occur at several locations in the northernmost North Atlantic.

In experiments with increased greenhouse gas concentrations, most GCMs simulate a decrease in the strength of the THC. This is caused by a decrease in the density of the surface water in the northern North Atlantic, which suppresses ocean convection. Both increased water temperature and reduced salinity associated with increased precipitation and river runoff may reduce the water density, but the precise mechanisms seem to be model-dependent (Cubasch et al. 2001). More importantly, the magnitude of the change differs greatly between different models. While most of the models studied by Cubasch et al. (2001) simulated a 30–50% decrease in the THC by the year 2100 when forced with a middle-of-the-range forcing scenario, some of them showed only a small decrease and one (Latif et al. 2000) no decrease at all. None of these models simulated a complete shutdown of the THC in the 21st century, although some simulations (e.g. Stocker and Schmittner 1997; Stouffer and Manabe 2003) suggest that this might be possible later.

Another important question is the sensitivity of the European climate to changes in the THC. In some simulations with increasing greenhouse gas concentrations, weakening of the THC leads to slight local cooling in the northern North Atlantic. However, the cooling is generally limited to a small area. Thus, higher temperatures are simulated in Europe despite reduced THC intensity (as shown by the results presented in this report), although the decrease in THC may act to reduce the magnitude of regional warming.

However, there have been at least two model simulations in which changes in the THC have lead to slight cooling along the north-western coasts of Europe. In the GISS2 CMIP2 simulation (Rus-

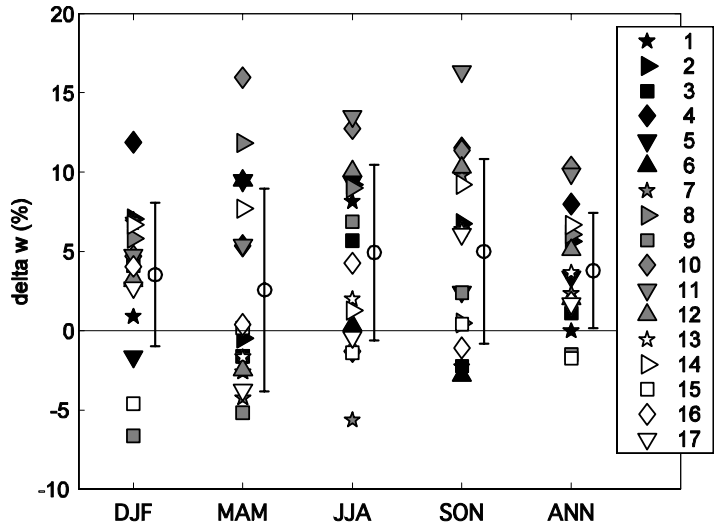

Fig. 3.11. Differences in percent between control and scenario for the seasonal means of the geostrophic wind speed from 17 CMIP2 GCM simulations. The mean and the error bar (± one standard deviation) of the changes in the 17 GCMs are also plotted (from Chen et al. 2006)

sell and Rind 1999), slight cooling is simulated in northern and western Scandinavia. Most of the Baltic Sea Basin warms up even in this model, but the warming is weaker than in the other CMIP2 simulations. A later version of the same model simulates stronger warming in northern Europe (Russell et al. 2000), but results similar to those of Russell and Rind (1999) were recently reported for another model by Schaeffer et al. (2004). In both cases the cooling in northern Scandinavia is an extension of stronger cooling in the sea area between Scandinavia and Svalbard. Schaeffer et al. (2004) show that the cooling is caused by a local expansion of sea ice triggered by a shutdown of ocean convection in this area. Other convection sites remain active in their model, so that the overall intensity of the THC is only moderately reduced. Their analysis suggests that the impact of THC changes on the atmospheric climate depends not only on the overall change in THC intensity but also on the regional details of the change. The atmospheric climate appears to be particularly sensitive to changes in ocean convection near the ice edge.

In summary, there is uncertainty in both the future changes in the Atlantic THC and the sensitivity of the European climate to these changes. However, models give at most very limited support to the idea that changes in the THC would turn the greenhouse-gas-induced warming to cooling. Furthermore, the risk of cooling appears to decrease with increasing distance from the northwestern coastlines of Europe.

3.3.3.3 *Large-scale Wind*

Analysis of surface wind at regional scale for present climate is rare, as are such studies in the anthropogenic climate change context. This is due to the facts that homogeneous wind measurements hardly exist (Achberger et al. 2006) and analysis of model simulations is usually focused on temperature and precipitation. The few works dealing with change in wind concern wind high up in the atmosphere (Pryor and Barthelmie 2003), surface wind (10 m) from reanalysis (Pryor et al. 2005a; "reanalysis" is described in Sect. 3.5.1.1), or geostrophic wind derived from surface pressure data (Alexandersson et al. 2000; see also Sect. 2.1.5.4). Recently, Chen and Achberger (2006) analysed surface wind measurements at a few Swedish stations in relation to the large scale geostrophic wind over the Baltic Sea. They expressed this in terms of circulation indices (Chen et al. 2006; see also Fig. 3.16) as well as gridded 10 m wind in relation to the geostrophic wind of the NCEP reanalysis for the grid box over Stockholm (57.5–60° N, 15–17.5° E). They concluded that there is a strong relationship between the observed station and the grid surface wind speeds, as well as with the geostrophic wind speeds. This opens the possibility of estimating

changes in regional surface wind using information on geostrophic wind derived from surface pressure data. They used simulated sea level pressure from the standardised global climate model simulations of the CMIP2 project (Meehl et al. 2000; see Sect. 3.3.1) to estimate changes in the surface wind over the Baltic region centered around Stockholm.

The GCM-simulated changes in the geostrophic wind are estimated by comparing means from the last 30-year period in the enhanced greenhouse runs with means from the entire 80-year period in the control runs. The last 30 years of the CMIP2 scenario approximately represent the period when doubling of CO_2 from present day levels is reached, and the difference between the future and present climates can be considered as a response to the doubled CO_2.

Since 17 different GCMs were used, the spread of the estimates can be taken as a measure of the uncertainty associated with global climate models (Chen et al. 2006). Figure 3.11 displays the relative change in geostrophic wind. As there exists a close linear relationship between the large scale geostrophic and the grid surface (10 m) winds over the period 1948–2004, the percent change in the geostrophic wind speed would reflect the percent change in the surface wind if the linear relation also holds in the future. Whether this assumption will be valid or not depends on the changes in the vertical stability of the atmosphere. The majority of models indicate an increase in the wind speed, mainly caused by an increased westerly wind. With the help of a t-test at the 5% level, it was determined that none of the negative changes are considered significant, while some of the positive changes in each season are significant (2, 2, 3, 3 and 5 of 17 for winter, spring, summer, autumn and annual means, respectively). The mean changes for winter, spring, summer, autumn and annual means are 3.5%, 2.6%, 4.9%, 5% and 3.8%, respectively.

3.3.4 Probabilistic Projections of Future Climate Using Four Global SRES Scenarios

According to present understanding, it is likely that future radiative forcing will fall within the range defined by the four SRES scenarios B1, B2, A2 and A1FI (for a brief description of the scenarios, see Annex 6). Therefore, it is reasonable to employ this set of SRES scenarios in constructing anthropogenic climate change projections, instead of a single CMIP2 or SRES scenario. Each SRES scenario is based on internally consistent assumptions about future development, in contrast to the idealised CMIP2 scenario.

In this subsection we concentrate on presenting anthropogenic climate change projections for the time period 2070–2099, relative to the baseline period 1961–1990. This is a commonly studied period as the ratio of climate change signal to noise due to internal variability is higher than for earlier years. Moreover, the various SRES scenarios do not diverge much until the middle of the 21st century (Fig. 3.2d). Scenarios for time periods earlier than 2070–2099 will be discussed briefly at the end of this subsection.

As far as the authors are aware, there exists no published research dealing with SRES-based climate projections just for the Baltic Sea Basin. Therefore, we have carried out the same calculations made in Ruosteenoja et al. (2007), tailoring the analysis for this region.

In the IPCC Data Distribution Centre, SRES-forced simulations were available for seven GCMs (Table 3.1). Of these models, CCSR/NIES2 simulates very large increases in temperature and precipitation compared to the remaining models (Fig. 3.10a), the projections of the other six models being much closer to one another. Furthermore, the control climate of CCSR/NIES2 is far too cold. Giorgi and Mearns (2002) suggested that, in order for a GCM to have good reliability in simulating regional anthropogenic climate change, the model should simulate the present-day climate with a small bias and climate projections should not be too different from those given by other GCMs. CCSR/NIES2 fails to fulfill either of these conditions. In addition, the spatial resolution of that model is lower than in any other GCM for which SRES runs are available (see Table 3.1). Consequently, we omit CCSR/NIES2 in this analysis. The six models incorporated in the analysis have a horizontal grid spacing of ~ 400 km or smaller in the Baltic Sea Basin.

The responses to the A2 and B2 forcing scenarios have been simulated by all six of the models (see Table 3.1). The low-forcing B1 response was available for HadCM3 and CSIRO Mk2, while the high-forcing A1FI response was only available for HadCM3. Furthermore, HadCM3 was the only model for which ensemble runs were available, the ensemble size being three for the A2 and two for the B2 scenario. For most of the models, projections for the highest (A1FI) and lowest

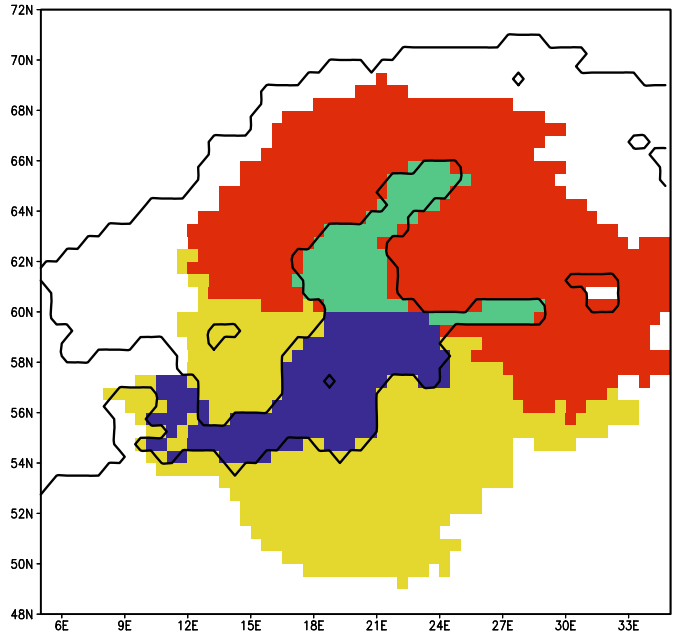

Fig. 3.12. The four subregions employed in representing the probability intervals of temperature and precipitation change

(B1) forcing scenario were composed employing a super-ensemble pattern-scaling technique, developed and assessed in Ruosteenoja et al. (2007). This method uses linear regression to represent the relationship between the local GCM-simulated temperature/precipitation response and the global mean temperature change simulated by a simple climate model. The method has several advantages, for example, the noise caused by natural variability is reduced, and the method utilises the information provided by GCM runs performed with various forcing scenarios effectively. The super-ensemble method proved especially useful in a situation with only one A2 and one B2 simulation available for an individual GCM. In such a case, the conventional time-slice scaling from an individual GCM response would excessively transfer noise to the scaled response.

In anthropogenic climate change impact research, it is generally not adequate only to consider a deterministic estimate of the change, but it is also of interest to know a range inside which the projected anthropogenic climate change is expected to fall. We constructed 95% probability intervals of spatially averaged temperature and precipitation change for two maritime and two continental regions of the Baltic Sea Basin. In winter in particular, there is a distinct south-west to north-east gradient in the geographical distribution of average model-simulated temperature change.

The mean of 20 CMIP2 simulations is given in Fig. 3.9, and a qualitatively similar pattern was obtained by averaging the six SRES simulations (not shown). Therefore, both the Baltic Sea and the continental runoff area were divided into a south-western and north-eastern subregion (Fig. 3.12). The NE maritime region covers the Gulf of Finland and the Gulf of Bothnia, the SW region the Baltic Proper. Considering hydrological applications, the two continental subregions correspond to the runoff areas of the maritime subregions. In individual GCMs horizontal resolution is much coarser than in Fig. 3.12, and therefore the results are not sensitive to the details of the subdivision.

Since we have analysed six GCMs only, modelled anthropogenic climate change projections applied as such do not give a statistically representative picture of regional anthropogenic climate change. Instead, we have fitted the normal (Gaussian) distribution to the set of model projections. The validity of the normal distribution approximation was assessed in Ruosteenoja et al. (2007). In all, the projections of the various GCMs were found to follow the normal distribution fairly well. Utilising the Gaussian approximation, we can con-

struct 95% probability intervals (i.e. 2.5–97.5%) for the temperature (T) and precipitation (P) change:

$$I_{\Delta T} = \overline{\Delta T} \pm 1.96 s_{\Delta T};\ I_{\Delta P} = \overline{\Delta P} \pm 1.96 s_{\Delta P}$$

where the means (denoted by an overline) and standard deviations (s) are calculated from the responses of the six models, separately for each season, region and forcing scenario.

In calculating the means and standard deviations needed to determine the probability intervals, the total weight assigned to the HadCM3 ensemble runs was twice that given to each of the other models. Probability intervals for temperature change are given in absolute terms, while precipitation changes are expressed here in percentages to facilitate application of the results to impact studies. In transforming the precipitation changes into percentages ($100\% \times DP/P$), the denominator P is the baseline-period precipitation averaged over the six GCMs, the weights being as stated above.

The 95% probability intervals for temperature change for each season, region and scenario are depicted in Fig. 3.13. Even at the lower end of the interval, the inferred temperature change is invariably positive. In winter and spring, the north-eastern part of the Baltic Sea Basin tends to warm more than the south-eastern one, while in the other seasons differences among the regions are smaller. As far as the medians of the intervals are concerned, the warming is a monotonic function of the strength of the radiative forcing, the A1FI forcing producing nearly double warming compared to B1.

However, the probability intervals are quite broad, reflecting the large scatter among the projections of the various models. For example, in both north-eastern regions the extreme estimates for springtime temperature response to the A1FI forcing range from < 3 °C to more than 10 °C. Another striking feature is the fact that the probability intervals representing different forcing scenarios overlap strongly. Even for the B1 forcing, the upper estimates are 4–6 °C, the lower estimates mostly being ∼1–2 °C.

The 95% probability intervals for precipitation change are presented in Fig. 3.14. With the exception of some regions in the intermediate seasons, the 95% probability intervals intersect the zero line. Consequently, in most cases even the sign of the future precipitation change cannot be established firmly. Especially in winter, the projections provided by the various models diverge strongly, and probability intervals of the change are broad. Compared with the large uncertainties in the projections, differences among the various subregions are fairly small. In studying the median estimate, summertime precipitation seems to change little, by ±10%. In other seasons an increase of 10–30% is projected.

As a rule of thumb, other probability intervals can be derived from Figs. 3.13 and 3.14 in a straightforward manner by adjusting the length of the bar while keeping the middle point unchanged. For instance, to obtain the 90% interval (i.e., an interval excluding 5% of probability density at *both* ends) the bar lengths must be multiplied by the factor 1.645/1.960, in accordance with the fitted normal distribution.

The time trends of change in temperature and precipitation for the four emissions scenarios are shown in Fig. 3.15. In the response to the A2 radiative forcing scenario, temperature increases fairly linearly in time (Fig. 3.15a). For the A1FI scenario, warming is more rapid in the second half of the century, while both B scenarios show decreasing rates of warming during this time. The scenarios deviate little from one another before 2030. However, the actual temperatures in individual decades are affected by natural variability as well as by anthropogenic forcing. In the curves depicted in Fig. 3.15a, this influence is suppressed by taking an average of several models and by the application of temporal smoothing. As a consequence of internal natural variability, one can expect that the actual tridecadal mean temperatures may fluctuate up to 1 °C around the general warming trend (the estimate for the magnitude of natural variability is given in Fig. 3.15a). These assessments do not take into account possible future changes in external natural forcing agents, such as the intensity of solar radiation.

In the simulations of future precipitation, as shown in Fig. 3.15b, the influence of natural variability is thought to be much stronger than in the temperature projection. For example, the B2-forced precipitation change shows an apparent rapid increase during the coming decades, whilst later in the century the rate of change appears to be much slower. However, it is difficult to know if this is a reliable feature of the B2 scenario or just a consequence of the fact that the effects of natural variability are not filtered out completely even when averaged over several models.

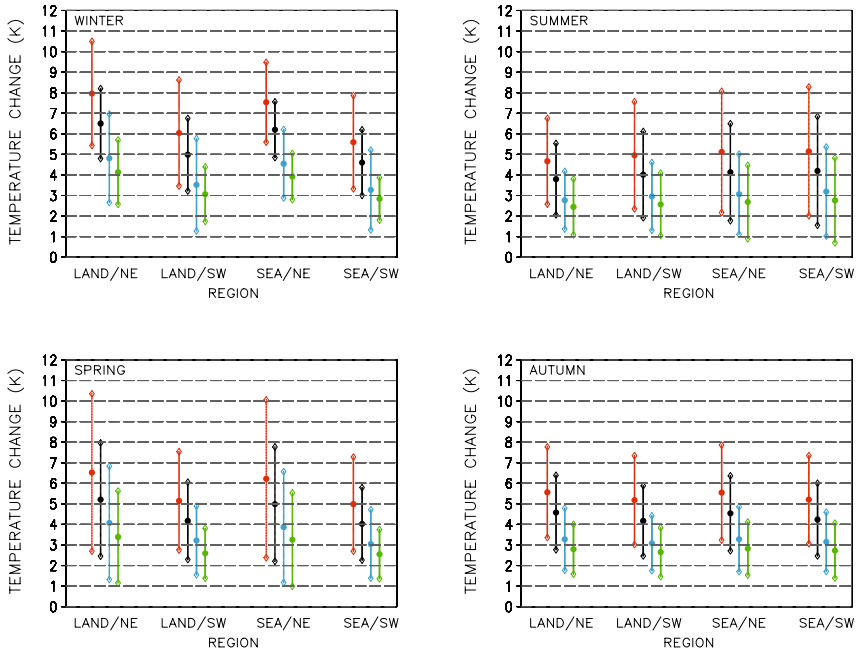

Fig. 3.13. Seasonal GCM-driven 95% probability intervals of absolute temperature change (*vertical bars*) from 1961–1990 to 2070–2099 for four subregions (defined in Fig. 3.12), derived from SRES-forced simulations performed with six GCMs. Intervals are given separately for the A1FI (*red*), A2 (*black*), B2 (*blue*) and B1 (*green*) scenarios. The dot in the centre of the bar denotes the median of the interval

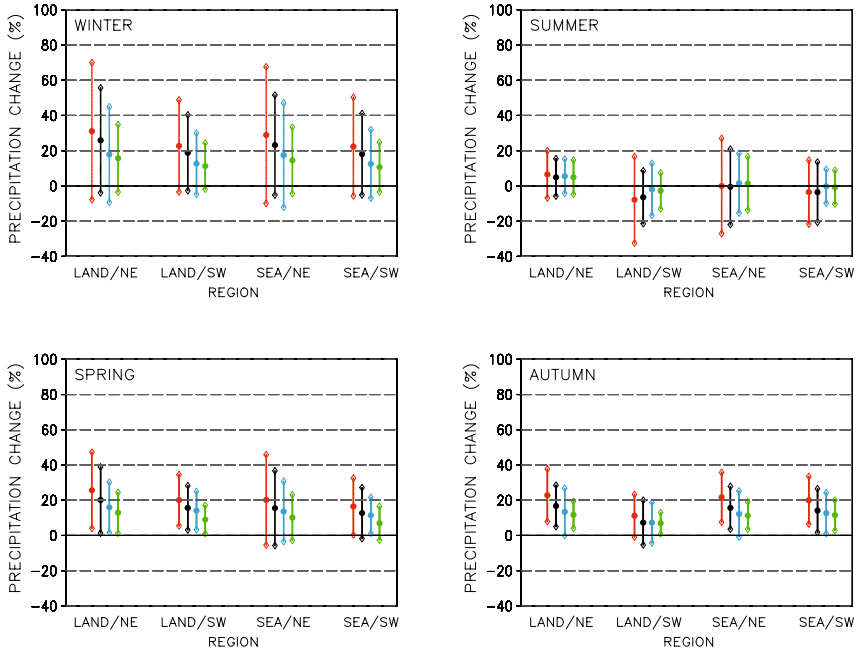

Fig. 3.14. Seasonal GCM-derived 95% probability intervals of precipitation change in percent. Intervals are given separately for the A1FI (*red*), A2 (*black*), B2 (*blue*) and B1 (*green*) scenarios. The dot in the centre of the bar denotes the median of the interval

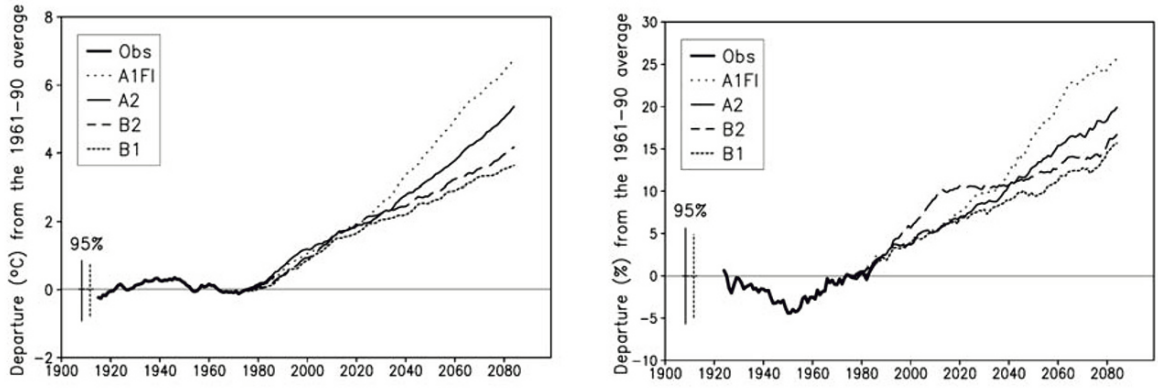

Fig. 3.15. Annual mean temperature (*left*) and precipitation anomalies for Finland relative to the mean of the baseline period 1961–1990. Before the 1980's the anomalies are based on observations, after that on the mean of projections given by four GCMs (HadCM3, ECHAM4, NCAR-PCM and CSIRO-Mk2). Projections are given separately for the A1FI, A2, B2 and B1 SRES radiative forcing scenarios. Curves are smoothed by applying 30-year running means. The vertical bars on the left indicate the 95% probability intervals for differences between two arbitrarily-chosen 30-year mean temperatures/precipitations in a millennial control run with unchanged atmospheric composition, performed with two coupled GCMs (*left bar* – HadCM3; *right bar* – CGCM2); these bars give a measure for internal natural variability (adapted from Jylhä et al. 2004)

Climate models are evolving continuously, and we can anticipate that their ability to simulate the response to anthropogenic climate forcing will improve. The results discussed in this subsection are based on a fairly small number of climate models. In the future, new more accurate models are likely to improve our picture of expected anthropogenic climate change.

3.4 Anthropogenic Climate Change in the Baltic Sea Basin: Projections from Statistical Downscaling

Statistical downscaling (also called empirical downscaling) is a way to infer local information from coarse scale information by constructing empirical statistical links between large scale fields and local conditions (e.g. Zorita and von Storch 1997). Such statistical links can be used to develop detailed local climate scenarios based upon the output from global climate models. A number of statistical downscaling studies have been performed for the Baltic Sea Basin during the last few years (Hanssen-Bauer et al. 2005). Statistical downscaling often involves analysis of observed predictands and predictors, establishing downscaling models between the two, and applying them to global climate model outputs. This section focuses on the last step for the Baltic region. Special attention is paid to future projections.

3.4.1 Statistical Downscaling Models

Most of the downscaling studies for the Baltic Sea Basin have so far been focused on monthly mean temperature and precipitation (e.g. Murphy 1999, 2000), although other variables have also been used as predictands.

For example, Linderson et al. (2004) tried to develop downscaling models for several monthly based statistics of daily precipitation (e.g. 75 and 95 percentiles and maximum values for daily precipitation) in southern Sweden, but found that skillful models can only be established for monthly mean precipitation and frequency of wet days. Kaas and Frich (1995) developed downscaling models for monthly means of daily temperature range (DTR) and cloud cover (CC) for 10 Nordic stations. Omstedt and Chen (2001), Chen and Li (2004), and Chen and Omstedt (2005) developed downscaling models for annual maximum sea ice cover over the Baltic Sea and sea level near Stockholm. Even the phytoplankton spring bloom in a Swedish lake has been linked to large scale atmospheric circulation and may thus be projected by statistical downscaling (Blenckner and Chen 2003).

Several large scale climate variables have been used as predictors of the statistical models. Due to its strong influences on the local climate (e.g. Chen and Hellström 1999; Busuioc et al. 2001a,b), atmospheric circulation is usually the first candidate as predictor. Among various ways to characterize the circulation, the Sea Level Pressure (SLP) based geostrophic wind and vorticity, u, v and ζ (see Fig. 3.16), are widely used (e.g. Chen 2000; Linderson et al. 2004).

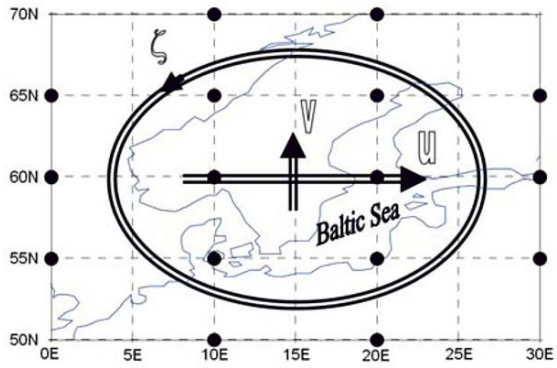

Fig. 3.16. Map showing the predictor domain of the statistical model (adapted from Chen et al. 2006)

In their downscaling study of CC and DTR, Kaas and Frich (1995) stated that the inclusion of tropospheric temperature information among the predictors is of fundamental importance for estimating greenhouse gas induced changes. They thus used both the 500–1000 hPa thickness and the sea level pressure (SLP) fields as predictors. Several potential "signal-bearing" predictors have been tested for downscaling precipitation. Hellström et al. (2001) used large-scale absolute humidity at 850 hPa (q850) as predictor for precipitation, in addition to circulation indices. They conclude that changes in q850 seem to convey much of the information on precipitation changes projected by ECHAM4. Linderson et al. (2004) tested several predictors for monthly mean precipitation and frequency of wet days, including large-scale precipitation, humidity and temperature at 850 hPa and a thermal stability index. They concluded that large-scale precipitation and relative humidity at 850 hPa were the most useful predictors in addition to the SLP based predictors u, v and ζ. Relative humidity was more important than precipitation for downscaling frequency of wet days, while large-scale precipitation was more important for downscaling precipitation.

3.4.2 Projections of Future Climate from Statistical Downscaling

3.4.2.1 *Temperature*

Benestad (2002b, 2004) downscaled temperature scenarios for localities in northern Europe using 17 climate simulations from 10 different global climate models, mainly based on the emission scenario IS92a. A total of 48 downscaled temperature scenarios were produced by using different global simulations, predictors and predictor domains. Though the models show a considerable spread concerning projected warming rates, some results seem to be robust. The projected warming rates are generally larger inland than along the coast. The 48 scenario ensemble mean projected January warming rate during the 21st century increases from slightly below 0.3 °C per decade along the west coast of Norway to more than 0.5 °C per decade in inland areas in Sweden, Finland and Norway (Benestad 2002b). This is shown in terms of probabilities by Benestad (2004), who concludes that under IS92a, the probability of a January warming of 0.5 °C per decade or more is less than 10% along the Norwegian west coast, but more than 70% in some inland areas in Sweden and Finland. Another robust signal is that the projected warming rates in Scandinavia are larger in winter than in summer. Some models also show a tendency for larger warming rates at higher latitudes, though distance to the open sea seems to be more important than latitude.

3.4.2.2 *Precipitation*

Some statistically downscaled scenarios for precipitation were produced applying only SLP-based predictors (Busuioc et al. 2001b, Benestad 2002b). These may be used to evaluate possible consequences of changes in the atmospheric circulation for future precipitation but not for estimating the total effect of increased concentrations of greenhouse-gases on precipitation conditions. The following is thus focused on precipitation studies including additional predictors.

Hellström et al. (2001) used the SLP-based predictors (geostrophic wind and vorticity: u, v, ζ) and large-scale q850 to deduce precipitation scenarios for Sweden from the global models HadCM2 and ECHAM4/OPYC3. Changes in precipitation conditions were projected by studying the differences between 10-year control and scenario timeslices. The downscaled precipitation scenarios for

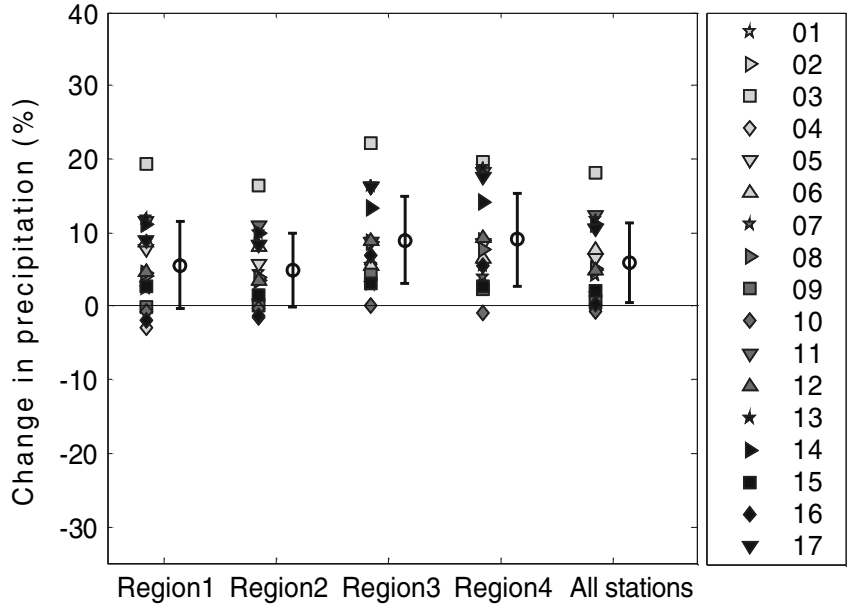

Fig. 3.17. Regional changes in percent for downscaled annual precipitation for four regions in Sweden and for all of Sweden. Region 1 = southernmost, Region 2 = south, Region 3 = north, Region 4 = northernmost. The numbered models are specified in Fig. 3.11. The mean and the error bar (± one standard deviation) of the changes in the 17 GCMs are also plotted (adapted from Chen et al. 2006)

winter and spring show increased precipitation in northern and north-western Sweden (approximately +20%) and reduced precipitation (approximately −20%) in southern Sweden.

During autumn both models project a substantial increase in north-western Sweden, but only minor changes in the southernmost part. During summer HadCM2 projects a substantial increase over the entire country, while ECHAM4/OPYC3 indicates an increase in northern and a reduction in central and southern Sweden. Hellström et al. (2001) conclude that change in vorticity is the greatest contributor to the projected precipitation changes in southern Sweden, while q850 have greater effect in the northern parts of the country. The modelled reduction in spring and winter precipitation in southern Sweden is linked to reduced vorticity, while the projected all-season precipitation increase in northern Sweden is mainly attributed to increased humidity.

Based on the Canadian Global Circulation Model 1 (CGCM1), Linderson et al. (2004) established scenarios of precipitation amount and frequency of wet days for the Scania region in southern Sweden. The CGCM1 simulation applied a greenhouse forcing corresponding to the observed one during the 20$^{\text{th}}$ century and thereafter the IS92a emission scenario up to the year 2100. The downscaled scenario shows a significant increase of the annual mean precipitation ($\sim$ 10%) and a slight decrease ($\sim$ 1.5%) in the frequency of wet days. The downscaled increase is slightly more than the GCM based large scale change in the annual precipitation (8%), which may be interpreted as an enhanced effect of local topography implicitly included in the statistical downscaling model (Achberger 2004).

The results indicate an increase in precipitation intensity almost all year round, but especially during winter. The increase in precipitation during winter and spring is associated with an increase in westerly flow and vorticity, but also with an increase in the large-scale precipitation. The summer decrease is linked to a decrease in vorticity and westerly flow and an increase of northerly flow. The circulation changes, however, may to some extent be specific to CGCM1.

Chen et al. (2006) downscaled precipitation scenarios for Sweden based on the 17 CMIP2 GCMs (Meehl et al. 2000; Sect. 3.3.1 introduces CMIP2), using large scale precipitation as predictor in addition to geostrophic wind and vorticity. They compared the precipitation conditions during years 50–80 of the scenario period (in CMIP2 the dou-

bling of CO_2 occurs in year 70) with an 80-year control run, and concluded that the ensemble of scenarios suggests an overall increase in annual precipitation, as shown in Fig. 3.17. The increase in precipitation is more significant in northern than in southern Sweden. This overall positive trend can be attributed to the increased large-scale precipitation and the westerly wind. The seasonal precipitation in autumn, winter and spring is expected to increase, whereas there is an indication of decreasing summer precipitation in the southern half of the country. The estimated uncertainty is nearly independent of region. However, there is a seasonal dependence; the estimates for winter show the highest level of confidence, and the estimate for summer the least.

3.5 Anthropogenic Climate Change in the Baltic Sea Basin: Projections from Regional Climate Models

Dynamical downscaling describes the process of downscaling from global scales to regional or local scales using dynamical models. For climate studies, this typically consists of applying a coupled atmosphere–land surface model to a limited area of the globe at scales considerably finer than those used for global climate models. For example, horizontal scales are typically some tens of kilometres versus hundreds of kilometres for GCMs. Like statistical downscaling, dynamical downscaling requires driving inputs from a global model. However, dynamical downscaling differs from statistical downscaling in that it includes explicit representation of physical processes for every grid square included in its domain. Critical variables from GCM simulations define driving inputs at the boundaries of the regional climate model (RCM) domain.

3.5.1 Interpreting Regional Anthropogenic Climate Change Projections

Regional climate modelling has been developed and used for dynamical downscaling of GCM results over the past 15 years. The first studies for Europe, including the southern half of the Baltic Sea Basin, were those of Giorgi et al. (1990) and Giorgi and Marinucci (1991). Since their introduction, the spatial and temporal resolution of RCMs has become finer and the level of output detail has increased considerably (e.g. Giorgi et al. 1992; Christensen et al. 1998; Jones et al. 1995 and 1997; Christensen et al. 2007).

Only a few studies have specifically focused on the Baltic Sea Basin (e.g. Jacob et al. 2001; Räisänen and Joelsson 2001; Kjellström and Ruosteenoja 2007), but a succession of European Union funded research projects with focus on regional downscaling over Europe has produced a host of European-wide studies with results relevant for the Baltic Sea Basin (i.e. Regionalization, RACCS, MERCURE, PRUDENCE, MICE, ENSEMBLES).

There is uncertainty associated with regional anthropogenic climate change projections, which can be summarised as the combination of biases related to the formulation of the regional climate model, lateral boundary conditions and initial conditions from the driving global model, and choice of emissions scenario. This section first addresses the question of the formulation of the RCMs by reviewing experiments in which the RCMs should represent the present climate. This is followed by an inventory of available RCMs and anthropogenic climate change experiments, and then results for projections of the future climate.

3.5.1.1 *Simulation of Present-day Climate from Regional Climate Models*

An important step in climate modelling is to evaluate how well models perform for the present climate (e.g. Achberger et al. 2003). This typically consists of performing model simulations for retrospective observed periods using boundary conditions that best represent observations. In lieu of actual observations at RCM boundaries, "reanalysis" data are often used. These data sets consist of results from numerical weather prediction models that are driven (and constrained) by as many actual observations as possible to produce representation of meteorological variables on a uniform model grid at sub-daily time scales (Uppala et al. 2005). Reanalysis data produced within Europe to date include ERA-15 (1979–1993) and ERA-40 (1957–2001). Other reanalysis data that are commonly used are the NCEP reanalysis data (1948–present, Kalnay et al. 1996; Kistler et al. 2001).

The subject of RCM evaluation was the theme of the European project MERCURE, which used reanalysis data from ERA-15 as reported by Hagemann et al. (2002, 2004) for the Baltic Sea Basin. Five regional models were analysed. In general, temperature and precipitation values aver-

aged over larger areas like the Baltic Sea Basin matched closely with results from observations and the driving reanalysis data. For the Baltic Sea Basin the authors concluded that although average precipitation is generally overestimated to some extent, except during summer, the annual cycle is well described. For temperature, two of the models show a very close match to the observed annual cycle, while two of the others show an exaggerated seasonal cycle with biases of ±2 °C for individual months. For other quantities, like model generated runoff, evapotranspiration and snowpack, the agreement between individual models and observations is not as good as for temperature and precipitation. Examples include both under- and overestimations for individual months as well as leads and lags of up to 2 months in the timing of the seasonal cycles. A further conclusion was that the higher resolution of RCMs resulted in more realistic smaller-scale variation as compared to GCMs, for example better orographic precipitation and better temporal detail. Additional aspects of the same simulations were analysed by Frei et al. (2003) and by Vidale et al. (2003).

A prominent deficiency of European climate simulations is a tendency toward excessive summer drying that most RCMs show, especially in southeastern Europe, but also in the southern part of the Baltic Sea Basin for some RCMs. This is characterised by temperatures that are too high and both precipitation and evapotranspiration that are too low. This was also noted in the first European multi-RCM project using reanalysis data, as reported in Christensen et al. (1997). Jones et al. (2004), using another RCM, attributed this phenomenon to model deficiencies, in particular for cloud and radiation processes.

In summary, RCMs have been shown to reproduce the mean climate and observed climate variability over Europe for the last decades. This includes not just the large-scale circulation but also other variables. For instance, near-surface temperature is most often simulated to within 1–2 °C from the observations over areas similar in size to the Baltic Sea Basin. Also, the seasonal cycle of precipitation is reproduced to within the uncertainties given by the observational data sets. Despite this agreement between the observed and simulated climate, individual RCMs do show more substantial errors for some variables in different regions and seasons. Furthermore, extreme values are by their nature difficult to validate and an extensive evaluation of model performance in terms of simulating extreme conditions is lacking. However, it can be noted that errors in simulating extreme conditions often tend to be larger than errors in mean conditions. This is discussed in more detail in Sect. 3.6.

An example of a common deficiency in the RCMs is the inability of RCMs to simulate high wind speeds over land without an additional gust parameterization (Rockel and Woth 2007).

3.5.1.2 *Regional Climate Models and Anthropogenic Climate Change Experiments*

Regional anthropogenic climate change projections covering the entire Baltic Sea Basin first became available with the work reported by Jones et al. (1995, 1997). A general compilation of RCMs and earlier studies was undertaken by the IPCC (Giorgi et al. 2001). Since then, a number of simulations have been performed, some of which are compared in Christensen et al. (2001) and Rummukainen et al. (2003) for the Nordic region.

In the European project PRUDENCE, ten different regional climate models were used to carry out more than 25 experiments, a majority of which were based on a common global anthropogenic climate change experiment (Christensen et al. 2007). The PRUDENCE matrix of experiments addressed some of the uncertainties mentioned above (Déqué et al. 2007). These most recent studies were based on anthropogenic climate change simulations using a 30-year period as a control to represent the present climate and a 30-year future period based on a documented emissions scenario.

A summary of the RCM future climate simulations referred to in the following discussion is shown in Table 3.2. Here, and in Sect. 3.6, focus is on reporting projections for the key variables of temperature, precipitation, wind and snow. The ability of the RCMs to reproduce the control climate, typically for the period 1961–1990, is first discussed. Future climate scenario experiments for the period 2071–2100 are then presented. In addition to material from published literature, this includes the most recently available results from the PRUDENCE data centre (http://prudence.dmi.dk/). Seasonal averages are highlighted from two specific PRUDENCE RCMs – RCAO and HIRHAM – that were used to downscale simulations from two GCMs – HadCM3/HadAM3H and ECHAM4/OPYC3 – forced by the SRES-A2 emissions scenario (Nakićenović et al. 2000; see also Annex 6). Thus,

a range of experiment results reflecting some of the uncertainties originating from both boundary conditions and RCM formulation differences is presented.

In addition, scatter plots for different subregions of the Baltic Sea Basin that include simulations addressing further aspects of uncertainty are presented to illustrate a more comprehensive spread of anthropogenic climate change projections in the region. This includes simulations with numerous RCMs, GCM ensemble simulations downscaled with the same RCM, RCM simulations with different horizontal resolution, and simulations using additional emissions scenarios. It should be noted, however, that the GCMs and emissions scenarios reported here are only a subset of those available (cf. Sect. 3.3).

3.5.2 Projections of Future Climate from Regional Climate Models

3.5.2.1 *Temperature*

The air temperature discussed below refers to the two-meter level air temperature in the models. This corresponds to a typical height common to most observation stations.

Temperature, control climate

Temperature biases in the Baltic Sea Basin for control experiments downscaled with RCMs have been shown to be generally positive for the winter season when compared to observations (Räisänen et al. 2003; Giorgi et al. 2004a). However, these biases are typically less than 2 ˚C. An exception is larger warm biases in the mountainous interior of northern Scandinavia. These larger biases, which are also seen in the global models (cf. Sect. 3.3.3), may partly be related to the fact that the observations come primarily from cold valley stations while RCM output is averaged from gridboxes covering a range of elevations, as discussed in Räisänen et al. (2003). The milder winter climate shown in these studies can be related to the excessive north–south pressure gradient over the North Atlantic inherited from the global models (cf. Sect. 3.3.3). It should be noted that the size and even sign of the temperature bias is sensitive to the boundary conditions (cf. Fig. 3.6a).

Regarding summer temperature, Räisänen et al. (2003) and Giorgi et al. (2004a) found a relatively large bias (1–2 ˚C) in summer temperature specific to the south-eastern part of the Baltic Sea Basin, while biases in spring and autumn were small for the entire region. Vidale et al. (2007) also showed a positive bias in temperature in the south-eastern part of the Baltic Sea Basin for one of the RCMs that they analysed. This bias in the south-eastern part of the Baltic Sea Basin is thought to be related to the summer drying bias mentioned above for the reanalysis boundary experiments in south-eastern Europe (cf. Sect. 3.5.1.1).

Seasonal cycle of temperature, future climate

In future scenarios, as snow cover retreats north and east, the climate in the Baltic Sea Basin undergoes large changes, particularly during the winter season. A common feature in all regional downscaling experiments is the stronger increase in wintertime temperatures compared to summertime temperatures in the northern and eastern parts of the Baltic Sea Basin (e.g. Giorgio et al. 1992; Jones et al. 1997; Christensen et al. 2001; Déqué et al. 2007), as shown in Fig. 3.18. This pattern of anthropogenic climate change is also seen from the global climate models (e.g. Fig. 3.9), but here, with higher horizontal resolution, regional features have a more pronounced impact on the results. For instance, the strong reduction in sea ice in the Bothnian Bay (presented in Sect. 3.8) leads to a substantial increase in air temperature over the Bothnian Bay.

The projected temperature change for summer is shown in Fig. 3.19. Warming in this season is most pronounced further south in Europe, and consequently, it is to the south of the Baltic Sea that the warming is strongest in the Baltic Sea Basin. Figures 3.20 and 3.21 show a wider range of RCM model results, whereby additional experiments are included as outlined in the figure caption. These figures summarise change in temperature against change in precipitation for northern and southern subregions of the Baltic Sea Basin. In some models the summertime warming south of the Baltic Sea is as large, or even larger, than that during winter.

As seen in Fig. 3.19, a local maximum over the Baltic Sea stands out in the experiments forced with boundary conditions from HadAM3H. This feature is associated with a strong increase in Baltic Sea SSTs (sea surface temperatures) for these experiments, which is larger than in any of the other GCMs discussed in Sect. 3.3.4 (Kjellström and Ruosteenoja 2007).

Table 3.2. List of studies that include RCM simulations of future climate covering parts of the Baltic Sea Basin. The scenarios SRES-A2 and SRES-B2 refer to the special report on emission scenarios from the IPCC (Nakićenović et al. 2000). [1]Pattern-scaling to a common time frame was performed; the original control and scenario simulations covered different time periods. [2]Pattern-scaling to a common emission scenario was applied; the original simulations used different scenarios (cf. Christensen et al. 2001). [3]PRUDENCE experiments

Reference	RCM	Resolution	GCM	Scenario	Timeperiod
Giorgi et al. (1992)	MM4	70 km	CCM	$2 \times CO_2$	–
Jones et al. (1995, 1997)	HadRM	50 km	HadCM	$2 \times CO_2$	–
Déqué et al. (1998)	Arpège stretched	60–700 km	N/A	$2 \times CO_2$	2×10 yrs
Räisänen et al. (1999)	RCA1	44 km	HadCM2	GHG	Pre-ind. (10 yrs) & 2039–2049
Räisänen et al. (2001)	RCA1	44 km	HadCM2 ECHAM4/OPYC3	GHG	Pre-ind. (10 yrs) & 2039-2049 10 yrs from 1980s & 2070s
Christensen et al. (2001, 2002)	RCA, HIRHAM	18,44,55 km	ECHAM4/OPYC, HadCM2	GHG, GHG +sulf+trop. O_3	10–20 yrs from 1990s & 2050s[1]
Rummukainen et al. (2003)	RCA, HIRHAM	18,44,55 km	ECHAM4/OPYC HadCM2	B2[2]	10–20 yrs from 1990s & 2050s[1]
Räisäinen et al. (2003)	RCAO	50 km	HadCM3/HadAM3H ECHAM4/OPYC3	A2, B2	1961–1990, 2071–2100
Christensen and Christensen (2004)	HIRHAM	50 km	HadAM3H ECHAM4/OPYC3	A2	1961–1990, 2071–2100
Räisänen et al. (2004)	RCAO	50 km	HadCM3/HadAM3H ECHAM4/OPYC3	A2, B2	1961–1990, 2071–2100
Moberg and Jones (2004)	HadRM3P	50 km	HadCM3/HadAM3P	–	1961–1990
Kjellström (2004)	RCAO	50 km	HadCM3/HadAM3H ECHAM4/OPYC3	A2, B2	1961–1990, 2071–2100
Giorgi et al. (2004a,b)	RegCM	50 km	HadCM3/HadAM3H	A2, B2	1961–1990, 2071-2100
de Castro et al. (2007)	9 RCMs[3]	≈ 50 km	HadCM3/HadAM3H	A2	1961–1990, 2071–2100
Déqué et al. (2007)	10 RCMs[3]	≈ 50 km	HadCM3/HadAM3H ECHAM4/OPYC3 Arpège/IFS	A2, B2	1961–1990, 2071–2100
Jylhä et al. (2007)	7 RCMs[3]	≈ 50 km	HadCM3/HadAM3H ECHAM4/OPYC3	A2, B2	1961–1990, 2071–2100
Kjellström et al. (2007)	10 RCMs[3]	≈ 50 km	HadCM3/HadAM3H ECHAM4/OPYC3	A2, B2	1961–1990, 2071–2100
Vidale et al. (2007)	10 RCMs[3]	50 km	HadCM3/HadAM3H ECHAM4/OPYC3	A2, B2	1961–1990, 2071–2100
Ferro et al. (2005)	HIRHAM	50 km	HadAM3H	A2	1961–1990, 2071–2100
Beniston et al. (2007)	10 RCMs[3]	≈ 50 km	HadCM3/HadAM3H ECHAM4/OPYC3	A2, B2	1961–1990, 2071–2100
Pryor and Barthelmie (2004)	RCAO	50 km	HadCM3/HadAM3H ECHAM4/OPYC3	A2, B2	1961–1990, 2071–2100
Rockel and Woth (2007)	8 RCMs	≈ 50 km	HadCM3/HadAM3H	A2, B2	1961–1990, 2071–2100
Leckebusch and Ulbrich (2004)	HadRM3H	≈ 50 km	HadCM3/HadAM3H	A2, B2	1960–1989, 2070–2099
Rummukainen et al. (2004)	RCAO	50 km	HadCM3/HadAM3H ECHAM4/OPYC3	A2, B2	1961–1990, 2071–2100
Pryor et al. (2005b)	RCAO	50 km	HadCM3/HadAM3H ECHAM4/OPYC3	A2, B2	1961–1990, 2071–2100

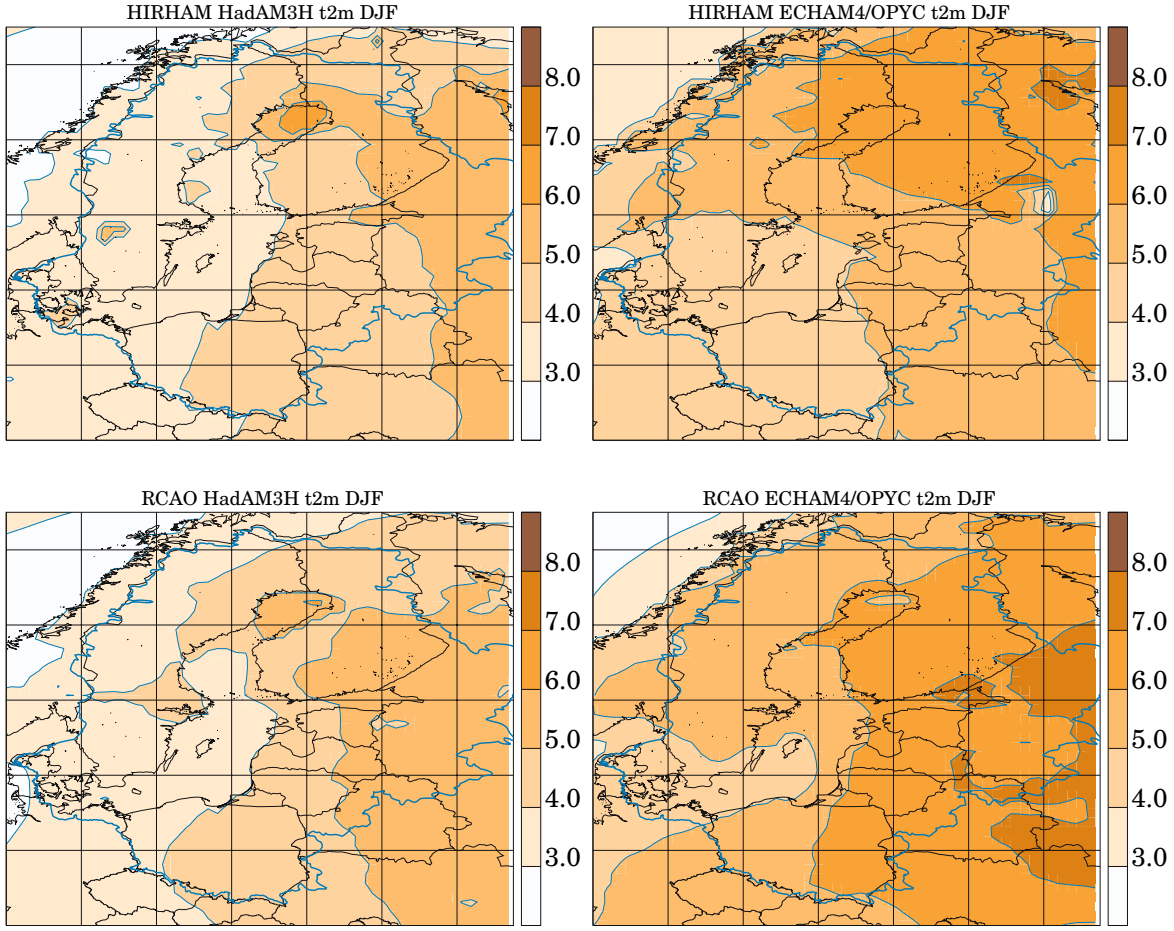

Fig. 3.18. RCM simulated temperature change in ˚C for winter (DJF) between the periods 1961–1990 and 2071–2100 using the SRES-A2 emissions scenario. The upper plots show results from the HIRHAM Model and the lower plots are from the RCAO Model. Plots on the left used GCM boundary conditions from HadAM3H; plots on the right used ECHAM4/OPYC3. The Baltic Sea Basin is indicated by the thick blue line (*note: ECHAM4/OPYC3 scenario simulations used as boundaries are different for the two RCM downscaling experiments, see Sect. 3.5.2.3*)

Experiments to investigate this further with the help of a regional coupled atmosphere–ocean model showed the excessive SSTs used in HadAM3H to be unrealistic (Kjellström et al. 2005). Such anomalies from GCMs can have consequences for the hydrological cycle over the Baltic Sea and parts of the surrounding land areas.

Figures 3.20 and 3.21 show area mean changes of temperature and precipitation for winter and summer, respectively, for 25 of the PRUDENCE experiments, which included 10 different RCMs, some run for three different GCM ensemble members, three different driving GCMs and two emission scenarios. The figures summarise results for the same four areas shown in Fig. 3.12 (two over land and two over sea). The overall ranges in temperature in Fig. 3.20 are smaller than the ranges estimated for the SRES-A2 and SRES-B2 experiments based on 6 GCMs, as illustrated in Fig. 3.13.

This implies that the largest uncertainty in these regional climate projections is due to the boundary conditions from the GCMs, as shown by Déqué et al. (2007). Nevertheless, there is additional uncertainty illustrated in Fig. 3.20 that is due to the formulation of the individual RCMs.

The open dots in the plot show the different projections from the common experiment performed in PRUDENCE, in which the RCMs were forced by lateral boundary conditions and SSTs from one GCM (HadAM3H). This experiment illus-

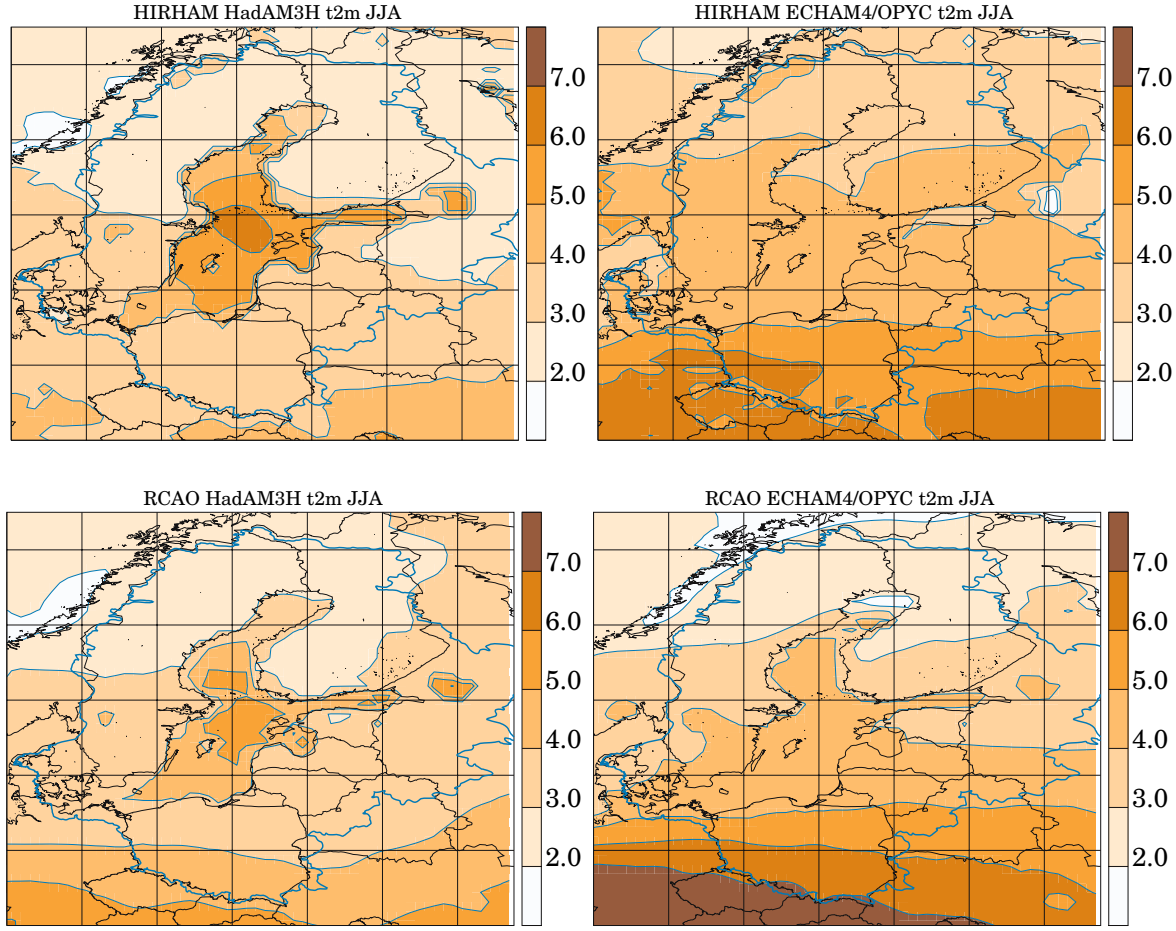

Fig. 3.19. RCM simulated temperature change in ℃ for summer (JJA) between the periods 1961–1990 and 2071–2100 using the SRES-A2 emissions scenario. The upper plots show results from the HIRHAM Model and the lower plots are from the RCAO Model. Plots on the left used GCM boundary conditions from HadAM3H; plots on the right used ECHAM4/OPYC3. The Baltic Sea Basin is indicated by the thick blue line (*note: ECHAM4/OPYC3 scenario simulations used as boundaries are different for the two RCM downscaling experiments, see Sect. 3.5.2.3*)

trates that there is a considerable spread between the projections due to RCM formulation. This spread is even larger during summer, as shown for the land areas in Fig. 3.21 (since the excessive HadAM3H Baltic Sea summer SSTs are unrealistically high, as discussed above, all experiments utilising those as lower boundary conditions have been excluded from the sea regions in Fig. 3.21). Compared to the ranges given by the GCMs in Fig. 3.13 the ranges from Fig. 3.21 are almost as large, indicating the relative importance of RCM uncertainty in climate projections for summer in this region.

Interannual variability of temperature, future climate

Räisänen et al. (2003) and Giorgi et al (2004a) showed that the interannual variability of temperature was simulated well in their respective control simulations as compared to gridded observations (CRU data). In the future anthropogenic climate change simulations analysed by Räisänen et al. (2003), interannual variability decreased in northern Europe during winter. They related this to the reduction in snow and ice in mid and high latitudes, as also seen in global models (Räisänen 2002). They also found large differences between different emission scenarios that they attributed to a relatively low signal-to-noise ratio.

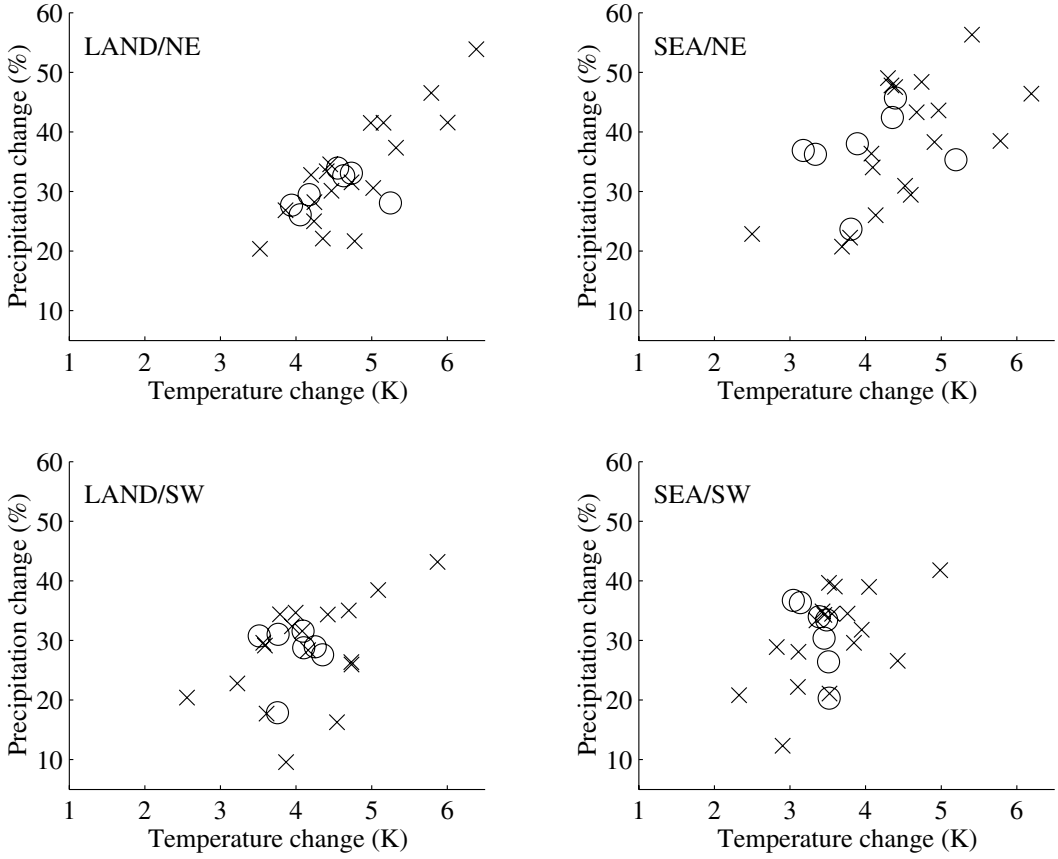

Fig. 3.20. Changes in winter (DJF) area mean temperature and precipitation for the areas defined in Fig. 3.12 The "◯" symbol denotes 7 RCMs from the common PRUDENCE experiment based on the same GCM (HadAM3H). The "×" symbol denotes other regional downscaling experiments from PRUDENCE, which included different driving GCMs, different emission scenarios, higher horizontal resolution and several ensemble members

Giorgi et al. (2004b) found increasing interannual variability south of the Baltic Sea during summer (JJA) and autumn (SON) in two future scenarios, SRES–A2 and SRES–B2. Schär et al. (2004) and Vidale et al. (2003) also found increasing interannual summer (JJA) temperature variability for Central Europe, including the southern part of the Baltic Sea Basin. The standard deviation of the interannual variability increased by 20 to 80% between the different RCMs in their study, all of which used the same emissions scenario. They linked this to the dynamics of soil-moisture storage and the associated feedbacks on the surface energy balance and precipitation.

Diurnal temperature range, future climate

The diurnal temperature range (DTR) is defined as the average difference between daily maximum and minimum temperatures. In future anthropogenic climate change scenarios, both Christensen et al. (2001) and Rummukainen et al. (2003) found a stronger decrease of the DTR in fall and winter than during summer for the Nordic region. The reduction around 2050 amounts to 0.6 ± 0.4 °C in winter, where the central value is the mean from all experiments and the range is given by the spread within the ensemble.

Räisänen et al. (2003) also found a larger change in DTR in northern Europe during the period late autumn to spring than in summer. The reduction of DTR in their scenarios, analysed over Sweden for the period 2071–2100, was of the order of 1 °C for the winter months. They also noted that the night-to-day temperature variability in northern Europe is small during mid-winter and that much of the simulated changes in DTR may be affected by irregular day-to-day variations.

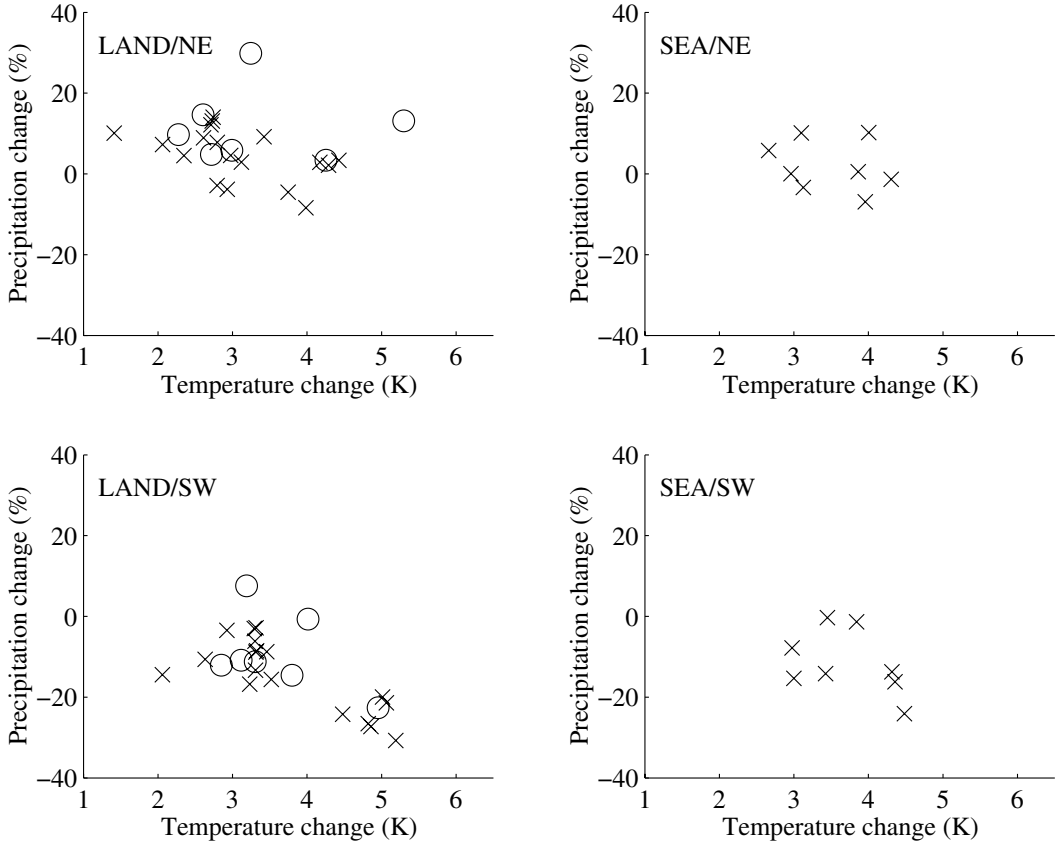

Fig. 3.21. Changes in summer (JJA) area mean temperature and precipitation for the areas defined in Fig. 3.12 The "◯" symbol denotes 7 RCMs from the common PRUDENCE experiment based on the same GCM (HadAM3H). The "×" symbol denotes other regional downscaling experiments from PRUDENCE, which included different driving GCMs, different emission scenarios, higher horizontal resolution and several ensemble members (*note that the common experiment is not shown for the sea areas due to unrealistically high Baltic Sea summer SSTs in HadAM3H*)

It should be noted that some models have problems in adequately simulating daily maximum and minimum temperatures for control periods (Moberg and Jones 2004; Kjellström et al. 2007; see also Sect. 3.6.2.1).

3.5.2.2 *Precipitation*

Precipitation, control climate

Inadequate observations contribute to difficulties in verifying precipitation results from climate models. Jones et al. (1995) compared large-scale precipitation over Europe from an RCM and its driving model to observed precipitation climatology (Legates and Wilmott 1990). They showed the RCM precipitation to be around 30% higher than the driving GCM and higher than observations, except for summer. They concluded that the large scale precipitation from the RCM could be realistic anyway, as observed precipitation was probably underestimated due to gauge undercatch errors, particularly for winter (see also Annex 5).

Several studies (Christensen et al. 1998; Rummukainen et al. 2001; Rutgersson et al. 2002) have similarly concluded that RCM precipitation in northern Europe is higher than the driving models and generally higher than observed data sets except for summer. Christensen et al. (1998) linked positive precipitation biases to exaggerated cyclone activity and high SSTs in the GCM control simulation, as compared to observations. They also attributed some of the bias to undercatch in precipitation observations.

The credibility of precipitation in climate models does not depend only on mean values. Hellström et al. (2001) studied the annual cycle of

precipitation in Sweden and Hanssen-Bauer et al. (2003) focused on regional variability in Norway. Both concluded that RCM simulations improved significantly, according to the driving GCM. Rummukainen et al. (2001) further concluded that although a large part of RCM biases can be attributed to the driving models, the RCMs added value to GCM simulations.

However, division of precipitation into intensity classes reveals a "drizzle problem", which is that the models exhibit too many days with light precipitation (defined as less than 1 mm day^{-1}) and too few dry days (defined as less than 0.1 mm day^{-1}), compared to observations (Christensen et al. 1998). The problem was shown to be more pronounced at finer RCM resolutions. According to Räisänen et al. (2003), relative interannual variability of precipitation from RCMs seems to be underestimated in the Baltic area, probably connected to the unrealistically high number of rainy days.

In more recent studies, Hagemann and Jacob (2006) compared the PRUDENCE RCM results to two observed precipitation databases that attempt to correct for gauge undercatch (CMAP, Xie and Arkin 1997; and GPCP, Huffman et al. 1997). They showed annual precipitation values for the Baltic Sea Basin to be close to an average of the two databases. They argued that the average of the two databases should exhibit realistic corrections for winter precipitation. Kjellström and Ruosteenoja (2007) also compared Baltic Sea Basin precipitation to observed databases (GPCP as above; and CRU, New et al. 1999). Their analysis of the seasonal cycle showed a general overestimation of winter precipitation. They also suggested that observational databases over the sea may be biased toward high summer precipitation due to erroneous influence of coastal precipitation.

Winter precipitation, future climate

As with results from global model experiments, regional projections for winter precipitation show increases over most of Europe (e.g. Déqué et al. 1998). Details of the geographical distribution for precipitation changes vary with different RCM simulations, however. The main source of disagreement in the RCM results is likely the different large-scale anthropogenic climate change signals from the GCM simulations employed. These differences are not just due to the consequences of different model formulations, but are also due to the fact that slow climate variations like the NAO can have different phases in the global simulations used to drive the RCMs.

The analysis by Déqué et al. (2007) of the multiple PRUDENCE simulations systematically attributes variations in results to different RCMs, emissions scenarios, GCM boundaries and variation between GCM ensemble members. For winter precipitation over the Baltic area, GCM boundary conditions are estimated to account for some 61% of the total variance and the choice of RCM for some 34% (Déqué, pers. comm. 2005). In summer, these roles are reversed with 74% of the variation attributable to choice of RCM for the Baltic area. However, there is an even wider distribution between choice of RCM, GCM and emissions scenario for most other European subregions.

This can be illustrated through an examination of Fig. 3.22, which shows winter precipitation change. The large-scale anthropogenic climate change in the ECHAM4/OPYC3 simulation leads to an intensification of the zonal flow, basically increasing the number and intensity of low-pressure systems from the Atlantic that hit Norway. The HadAM3H model turned the flow in a more south-easterly direction, leading to a decrease in precipitation in mid-Norway.

Simulations from the PRUDENCE common experiment tend to agree about an increase of more than 25% in a southwest to northeast band from England to Finland. In Fig. 3.20 this increase in winter precipitation can also be seen in the four subregions. The ECHAM4/OPYC3 experiments using the RCAO (Räisänen et al. 2003, 2004) and HIRHAM models (Christensen and Christensen 2004) show less agreement, as seen in Fig. 3.22. While both simulations exhibit increased precipitation of over 25% for most of northern Europe, the increase in precipitation is larger and covers an area much farther east in the RCAO simulation.

It is important to note that the boundary fields for these two sets of simulations are the same for the control period but not for the scenario period. The two simulated 2071–2100 time periods have different NAO phases, which is reflected in the downscaling results (see e.g. Ferro 2004). Hence, the larger difference between the two RCM projections using ECHAM4/OPYC3 scenario simulations compared to the two RCM projections using HadAM3H simulations can be attributed to differences in large-scale circulation in two different ECHAM4/OPYC3 scenario simulations.

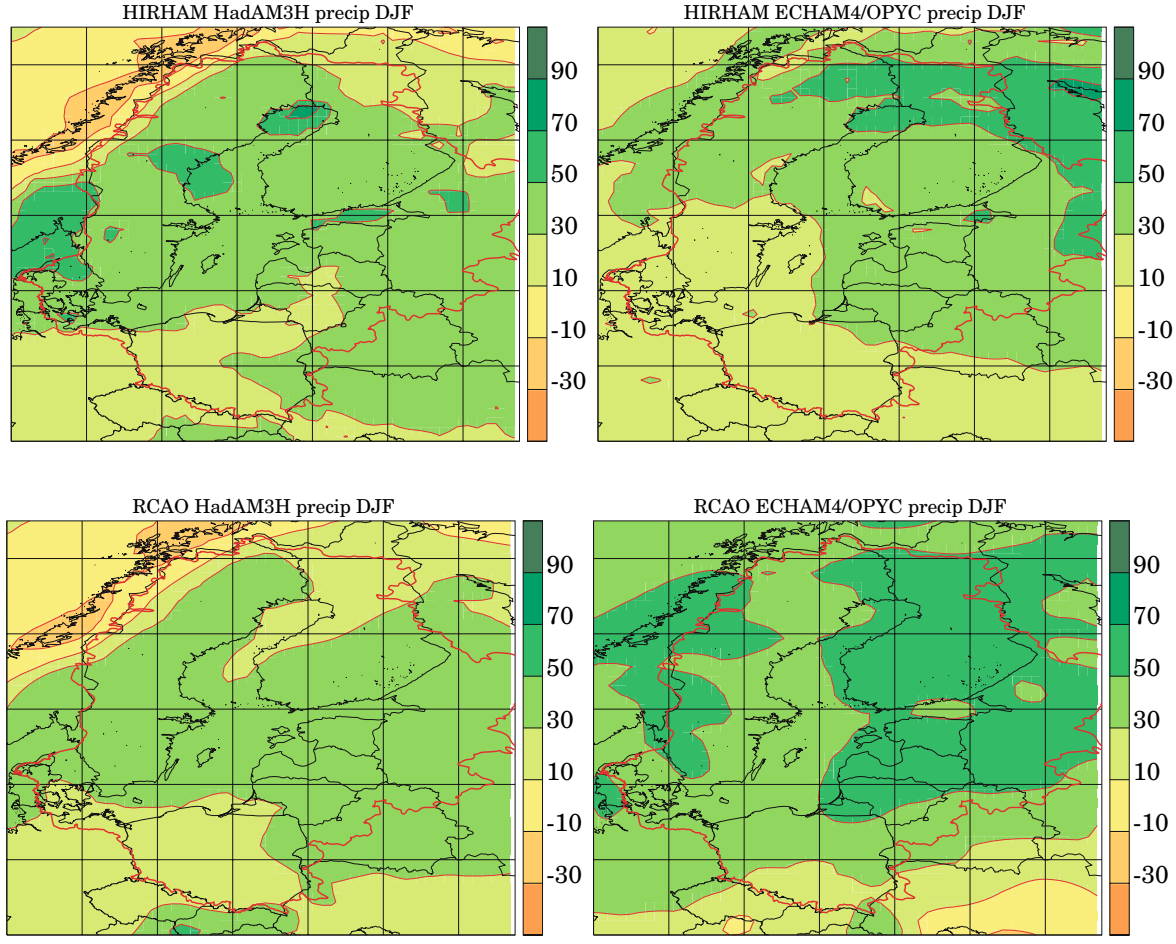

Fig. 3.22. RCM simulated precipitation change in percent for winter (DJF) between the periods 1961–1990 and 2071–2100 using the SRES-A2 emissions scenario. The upper plots show results from the HIRHAM Model and the lower plots are from the RCAO Model. Plots on the left used GCM boundary conditions from HadAM3H; plots on the right used ECHAM4/OPYC3. The Baltic Sea Basin is indicated by the thick red line (*note: ECHAM4/OPYC3 scenario simulations used as boundaries are different for the two RCM downscaling experiments, see Sect. 3.5.2.3*)

Summer precipitation, future climate

For future summers, regional anthropogenic climate change simulations show increases in precipitation for northern parts of the Baltic Sea Basin and decreases to the south, as shown in Fig. 3.23 for four simulations. This results in only a small average change for the basin as a whole. The dividing line between increase and decrease for the full range of PRUDENCE simulations generally goes across the southern half of Norway and Sweden continuing eastward through the Baltic countries (Kjellström and Ruosteenoja 2007).

As discussed above (Sect. 3.5.2.1) SSTs from simulations driven by HadAM3H show a large anomalous summer heating of the Baltic Sea, which in turn leads to a local increase in precipitation (Kjellström and Ruosteenoja 2007). Representation of summer precipitation over parts of the Baltic Sea Basin is therefore particularly sensitive to how thermal conditions in the Baltic Sea itself are input to the RCMs.

Precipitation and temperature, future scenarios

Figures 3.20 and 3.21 provide a comprehensive comparison of the projected anthropogenic climate change signals in temperature and precipitation between RCMs in the northern and southern sub-

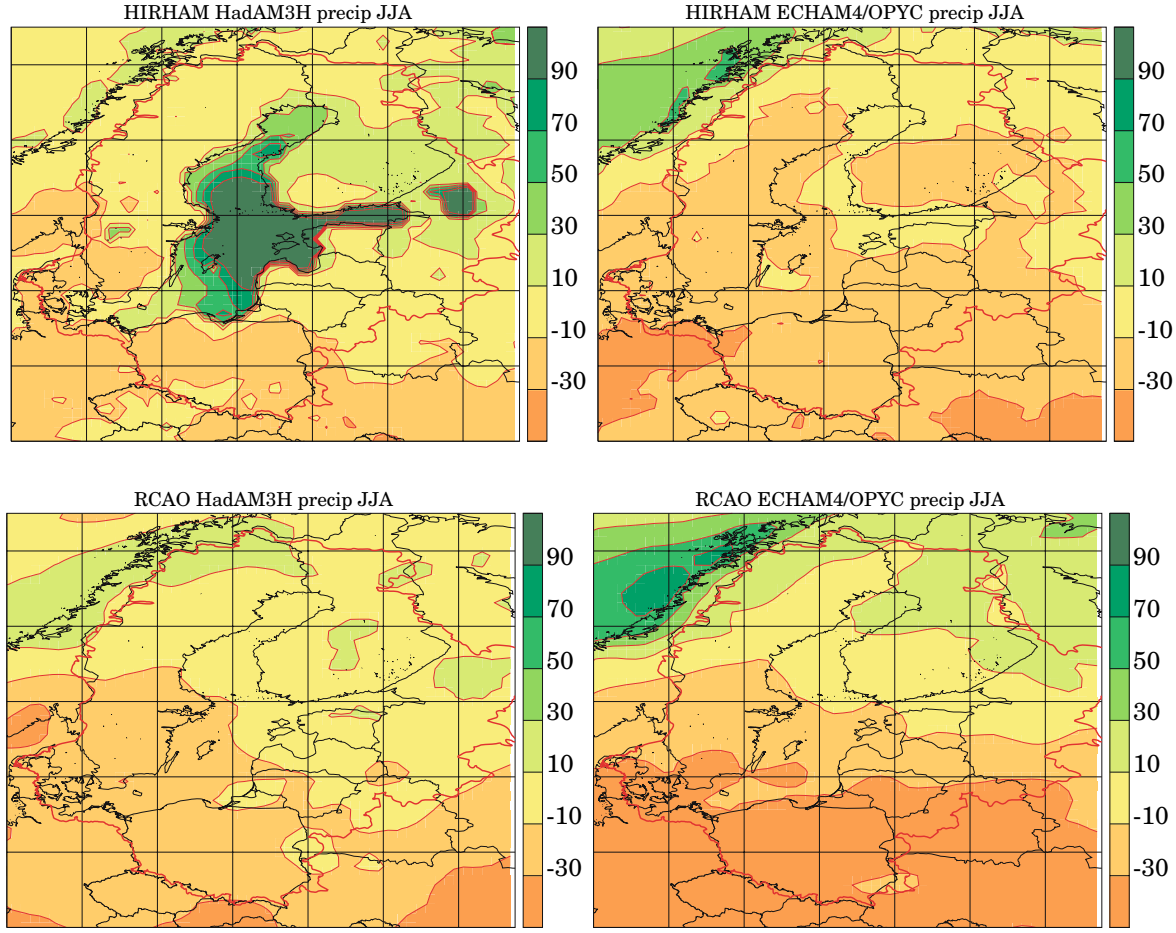

Fig. 3.23. RCM simulated precipitation change in percent for summer (JJA) between the periods 1961–1990 and 2071–2100 using the SRES-A2 emissions scenario. The upper plots show results from the HIRHAM Model and the lower plots are from the RCAO Model. Plots on the left used GCM boundary conditions from HadAM3H; plots on the right used ECHAM4/OPYC3. The Baltic Sea Basin is indicated by the thick red line (*note: ECHAM4/OPYC3 scenario simulations used as boundaries are different for the two RCM downscaling experiments, see Sect. 3.5.2.3*)

regions of the Baltic Sea Basin. The trend is for wintertime climate to become milder and generate more precipitation in both sub-regions. As discussed for the GCMs in Sect. 3.3.3.1, there tends to be a positive correlation between increasing temperature and precipitation, particularly over the north-eastern land area in most RCMs – the warmer the wetter. During summer there is no such correlation in the north, where all models get warmer to a different degree and most get wetter by between 5 to 20%. In the south, there is a tendency of an inverse correlation for summer – the warmer the drier.

3.5.2.3 *Wind*

To date, studies on future wind changes using RCMs were based mainly on two sets of simulations. One such set was performed within SWECLIM (Swedish Regional Climate Modelling Programme) and is described in detail by Rummukainen et al. (2000; 2004). The other set is more recent and includes eight different RCMs from the PRUDENCE project (Christensen et al. 2002). The results presented below focus mostly on results from the same two RCAO control simulations discussed above for temperature and precipitation. Wind speed in the following discussion refers to the mean velocity of the near surface

wind. This is generally the model wind speed at a height of 10 m from the surface.

Several parameters can be used to describe the temporal and spatial changes in wind speed and direction. A summary of the relevant quantities is given by Pryor and Barthelmie (2004). Besides generally applied parameters such as means, autocorrelations and percentiles, they also described quantities especially useful for the windpower industry. These are the Weibull distribution and energy density, which are described in detail by the Danish Wind Industry Association (www.windpower.org).

Wind, control climate

Pryor and Barthelmie (2004) compared wind speed from the two RCAO control simulations to NCEP reanalysis data for the period 1961–1990. They found that these RCM simulations accurately represented the dominant wind direction from southwest to southeast. However, they underestimated the prevalence of westerly winds in a band oriented southwest to northeast across the centre of the Baltic Sea Basin and overestimated the frequency of northeasterly and easterly winds in the south of the basin. Qualitatively RCAO driven by HadAM3H showed greater similarity to the NCEP reanalysis data than RCAO driven by ECHAM4/OPYC3.

Comparing to gridded observations (CRU data), Räisänen et al. (2003) found that the simulated seasonal cycle of wind speed in the RCAO simulations was in good agreement for the Baltic Sea Basin as a whole. However, summer minimums occurred one month earlier (July) in the control simulations compared to observations. In amplitude, both simulations overestimated the average observed wind speeds in winter and underestimated them in summer. Räisänen et al. (2003) ascribe this to two possible factors: 1) deficiencies in the RCM in simulating the boundary layer near surface conditions, and 2) an uneven distribution of observation stations.

Wind, future climate

Overall, Pryor and Barthelmie (2004) found that the spatial patterns of wind results from RCAO driven by ECHAM4/OPYC3 show larger changes between control and scenario than RCAO driven by HadAM3H. This is particularly true for mean wind speed as shown in Figs. 3.24 and 3.25, energy density, and the upper percentiles of the wind speed distribution. They argued that the differences in the two projected SRES-A2 future climate simulations from RCAO are due to differences in mean sea level pressure and transient activity.

This is in line with the findings by Räisänen et al. (2003), who show future changes in mean annual wind speed to fall mostly between −4 to +4% over Scandinavia for RCAO driven by HadAM3H for both SRES-A2 and SRES-B2 scenarios. Corresponding results from RCAO driven by ECHAM4/OPYC3 are about 8% for SRES-A2 and slightly less for SRES-B2.

A statistical analysis by Pryor and Barthelmie (2004) showed only small similarities in mean wind speed change between the two RCAO simulations, both for winter and summer and even less so in the annual mean. They ascribe the large differences between the anthropogenic climate change signals to the different GCMs used to drive the RCM. Figures 3.24 and Fig. 3.25 show these differences related to choice of GCM for summer and winter.

Again, the different NAO phases in the boundary conditions from ECHAM4/OPYC3 show up in the winter climate. The more positive phase of NAO in the boundaries is indicative of stronger winds on average. This is due both to the stronger pressure gradient in itself and to the warmer climate with less stably stratified conditions on average.

Regarding the seasonal cycle, Räisänen et al. (2003) found that the largest increases in future climate wind speed occur in simulations driven by ECHAM4/OPYC3 in winter and early spring over Sweden and northern Europe, as shown for SRES-A2 in Fig. 3.24 for winter. They occur when the increase in north–south pressure gradient is largest. Over land areas, these increases are up to 12% for the SRES-A2 and some 7% for the SRES-B2 scenarios, as an average over Sweden for DJF. Corresponding simulations driven by HadAM3H show almost no change over land for winter. Figure 3.25 illustrates that there is an opposite trend for summer from these simulations, as they show a decrease in wind speed over most of the Baltic Sea Basin. However, statistical analysis showed that only the ECHAM4/OPYC3 driven results for winter are statistically significant at the 95% level.

Over the Baltic Sea itself, simulated wind changes are modified by stability effects associated with changes in SST and ice cover. The winter increases in the ECHAM4/OPYC3 driven RCM simulations are up to about 18% in SRES-

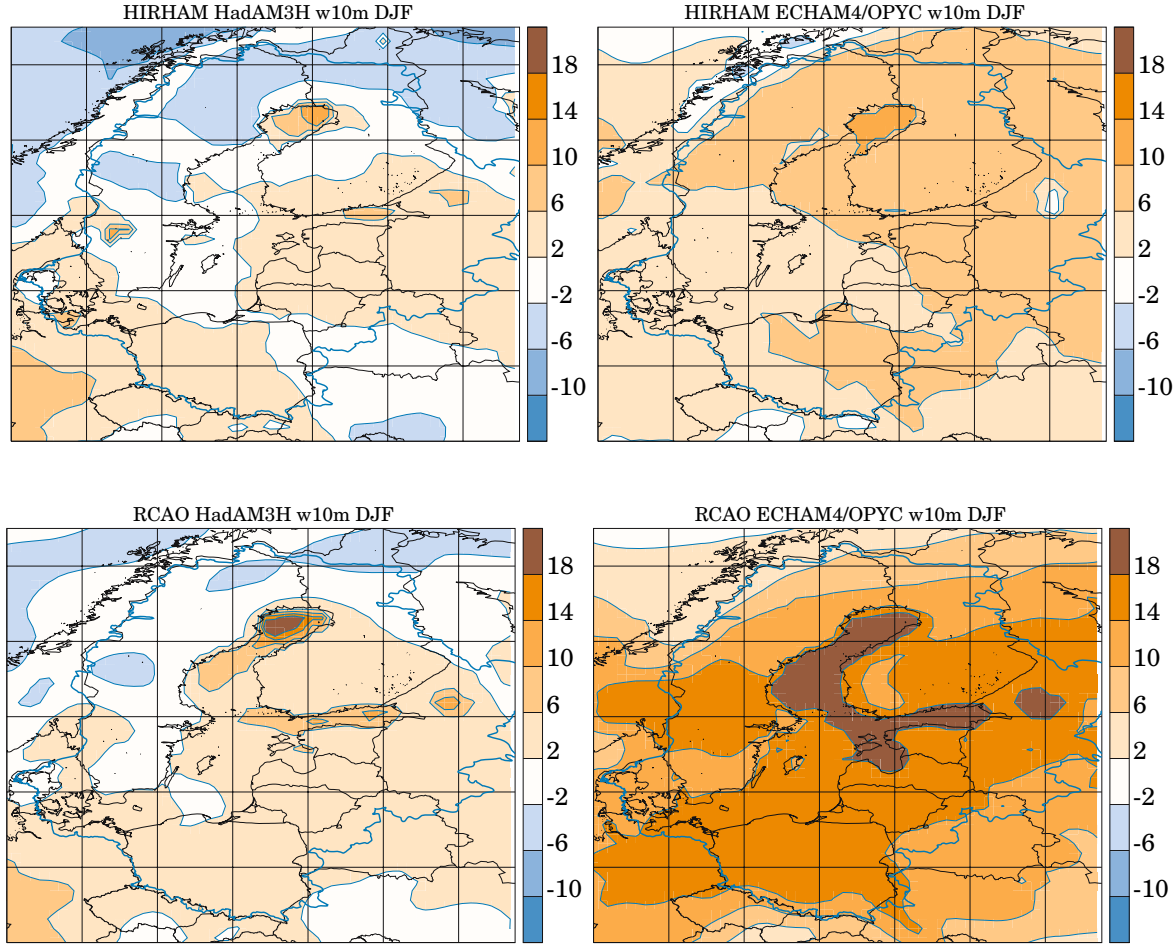

Fig. 3.24. RCM simulated wind speed change in percent for winter (DJF) between the periods 1961–1990 and 2071–2100 using the SRES-A2 emissions scenario. The upper plots show results from the HIRHAM Model and the lower plots are from the RCAO Model. Plots on the left used GCM boundary conditions from HadAM3H; plots on the right used ECHAM4/OPYC3. The Baltic Sea Basin is indicated by the thick blue line (*note: ECHAM4/OPYC3 scenario simulations used as boundaries are different for the two RCM downscaling experiments, see Sect. 3.5.2.3*)

A2 and 13% in SRES-B2, as an average over the entire Baltic Sea for DJF. Corresponding HadAM3H driven simulations show an increase of less than 5%, as an average over the entire Baltic Sea. The largest increases occur over the central and northern part of the sea, where ice cover decreases in the scenario runs. Summer changes over the Baltic Sea show a decrease of up to 7% for ECHAM4/OPYC3 driven simulations and an increase of about 5% for HadAM3H driven simulations, as an average over the entire Baltic Sea for JJA.

Regarding the latter, this reflects the large increase in Baltic Sea SSTs discussed above (Sect. 3.5.2.1), which leads to reduced surface stability and thereby higher wind speed (Räisänen et al. 2003).

Pryor and Barthelmie (2004) interpreted future wind changes with respect to the use of wind as an energy source by defining wind resource classes calculated from energy density in each model grid cell. This is defined as "poor" for energy density less than $70\,\mathrm{Wm}^{-2}$, or "good" for energy density greater than $140\,\mathrm{Wm}^{-2}$. Using these definitions, Pryor and Barthelmie (2004) found that the number of grid cells rated as "poor" decreased and the number of grid cells rated as "good" increased for almost all the simulations they analysed.

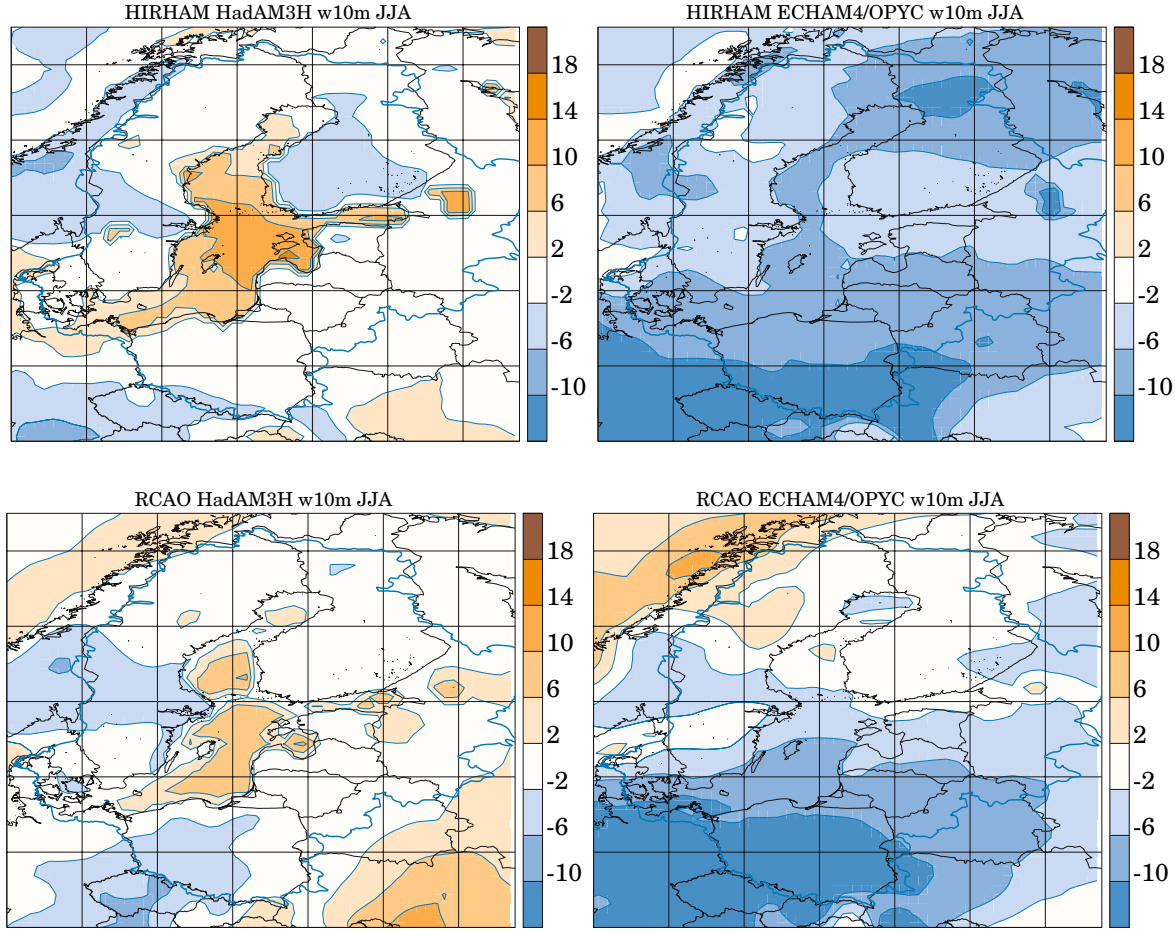

Fig. 3.25. RCM simulated wind speed change in percent for summer (JJA) between the periods 1961–1990 and 2071–2100 using the SRES-A2 emissions scenario. The upper plots show results from the HIRHAM Model and the lower plots are from the RCAO Model. Plots on the left used GCM boundary conditions from HadAM3H; plots on the right used ECHAM4/OPYC3. The Baltic Sea Basin is indicated by the thick blue line (*note: ECHAM4/OPYC3 scenario simulations used as boundaries are different for the two RCM downscaling experiments, see Sect. 3.5.2.3*)

3.5.2.4 *Snow*

Snow, control climate

Räisänen et al. (2003) found that the mean annual duration of snow season as simulated by RCAO is in good agreement with the observations of Raab and Vedin (1995) for Sweden. The mean annual maximum water content of the RCM snow pack tends to be slightly too low in southern Sweden and slightly too high in northern Sweden. A large positive bias occurs for the inland of northern Sweden (looking specifically at two available observation stations). This was attributed to orographic effects. In reality much of the precipitation in the north falls on the western side of the Scandinavian mountains. Due to orographic smoothing, the RCMs tend to generate more precipitation on the eastern side of the actual mountain divide.

Christensen et al. (1998) examined the dependence of snow cover on RCM resolution and found that a higher resolution significantly increases snow cover and delays spring snow melt due to the more realistic description of mountain topography. Räisänen et al. (2003) showed that differences due to GCM driving models were found to be modest, except for southern Sweden where ECHAM4/OPYC3 driven simulations show more snow and a longer snow season than for HadAM3H driven simulations. Jylhä et al. (2007) evaluated

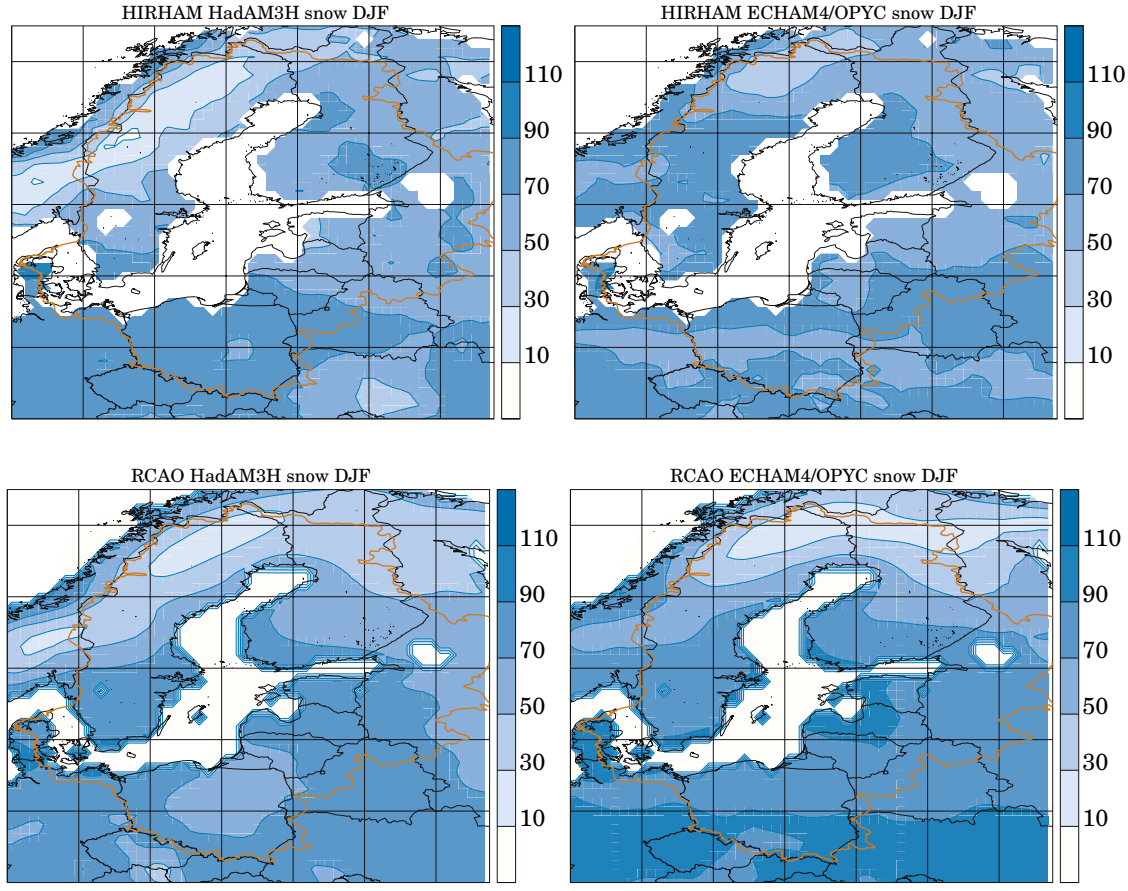

Fig. 3.26. RCM simulated snow depth reduction in percent for winter (DJF) between the periods 1961–1990 and 2071–2100 using the SRES-A2 emissions scenario. The upper plots show results from the HIRHAM Model and the lower plots are from the RCAO Model. Plots on the left used GCM boundary conditions from HadAM3H; plots on the right used ECHAM4/OPYC3. The Baltic Sea Basin is indicated by the thick red line (*note: ECHAM4/OPYC3 scenario simulations used as boundaries are different for the two RCM downscaling experiments, see Sect. 3.5.2.3*)

an ensemble mean of results from seven different PRUDENCE RCM simulations and found good agreement with the observations of Heino and Kitaev (2003) for the simulated number of days with snow cover (see also Annex 1.3.5).

Snow, future climate

Since snow changes follow changes in temperature, there is a general decrease in snow variables due to atmospheric warming in the RCM future scenarios. Results described by Räisänen et al. (2003) show a future decrease in mean annual maximum snow water equivalent everywhere over northern Europe from RCAO simulations. ECHAM4/OPYC3 driven results show a clear north–south gradient in change of snow water equivalent for both scenarios with only small deviations over Swedish inland areas. Reduction in snow water equvalent is some 60 to 80% in the southern part of the Baltic Sea Basin up to about latitude 62° N, some 40 to 60% between 62° N and 66° N, and less than 40% north of 66° N. There is also a clear region with relatively small changes down to 20% east of the Scandinavian mountains. For northern areas of the Baltic Sea Basin differences in results due to different driving GCMs are small, as shown in Fig. 3.26. Further south, for example in Denmark, the differences are larger in relative terms (Fig. 3.26) but small in absolute terms (Fig. 3.27).

Giorgi et al. (2004b) also found a general decrease in snow depth in their simulations with another RCM. There is a general decrease over the

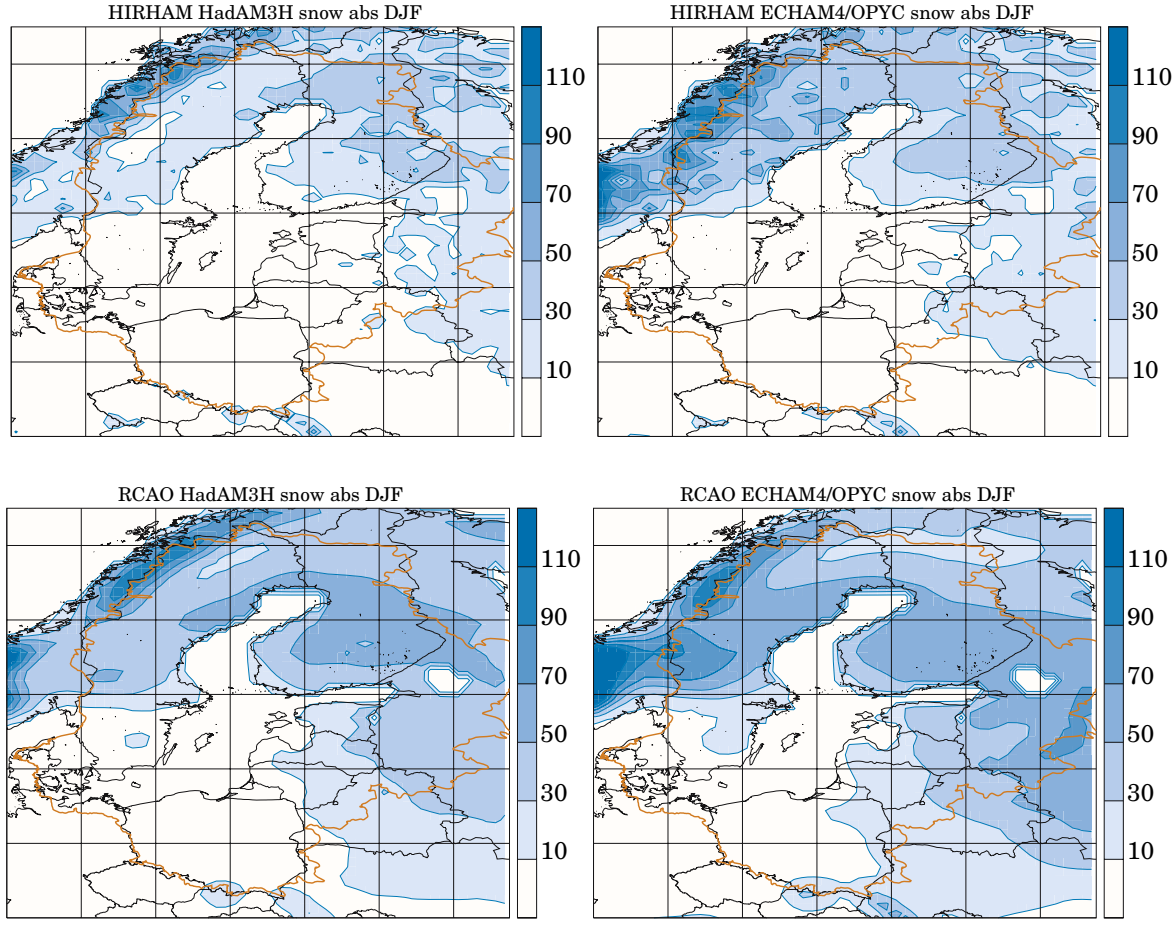

Fig. 3.27. RCM simulated snow depth reduction in mm of equivalent water for winter (DJF) between the periods 1961–1990 and 2071–2100 using the SRES-A2 emissions scenario. The upper plots show results from the HIRHAM Model and the lower plots are from the RCAO Model. Plots on the left used GCM boundary conditions from HadAM3H; plots on the right used ECHAM4/OPYC3. The Baltic Sea Basin is indicated by the thick red line (*note: ECHAM4/OPYC3 scenario simulations used as boundaries are different for the two RCM downscaling experiments, see Sect. 3.5.2.3*)

whole model domain. Over southern Sweden and Norway the decrease is about 50 to 100%. Over Denmark, Germany, and Poland and most parts of the Baltic States, where the present climate snow depth is already small, snow vanishes totally in the scenario simulations. These results were further confirmed by Jylhä et al. (2007). All seven RCMs analysed agreed about substantial decreases in snow depth. The mean annual decrease evaluated from the RCMs was shown to be some 50 to 70% for northern Europe and 75 to 90% for eastern Europe.

Räisänen et al. (2003) also found that the decrease in the duration of the snow season is greater in the SRES-A2 scenario than in SRES-B2. It is also greater in ECHAM4/OPYC3 driven simulations than in HadAM3H simulations. For all cases, the greatest changes (some 45 to 90 days) occur in the same area, a belt extending from central Scandinavia to the Baltic countries. This region showed a reasonable snow season in the control run, but with milder temperatures and is therefore more sensitive to scenario temperature increases than northern Scandinavia. South of this belt, the snow season was generally short even in the control run. Jylhä et al. (2007) found from the multimodel ensemble mean of RCMs driven with the HadAMH3 SRES-A2 scenario that mean changes were largest in areas that also had the largest decline in the number of frost days. This occurred primarily in mountainous areas and around the northern Baltic Sea, with a projected decrease of

more than 60 snow cover days. They also found that the portion of days with only a thin snow cover increases.

3.6 Projections of Future Changes in Climate Variability and Extremes for the Baltic Sea Basin

In the previous section, mean changes in atmospheric parameters were described. Such changes do not imply per se that extreme values also change in the same way. The occurrence of extremes is of great interest due to their considerable impact on mankind – e.g. droughts, floods and storms. Reinsurance companies, for instance, undertake their own investigations on extremes, since windstorms and floods are the two natural hazards that have caused the highest economic losses over Europe during the past century (Munich Re Group 1999).

3.6.1 Interpreting Variability and Extremes from Regional Anthropogenic Climate Change Projections

A common way to interpret climate variability and changes in extremes from regional anthropogenic climate change projections is to study the change in the distribution of key variables. Changes in mean and/or variance of the distribution function lead to different future projections. For some quantities, such as temperature, a normal distribution may be applied. More difficult to interpret are those quantities that generally cannot be approximated by a normal distribution, such as precipitation.

Some examples of how to interpret changes to normally distributed temperature are as follows:

- *Increase in mean* shifts the distribution function to a warmer climate. There will be fewer cold and more hot days, and more hot extremes.
- *Decrease in mean* shifts the distribution to a colder climate with fewer hot and more cold days, and more cold extreme events.
- *Increase in variance* broadens the distribution function, resulting in a larger variability of temperatures, but also in both more cold and extremely cold days and more hot and extremely hot days.
- *Decrease in variance* narrows the distribution function, leading to less variability and fewer extreme events, both cold and hot.

For more quantitative assessment of future changes, the percentiles of a distribution function can be calculated. Change in percentile values between 1^{st} to 5^{th} and between 95^{th} to 99^{th} are commonly used to define changes in extremes. The percentiles can be calculated either directly from the empirical distributions or from fitted distribution functions. As another approach for investigating changes in extremes, one can define a threshold value for the chosen variable and then determine the number of events exceeding this threshold for both present and future climates. For example, evaluating the number of times that the wind speed exceeds a certain value can be used to assess changes in storm events.

3.6.2 Projections of Future Climate Variability and Extremes

3.6.2.1 *Temperature Variability and Extremes*

Temperature variability and extremes, control climate

Overestimation of maximum temperatures in summer dominates in central and southern Europe and is associated with excessive drying of soils in the RCMs, as discussed in Sect. 3.5.1.1 (e.g. Vidale et al. 2007). In northern Europe, including the Baltic Sea Basin, the problem of dry soils and excessively high temperatures was not as large, and most PRUDENCE RCMs instead tended to underestimate the highest daily maximum temperatures (Kjellström et al. 2007). Räisänen et al. (2003) discussed the underestimation of high temperatures during summer in northern Europe, which they related to an over-representation of cloudy and rainy conditions in the RCAO simulations.

In winter, Räisänen et al. (2003) found that 30-year average minimum temperatures were too low for Sweden. Kjellström et al. (2007) showed that RCAO produces a cold bias for the 1^{st} percentile of the daily minimum temperatures over Scandinavia during winter, while the other RCMs exhibit a warm bias for these extreme temperatures. Further, they found that all the RCMs overestimate the 5^{th} percentile of diurnal average temperature for the 1961–1990 period when compared to the long observational records of daily temperatures in Stockholm, Uppsala and St. Petersburg, as shown in Fig. 3.28. Jylhä et al. (2007) found that the PRUDENCE RCMs generally capture the observed spatial patterns in the annual number of

frost days (defined as days with a minimum air temperature below 0 °C) and freezing point days (defined as days with a minimum air temperature below 0 °C and a maximum temperature above 0 °C, i.e. days during which the air temperature crosses the 0 °C threshold).

Kjellström et al. (2007) further compared the simulated daily maximum and minimum temperatures from the control climate of ten different RCMs to observations from a large number of European stations. They found considerable biases in some of the models. Taken as regional averages, these biases fall within ±3 °C in most regions for the 95th and 5th percentiles of daily maximum and minimum temperatures in summer and winter, respectively. A general tendency is that the biases are smaller for the more central percentiles than for the more extreme ones, and biases in the extremes are substantially larger than biases in the seasonal averages reported in Sect. 3.5.2.1. This implies that the conclusions regarding extremes are not as robust as those regarding seasonal averages.

Summertime warm temperatures, future climate

Kjellström (2004) investigated how probability distributions of diurnal averaged temperatures change in four different future scenarios. It was found that the asymmetry of these distributions changes differently depending on location and season. For summer, the changes are almost uniform over northern Scandinavia, while there are large differences between different parts of the probability distributions in the southern parts of the Baltic Sea Basin. The differences are manifested as a larger change of, for instance, the 99th percentile than the median, implying larger than average temperature increase on the warmest days. It was noted that the largest differences are found in areas where projected changes to components of the hydrological cycle are large, such as for cloud cover and soil moisture.

For the same set of simulations Räisänen et al. (2004) investigated changes in 30-year averages of yearly maximum and minimum temperatures. They found increases in maximum temperatures that were similar to the increases in summer mean temperatures for the Baltic Sea and Sweden while the maximum temperatures increased more than the average south of the Baltic Sea. The changes related to heat waves investigated by Beniston et al. (2007) showed that while the duration of heat waves (defined as the maximum length of all heat waves) increased only slightly, the number, frequency (defined as the total length of all heat waves) and intensity of heat waves increased substantially (by more than a factor of 5) in the Baltic Sea Basin.

Kjellström et al. (2007) showed that the differences between RCM projections of daily maximum temperatures are larger than differences between mean temperatures. For the Baltic Sea Basin some RCMs project the 95th percentile of daily maximum temperature to increase by 3 to 5 °C, while in others the increase lies from 5 to more than 10 °C. They also found that, although there is a large inter-model variability, the anthropogenic climate change signal is well beyond natural variability, as derived from the long series of daily temperature measurements in Stockholm, Uppsala and St. Petersburg, as seen in Fig. 3.28.

Wintertime cold temperatures, future climate

A snow covered surface is a crucial requirement to attain really low temperatures. The large wintertime temperature increase projected for northeastern Europe in Sect. 3.5.2.1 is to a large extent related to the withdrawal of the snow cover. Temperatures on the coldest days increase dramatically in the future scenarios. For instance, Kjellström (2004) showed individual daily increases of more than 15 °C in parts of eastern Europe and Russia, while the average daily temperatures increase more modestly by 3 to 7 °C. The largest differences between the increase of temperature on the coldest days and the increase in the median were found to be similar to the area where the length of the snow season decreases the most (cf. Sect. 3.5.2.4).

Ferro et al. (2005) showed some of the complex changes in the probability distributions for daily minimum temperatures in the Baltic Sea Basin, including greater changes on the coldest days as compared to the mean. Räisänen et al. (2004) showed a high degree of nonlinearity between the average increase in winter temperature and the increase in the 30-year average of yearly minimum temperatures. They also pointed out the fact that the average minimum temperatures in the control run simulations were too cold over Sweden, a fact that could contribute to the large anthropogenic climate change signal (see above). However, they concluded that this is unlikely to be the only cause of the large increases.

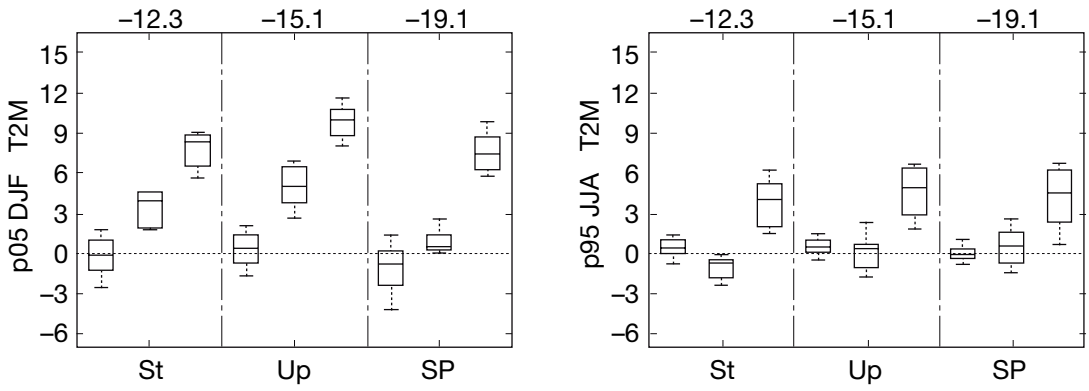

Fig. 3.28. Daily mean temperature deviation from the 1961–1990 observed median in ℃, values of which are shown along the top. Shown are the 5th percentile for winter on the left and the 95th percentile for summer on the right. Three stations are given – Stockholm (St), Uppsala (Up) and Saint Petersburg (SP). Three boxplots are shown for each station; the left shows the observed spread between different overlapping 30-year periods from the last 200 years, the middle shows the spread between the different RCMs for the control period, and the right shows RCM spread for the future SRES-A2 simulations. In each boxplot the box extends from the lower to the upper quartile, with the line inside the box denoting the median. The vertical lines extend from the lower (upper) quartile to the minimum (maximum) value. Values of the 1961–1990 observed median are shown along the top (based on data from Kjellström et al. 2007)

Kjellström et al. (2007) found, similarly to the case for high temperatures in summer, a larger inter-model variability for extremely low temperatures than for the mean. Some RCMs project changes in the 5th percentile of daily average temperatures of 4 to 7 ℃ while in others the changes are 7 to 12 ℃ in the Baltic Sea Basin. Again, and even more pronounced, it was shown that the projected changes of minimum temperatures are well outside of the observed climate variability during the last 200 years, as seen in Fig. 3.28.

3.6.2.2 *Precipitation Extremes*

Due to its very nature as infrequent, sporadic events occurring on small spatial scales, simulating extreme precipitation in RCMs is much more difficult than simulating mean precipitation. Hence, care has to be taken to extract meaningful results from RCM studies. To date, only limited evaluation has been performed.

Precipitation extremes, control climate

Christensen et al. (1998) investigated heavy precipitation (defined as exceeding 10 mm day^{-1}) in an RCM at two different resolutions (57 km and 19 km) and its driving GCM. The results were compared to observations over the Nordic countries. The RCM simulations showed a more representative number of high-intensity rain days than the GCM, with the finer resolution simulation showing the highest number.

Christensen et al. (2002) compared results from RCM simulations at 22 km resolution to 20 years of gridded observations over Denmark (Scharling 2000). They also showed high-intensity events to be more frequent with higher spatial resolution, but the regional model did not produce a sufficient number of extreme events even though the mean precipitation was realistic (see also Christensen and Christensen 2004). However, in contrast to the driving GCM, the high-resolution RCM simulation showed a realistic annual variation of the decay exponent (i.e. the exponent of an exponential fit to the probability of exceedance as a function of daily precipitation values). Räisänen et al. (2003) concluded that extreme precipitation was underestimated in RCMs. Semmler and Jacob (2004) looked at daily precipitation over the German state of Baden–Württemberg and found realistic magnitudes and regional variation for 10-year return periods compared to gridded observations.

Available validation studies are thus insufficient to provide definite statements about the relative merits of different regional climate models, or at what resolution they could best be applied. However, the studies do show that RCMs provide more realistic descriptions of extreme precipitation than GCMs.

Precipitation extremes, future climate

Christensen et al. (2001) compiled results of several independent regional simulations showing that heavy precipitation (defined as exceeding 10 mm day^{-1}) increased significantly over Scandinavia following a similar but less significant increase in mean precipitation over the same area. Räisänen and Joelsson (2001) showed that spatial aggregation of a simple statistic, the annual-maximum precipitation event, increased the statistical significance. Their 10-year simulations showed a significant increase of this quantity when averaged over the entire RCM domain, which encompassed central and northern Europe. The method was extended in Räisänen et al. (2004) and applied to 30-year simulations (as presented in Sect. 3.5). Christensen et al. (2002) found that the decay exponent decreased in summer, which indicates more intense extreme rainfall, although the statistical significance of this result was not assessed.

Some results for projected future changes in precipitation extremes are common for several downscaling experiments. The decrease of summer precipitation in southern Europe is seen in several numerical experiments (Cubasch et al. 2001; Giorgi et al. 2001). However, in spite of this reduction the extreme precipitation generally shows an increase (e.g. Christensen and Christensen 2003, 2004; Räisänen and Joelsson 2001; Räisänen et al. 2004; Beniston et al. 2007). Christensen and Christensen (2004) similarly show a larger increase for heavy precipitation than mean precipitation for two river catchments in the Baltic Sea Basin, Oder and Torne, as simulated with two different driving models, HadAM3H and ECHAM4/OPYC3. This result was also found to apply over the entire Baltic Sea Basin and the Baltic Sea itself; however, the anomalous increase in Baltic Sea SSTs from HadAM3H are problematic for this experiment (see Sect. 3.5.2.1).

A further analysis over Europe in Beniston et al. (2007) shows that several models share the tendency to exhibit increasingly positive changes for higher return periods (see also Kjellström 2004). However, some models (e.g. HadRM3H) have such large reductions in precipitation frequency that even the highest extremes have negative changes. Räisänen et al. (2004) found that the projected future reduction in precipitation in Central and Southern Europe is due to a reduction in precipitation frequency and not in intensity. They showed that average intensity changes only slightly, while extreme values tend to increase. Winter precipitation extremes were also analysed by Beniston et al. (2007). For most of Europe, including the Baltic Sea Basin, extreme winter precipitation was shown to increase, roughly proportional to the increase in mean precipitation.

3.6.2.3 *Wind Extremes*

Characteristics of changes in wind extremes can be expressed by several different parameters, for example as changes in the upper percentiles (e.g. 90$^{\text{th}}$, 95$^{\text{th}}$, 99$^{\text{th}}$) of the daily mean wind or of the daily maximum wind speed. For calculations of higher wind speeds additional techniques are needed, such as gust parameterisation. Using such parameterisations, the number of storm peak events can be determined. Another method for assessing changes in storm events is applying a combination of maximum wind speed and pressure changes (Leckebusch and Ulbrich 2004).

Wind extremes, control climate

Rockel and Woth (2007) studied the 99$^{\text{th}}$ percentile of daily mean wind speed for SRES-A2 scenario simulations from eight different RCMs. For north-eastern Europe monthly averages of the 99$^{\text{th}}$ percentile from all the control simulations varied between about 13 to 17 m s^{-1} for January and 10 to 12 m s^{-1} for July (Fig. 3.29). However, over land these quantities can only be used to assess a qualitative change in wind speed, as regional models are hardly producing wind speeds above 17 m s^{-1} (cf. Sects. 3.5.1.1 and 3.5.2.3).

Wind extremes, future climate

An increase of strong winds over the whole Baltic Sea Basin was reported by Pryor and Barthelmie (2004). They investigated the change in the 90$^{\text{th}}$ percentile and found an increase in the southern part of the Baltic Sea Basin and southern to mid-Sweden of up to 0.7 m s^{-1} over land areas. Over the northern part of the basin, the increase was lower, less than 0.4 m s^{-1}. The largest increase occurs over the Baltic Sea itself, with more than 0.7 m s^{-1}. These numbers were taken from the RCAO simulation driven by ECHAM4/OPYC3; values from the corresponding simulation driven by HadAM3H are generally lower as discussed below (see also Sect. 3.5.2.3). Following Pryor

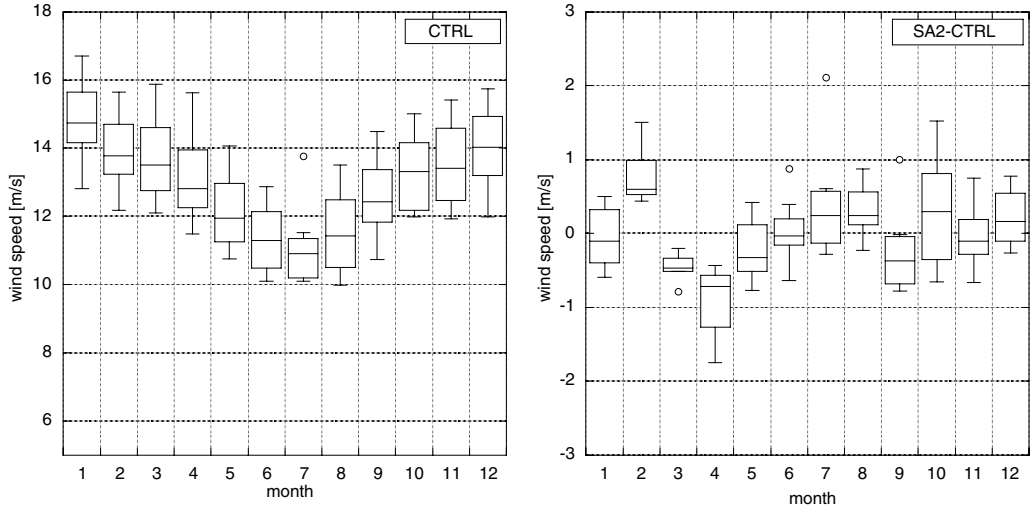

Fig. 3.29. 99$^{\text{th}}$ percentile of daily mean wind speed over Scandinavian land area from eight different RCMs driven by HadAM3H boundary conditions. The plot on the left shows results for the present climate (1961–1990). The plot on the right shows change in future climate for the SRES-A2 scenario (scenario 2071–2100 minus present day 1961–1990). Open circles denote outliers (i.e. where the distance from either the lower 25% or the upper 75% quartile is larger than 1.5 times the interquartile distance) (from Rockel and Woth 2007)

and Barthelmie, the differences in future change of extreme wind speed may be indicative of a change in the NAO teleconnection patterns. In agreement with dynamic scales, up to 50% of the interannual variability in the 90$^{\text{th}}$ percentile winter wind speeds in the Baltic Sea Basin can be attributable to variations in NAO (Pryor and Barthelmie 2003).

Rockel and Woth (2007) studied daily mean wind speed over land for SRES-A2 scenario simulations from eight different RCMs. Looking at the 90$^{\text{th}}$ percentile, half of the models determine a future increase in wind speed of around $1\,\mathrm{m\,s^{-1}}$ in February and a decrease of around $1\,\mathrm{m\,s^{-1}}$ in April over north-eastern Europe (Fig. 3.29). Individual models show values of up to $2\,\mathrm{m\,s^{-1}}$ (July) and nearly $-2\,\mathrm{m\,s^{-1}}$ (April). For September the 99$^{\text{th}}$ percentile of wind speed decreases between 0 and about $1\,\mathrm{m\,s^{-1}}$, with a model mean of $0.5\,\mathrm{m\,s^{-1}}$.

Generally, the changes in extreme wind speed follow those in mean wind speed (Räisänen et al. 2003). RCAO driven by ECHAM4/OPYC3 shows an increase of about 8%; in terms of annual maximum wind speed, the projected changes over Sweden are 8% and 6% for the SRES-A2 and SRES-B2 scenarios, respectively. RCAO driven by HadAM3H shows a decrease of about 4%; the corresponding changes in annual maximum wind speed are −3% and −2% over Sweden for the SRES-A2 and SRES-B2 scenarios, respectively. However, only the results from the RCAO simulations driven with ECHAM4/OPYC3 are statistically significant at the 95% level. The large-scale geographical patterns of change and differences between the different simulations of annual maximum wind speed broadly follow those of the annual mean wind speed (Räisänen et al. 2004). The largest increases occur in northern Europe in the regions of western Norway and Sweden.

The results described above are based directly on model calculated wind. As such, this wind speed does not realistically reflect the occurrence of wind peaks or gusts. Gusts occur on finer temporal and spatial scales than those resolved by RCMs. Thus, a sub-grid parameterisation is necessary to properly account for them. For two of the eight RCMs used in PRUDENCE, maximum wind speed results included gust parameterisation. Rockel and Woth (2007) studied the future change in the number of storm peak events (defined as wind speeds greater than $17.2\,\mathrm{m\,s^{-1}}$) for the SRES-A2 scenario with HadAM3H boundary conditions. They found an increase of about 10% over the southern part of the Baltic Sea Basin and a decrease of about 10% in the northern part for both models. In the middle of the Baltic Sea Basin the two models show opposite behaviour. One gives a decrease of about 10%, whereas the other shows storm peak events to increase by about 10%. As the same gust parameterisation is implemented

in both models, other differences in the models must be responsible for these discrepancies.

3.7 Projections of Future Changes in Hydrology for the Baltic Sea Basin

Hydrological regimes vary according to how the local and regional climate varies; looking toward future climate, both change and variability in climate will produce changes in hydrological conditions. This section focuses on the hydrological response to projected changes in climate for the Baltic Sea Basin. Hydrological studies focusing on anthropogenic climate change are often associated with analysing impacts to water resources, thus combining the science of anthropogenic climate change with applications for society. The following hydrological assessment strives primarily to summarise responses of the hydrological system and does not attempt to cover the full details of the studies on impacts included in the literature, although some overlap is unavoidable.

Most studies conducted within the Baltic Sea Basin do not cover the entire basin. Many are often of national interest and concentrate only on certain river basins. Therefore to be complete, a short summary of relevant studies is included here, even though they do not address the continental scale of the full Baltic Sea Basin.

3.7.1 Hydrological Models and Anthropogenic Climate Change

Although both global and regional climate models include representation of the hydrological cycle and resolve the overall water balance, they typically do not provide sufficient detail to satisfactorily address how a changing climate can impact on hydrology (Varis et al. 2004). Due to this, hydrological models are used to further investigate hydrological responses to anthropogenic climate change. Many researchers have estimated how hydrological conditions may change with anticipated climate change for a host of different drainage basins around the world (e.g. Arnell 1999; Bergström et al. 2001; Gellens and Roulin 1998; Grabs et al. 1997; Hamlet and Lettenmaier 1999; Kaczmarek et al. 1996; Sælthun et al. 1998; Vehviläinen and Huttunen 1997). The common approach for such studies is to first evaluate representative anthropogenic climate changes from the climate models and then to introduce these changes to a hydrological model for the basin in question. Many such studies were based on anthropogenic climate change results from global general circulation models (GCMs), some used statistical downscaling methods, and more recent studies included results from regional climate models (RCMs).

3.7.2 Interpreting Anthropogenic Climate Change Projections for Hydrology

Transferring the signal of anthropogenic climate change from climate models to hydrological models is not a straightforward process. In a perfect world one would simply use outputs from climate models as inputs to hydrological models, but meteorological variables from climate models are often subject to systematic biases. For example, in the Alpine region of Europe, many RCMs exhibit a dry summertime precipitation bias on the order of 25% (Frei et al. 2003). For northern Europe, including parts of the Baltic Sea Basin, precipitation biases tend toward overestimation (Hagemann et al. 2004; see also Sect. 3.5.1.1). Hydrological regimes are particularly sensitive to precipitation, and such biases strongly affect the outcome of hydrological model simulations. Uncertainties in observations further complicate the analysis of precipitation biases.

Due to climate model biases, most studies of the hydrological response to anthropogenic climate change to date have resorted to the practice of adding the change in climate to an observational database that is then used as input to hydrological models to represent the future climate (Andréasson et al. 2004; Bergström et al. 2001; Kilsby et al. 1999; Lettenmaier et al. 1999; Middelkoop et al. 2001; Sælthun et al. 1999). This common approach for impacts modelling has been referred to as the *delta change* approach (Hay et al. 2000), and variations of this approach have been the de facto standard in anthropogenic climate change impacts modelling for some time. According to Arnell (1998), this requires two important assumptions. One is that the base condition represents a stable climate both for the present and for a future without anthropogenic climate change. Secondly, the atmospheric model scenarios represent just the signal of anthropogenic climate change, ignoring multi-decadal variability. However, the longer the time period of climate model simulations, the more multi-decadal variability is smoothed out.

A major disadvantage of the delta change approach is that representation of extremes from future climate scenarios effectively gets filtered

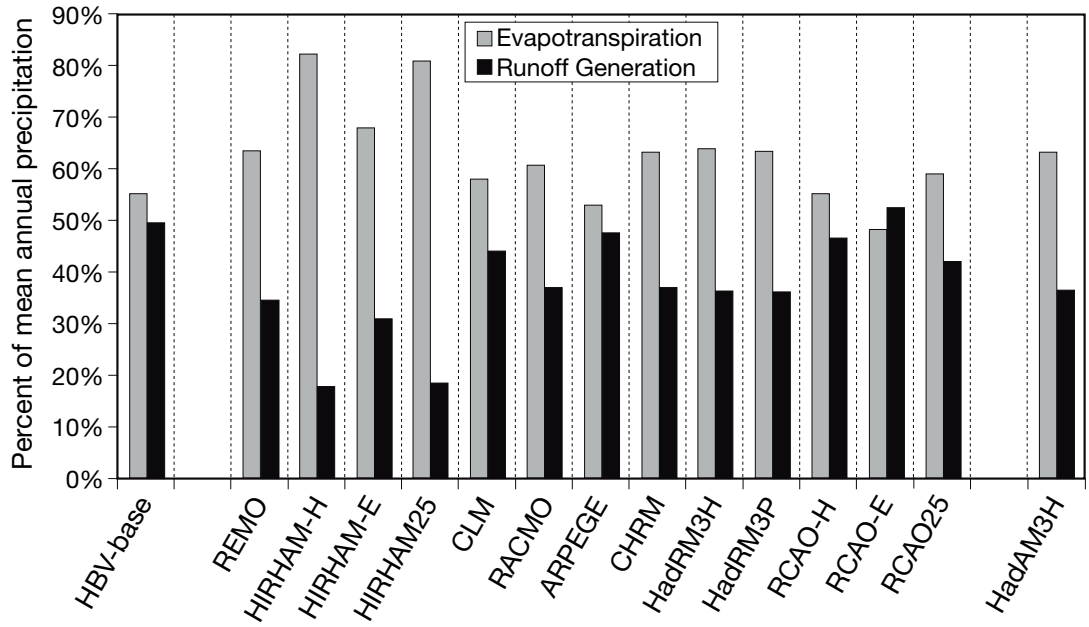

Fig. 3.30. RCM partitioning of precipitation into evapotranspiration and runoff generation over the total Baltic Sea Basin for control simulations representing the period 1961–1990. Also shown are calibrated results from the HBV-Baltic hydrological model (HBV-base; see Sect. 3.7.4), which are thought to give a reasonably accurate representation of the partitioning. All RCM simulations with the exception of 3 were forced by the global HadAM3H (*also shown*); the exceptions are HIRHAM-E and RCAO-E forced by ECHAM4/OPYC3, and HadRM3P forced by HadAM3P (from Graham et al. 2007b)

out in the transfer process. The delta change extremes are simply the extremes from present climate observations that have either been enhanced or dampened according to the delta factors. For this reason, researchers have recently been investigating more direct methods for representing the future climate in assessments of the hydrological response to anthropogenic climate change. This employs applying some form of scaling (modification) to RCM outputs to try to correct for biases before transfer to hydrological models. Such methods also have limitations, which can be severe, but they are more consistent with the RCMs and provide additional answers that are missing in the delta change approach (Arnell et al. 2003; Graham et al. 2007a; Lenderink et al. 2007).

Yet another approach is to use runoff results directly from climate models. This applies primarily to RCMs, where horizontal model scales are becoming finer and are approaching scales more representative of large-scale hydrological processes. RCM model runoff output is in the form of *runoff generation*, which is the instantaneous excess water per model grid square, without any translation or transformation for groundwater, lake and channel storage, or transport time. As such, this runoff value is difficult to compare to observations and it does not provide flow rates through rivers into the sea. *River routing* schemes can be used to route climate model runoff ($\mathrm{mm\,day^{-1}}$) to river discharge ($\mathrm{m^3\,s^{-1}}$) (Hagemann and Dümenil 1999; Lohmann et al. 1996); this mainly affects timing and seasonal distribution. However, since this approach makes no corrections to runoff volumes, water balance biases from the climate models greatly influence the results.

The partitioning of precipitation into evapotranspiration and runoff is critical for realistic representation of the hydrological cycle. Graham et al. (2007b) investigated the hydrological performance of 13 RCM control simulations over the Baltic Sea Basin with a simple comparison of the partitioning of annual RCM precipitation into evapotranspiration and total runoff generation, as shown in Fig. 3.30. They found that the majority of RCMs investigated tended to underestimate the partitioning of precipitation into runoff. This is likely due to a general overestimation of evapotranspiration in the basin.

3.7.3 Country Specific Hydrological Assessment Studies

As mentioned above, many hydrological studies do not cover the entire Baltic Sea Basin. This section gives a concise summary of known studies on a country specific basis. Some of these were conducted over the total territory of the country in question, while others concentrated on specific river basins or specific subbasins. Figure 3.31 shows a map giving the approximate locations of documented studies. A short section on each country follows. Note that although the Czech Republic, Slovakia and Ukraine also have areas within the Baltic Sea Basin, they are not included here due to their relatively small contributions of runoff.

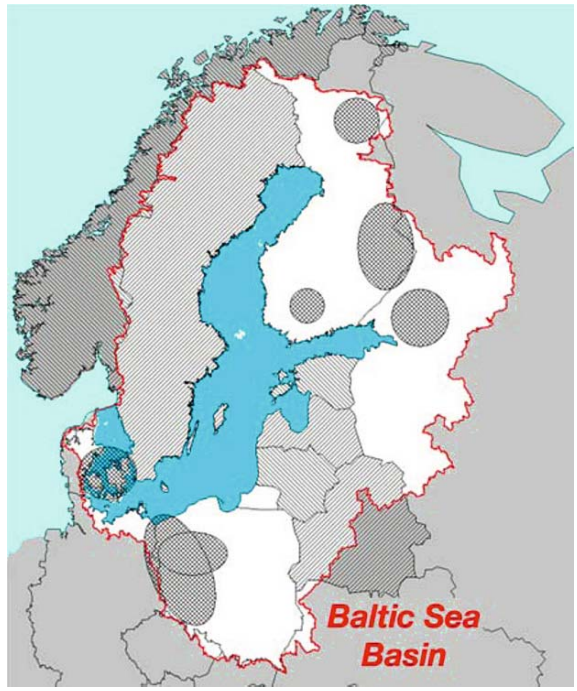

Fig. 3.31. Locations of country specific studies conducted to analyse the hydrological response to projected anthropogenic climate change in the Baltic Sea Basin. Countries that included their total territory in the studies are indicated with diagonal striping. Otherwise, the general location of basins studied is indicated with hatched circles

Belarus

One study was conducted and reported in the Assessment of Potential Impact of Climatic Changes in the Republic of Belarus (World Bank 2002) and in BALTEX conference proceedings (Kalinin 2004). Three different incremental climate scenarios were used, 1) an increase in temperature by 2 °C, 2) a decrease in precipitation by 10%, and 3) a combination of both changes. A water balance model was used to calculate monthly mean and annual mean river runoff and total evapotraspiration. The entire territory of Belarus was included.

According to the first scenario, river runoff would decrease by 10%, and total evapotranspiration would increase by 4.7% (World Bank 2002). According to the second scenario, river runoff would decrease by 24.5%, and total evaporation would decrease by 5.4%. In this case, the maximum runoff and total evaporation reduction would take place in July with 29.7% and 7%, respectively. In the third scenario runoff would decrease by 29.3% on average, and total evapotranspiration would decrease by 0.7% on average. The maximum runoff and total evapotranspiration reduction would take place in July with 45.2% and 5.1%, respectively. River runoff appeared to be quite sensitive to the simultaneous precipitation reduction and air temperature rise.

A further analysis looked at how a temperature increase of 1.5 °C by the year 2025 would affect groundwater. This showed a groundwater level recession of approximately 0.03–0.04 m relative to the current level (Kalinin 2004).

Denmark

Andersen et al. (2006) used 30-year HIRHAM RCM control and SRES-A2 simulations driven by ECHAM4/OPYC3 in the NAM rainfall-runoff model for the Gjern River basin. They found mean annual runoff to increase by 7.5% in the future climate. Seasonally, their results show considerably higher runoff during winter. They found summer runoff to increase in streams that are predominantly groundwater fed and to decrease in streams with a low base-flow index, typically loamy catchments. Summer runoff reductions of 40–70% were projected for the latter stream type.

Thodsen et al. (2005) and Thodsen (2007) looked at the impact of projected anthropogenic climate change on the Odense River, also using the NAM rainfall-runoff model with a HIRHAM SRES-A2 simulation (GCM unspecified). They found that runoff would increase for the period December to August, with as much as 30% in February. A decrease in runoff was shown for September to November, with as much as 40% in September.

They also found that extremes would be more pronounced, both at high flows and at low flows.

Estonia

A coordinated study using the same set of anthropogenic climate change scenarios generated by two GCMs was reported in the Country Case Study on Anthropogenic Climate Change Impacts and Adaptation Assessments in the Republic of Estonia (Tarand and Kallaste 1998) and other publications (Kallaste and Kuldna 1998; Järvet et al. 2000; Roosaare 1998). Additionally, another study using five incremental scenarios was conducted for the Lake Võrtsjärv (Järvet 1998).

The MAGICC model (Wigley and Raper 1987; 1992a; 1992b) and SCENGEN program were used for anthropogenic climate change scenario generation in the country case study (Keevallik 1998). Three alternative IPCC GHG emissions scenarios (IS92a, IS92c, IS92e) were combined with results of two GCM experiments (HadCM2 and ECHAM3). As a result, six anthropogenic climate change scenarios up to year 2100 were prepared for modelling anthropogenic climate change impact on river runoff. The three IPCC scenarios were qualitatively labeled as MIN (IS92c), MID (IS92a) and MAX (IS92e), as used in the discussion below.

Several different hydrological models and tools were used for the analysis of river runoff, evapotranspiration, groundwater and water supply. The water balance model WATBAL was used for river runoff with a monthly time step. The entire territory of Estonia, subdivided into western Estonia with strong influence from the Baltic Sea, and central and eastern Estonia with a more continental climate. The territory was further subdivided into 36 river basins. In some studies the watershed of the Väike-Emajõgi River was studied in greater detail.

Evapotranspiration was shown to increase under all six scenarios studied. The predicted changes would affect evapotranspiration more in the cold season than in the growing season. However, the change in the magnitude is much smaller on the annual scale, as the cold season evapotranspiration constitutes only 10–13% of the annual evapotranspiration. The most significant increase was simulated using the ECHAM3-MAX scenario. In absolute values, the ECHAM3-MAX scenario predicted evapotranspiration increases of 16 mm in June and about 4 mm in January.

The modelled changes in the mean annual runoff in different basins and scenarios range from −1% to +74%. The largest increases were found for the Emajõgi River, and for a number of small river basins. An increase in total annual runoff by 20–40% (HadCM2-MID) and 30–60% (ECHAM3-MID) was modelled for the year 2100.

Seasonal dynamics of runoff were analysed for several rivers and showed the projected runoff increase in winter to have the largest impact. The maximum increase for the Emajõgi River was projected for April or May (depending on the model and scenario). Runoff maximums in spring were shown to decrease considerably in the central and western parts of Estonia. This is related to the projection that the duration of snow cover would also decrease considerably. Among the single river basins studied, the projection for the small Lõve Rive on the Saaremaa Island stands out; it showed the lowest increase in every scenario.

Groundwater recharge was shown to increase on average by 20–40% according to these simulations with a maximum increase of up to 75% increase. The ratio of the groundwater contribution to river runoff would increase from 30 to 40%. The modelling results also indicated a rise of long-term mean annual groundwater levels by about 0.5–0.8 m in northern Estonia, and 0.2–0.4 m in southern Estonia. Furthermore, considerable changes would occur in the seasonal dynamics of the groundwater regime, with rising water levels in spring and autumn. This would tend toward an earlier onset of flooding.

Finland

As outlined by Bergström et al. (2003), three major studies concerning anthropogenic climate change and hydrology have been conducted in Finland. The Nordic research programme on Climate Change and Energy Production (CCEP; Sælthun et al. 1998) was carried out during 1991–1996. The multidisciplinary Finnish Research Programme on Climate Change (SILMU) was carried out during 1991–1995 (SILMU 1996; Vehviläinen and Huttunen 1997) and more recently, the ILMAVA project (ILMAVA 2002). Additional studies have focused on hydrological impacts and design floods (Tuomenvirta et al. 2000).

The CCEP research programme used an anthropogenic climate change scenario based on statistically downscaled information from four different General Circulation Models. The SILMU sce-

narios were based on an intercomparison study of GCM simulation results (Räisänen 1994). For the ILMAVA project (ILMAVA 2002), two SRES scenarios (A2 and B2; Nakićenović et al. 2000) from the HadCM3 GCM were used.

All of the studies used the operational watershed models of the Finnish Environment Institute (SYKE; Vehviläinen 1994), which are based on a Finnish version of the HBV-model (Bergström 1976). All studies thus far have used the delta change approach for transferring the anthropogenic climate change signal from climate models to hydrological models and have relied on GCM models.

The drainage basins used for hydrological studies were selected to represent different regions of Finland, as shown in Fig. 3.31. Starting with the CCEP project, subbasins from southern and northern Finland were used. In the SILMU project, a similar selection of drainage basins was chosen, but larger areas in the southeast were included. For the ILMAVA project, basins producing most of Finland's hydropower were chosen.

The trend of results from the more recent ILMAVA project is similar to results from the earlier CCEP and the SILMU projects. The projected anthropogenic climate change was shown to strongly affect the seasonal distribution of runoff and other water balance terms. With increased temperature, snow cover diminishes or almost vanishes in southern Finland, and its duration becomes shorter. Frequent thawing periods result in increased occurrence of winter floods and decreased spring floods. Summers become drier due to the longer summer season, and increases occur in both evapotranspiration and lake evaporation.

There are differences between the results of these studies, as seen for changes in runoff. Annual runoff from the Kemihaara subbasin (Kemijoki basin, northern Finland) was found to increase by 2% in the CCEP project, whereas in the SILMU project essentially no annual change was found. Results from ILMAVA showed annual runoff in this sub-basin to increase by 5 to 8%. In the Oulujoki drainage basin (mideastern Finland), the CCEP project reported nearly no change in annual runoff, but results from the ILMAVA project showed an annual increase of 2 to 7%. For the Vuoksi drainage basin (south-eastern Finland), changes in annual runoff varied between −1 to +4% (CCEP), −2% (SILMU) and 0 to +8% (ILMAVA). These differences were due primarily to differences of climate scenarios, especially regarding precipitation. However, it was also found that results were quite sensitive to how evapotranspiration and lake evaporation are represented.

Results from the SILMU project also showed that changes in maximum flows for large basins with a high concentration of lakes depend strongly on the location of the site within the lake system. For upper subbasins of large basins and basins without lakes, the maximum discharge decreased by 20 to 60% due to smaller spring floods. However, maximum inflows to the central lakes of large basins increased by some 3 to 17%, as snowmelt and precipitation accumulate into these lakes during winter, when no evaporation takes place. Thus, due to increased volume accumulating in large lakes, the maximum discharge of the lakes would increase.

Germany

No specific studies were found for German basins flowing into the Baltic Sea. However, runoff from German territory is included in projections of the hydrological response for the Oder River. See related studies under Poland.

Latvia

Related studies were reported in the Third National Communication of the Republic of Latvia under the United Nations Framework Convention on Climate Change (Ministry of Environmental Protection and Regional Development 2001), BALTEX conference proceedings (Butina et al. 1998a), and Proceedings of the Second International Conference on Climate and Water (Butina et al. 1998b; Jansons and Butina 1998).

Anthropogenic climate change scenarios from the UKMO GCM transient scenario (Murphy and Mitchell 1994) and the GENESIS GCM (Thompson and Pollard 1995) scenario were used. The results of the GENESIS GCM were represented in the form of monthly corrections to meteorological parameters received from maps of low resolution (Henderson-Sellers and Hansen 1995). Doubling of the atmospheric CO_2 concentration was assumed. The climate scenario predicts a 3–3.5 °C rise in air temperature and a 20–25% increase in precipitation.

All of Latvia was included in the Third National Communication. Studies by Butina et al. (1998b) were done in the Liulupe basin (17,600 km^2), its subbasin Viesite-Sudrabkalni, and the Berze

basin. Hydrological assessments were made using the HBV hydrological model (Bergström 1995).

According to the assessment in the Third National Communication, groundwater levels in the lowest coastal zone of Riga Bay could rise by 50–70 cm. Risk of floods would increase in the lower reaches of the large rivers Liulupe, Daugava and Gauja. Rising groundwater level could cause serious problems to people living in lowlands in the coastal zone where elevation above sea level is only 0.7 to 2.0 m.

Butina et al. (1998b) reported that, due to higher temperatures, more winter precipitation would fall as rain instead of snow. The spring snowmelt would shift from April to February or even earlier. River flow would be higher during all seasons according to the GENESIS scenario, but not for the UKMO GCM scenario. The UKMO GCM transient scenario showed river flow to increase by 11% on average (ranging from −7 to +36%), while, according to the GENESIS scenario, river flow would increase on average by 83% (ranging from 55 to 120%).

Jansons and Butina (1998) used the same scenarios to investigate changes in runoff and nutrient load for the small agricultural Berze catchment. According to the GENESIS scenario, annual flow would increase by 57%, but the UKMO GCM scenario showed no significant increase in flow. Flood peaks increased by 32% with GCM GENESIS input, while the UKMO GCM scenario predicted a decrease in flood peaks. The GCM GENESIS scenario generated an increase in summer flow, whereas a moderate decrease was projected using the UKMO GCM scenario.

Lithuania

Studies were reported in Lithuania's Second National Communication under the Framework Convention on Climate Change (Ministry of the Environment 2003) and in BALTEX conference proceedings (Rimkus 2001). The National Communication used scenario results from the GFDL GCM. Rimkus used results from five GCMs over Lithuania; these were HadCM2, ECHAM4, CGCM1, GFDL-R15 and CSIRO-Mk2.

According to the GFDL model, the average summer temperature by 2050 would exceed the recent average by 1.7 °C, and the average winter temperature would be 1.2–1.3 °C higher. The summer precipitation would increase slightly until 2020 and then start decreasing in the subsequent period. The amount of summer precipitation by 2050 would be 5–6% lower than the present level, and the winter precipitation would be 5–6.5% higher.

No hydrological models were used for the assessment described in the Second National Communication; only analysis of the climate model outputs was carried out. This included assessment of possible effects over all of Lithuania. One outcome from this study was that the extensive wetlands of the country would become dryer with accelerated succession.

Rimkus (2001) used an analysis of regression links between climate variables. Data from the nearest grid points were used to assess changes in snow water equivalent in Lithuania. Two cases were analysed: 1) the mean temperature for the snow accumulation period would rise by 1.5 °C and precipitation would rise by 8 mm (as expected around the year 2040); 2) the mean temperature of the snow accumulation period would rise by 3.0 °C and precipitation would increase by 14 mm (as expected around the year 2065).

Results from Rimkus (2001) showed that maximum snow depth in Lithuania would decrease significantly under anthropogenic climate change scenarios. For the reference period 1961–1990, maximum snow water equivalent was 40 mm on average, ranging from 21 to 60 mm. Average maximum snow water equivalent would decrease to 34 mm, with temperature and precipitation increasing by 1.5 °C and 8 mm, respectively. Average maximum snow water equivalent would decrease to 28 mm, with temperature and precipitation increasing by 3.0 °C and 14 mm, respectively.

Norway

In addition to the Nordic research programme on Climate Change and Energy Production (CCEP; Sælthun et al. 1998) during 1991-1996 (see also Finland and Sweden), two national projects on anthropogenic climate change and hydrological impacts have been performed in Norway (Bergström et al. 2003). These were "Climate change and water resources" (Sælthun et al. 1990) conducted prior to CCEP, and "Climate change and energy production potential" (Roald et al. 2002; Skaugen et al. 2002; Skaugen and Tveito 2002), which was carried out during 2000–2002.

Sælthun et al. (1990) used anthropogenic climate change scenarios based on the NCAR model (Washington and Meehl 1989). No downscaling

procedure was applied. Two climate scenarios were used: one based on what was considered the most probable changes of precipitation and temperature, and one based on greater changes. As described under Finland, CCEP used an anthropogenic climate change scenario based on statistically downscaled information from four different General Circulation Models (Sælthun et al. 1998). Local and regional climate scenarios have also been studied in the RegClim project since 1997. This has focused mainly on results originating from ECHAM4/OPYC3 simulations using the IPCC IS92a scenario. Regional downscaling from both statistical techniques (Hanssen-Bauer et al. 2000, 2001; Benestad 2002a) and RCM modelling (Bjørge et al. 2000) was used.

Runoff simulations were performed with the HBV Model (Bergström 1995). Evapotranspiration was estimated according to temperature based methods developed by Sælthun et al. (1990), which were further improved in later studies (Sælthun 1996). In Sælthun et al. (1990) 7 basins were used, in Sælthun et al. (1998) 10 basins, and in Roald et al. (2002) 42 basins. These basins are distributed over all of Norway and represent different hydrological regimes. Future water balance changes for the whole of Norway were also included in Roald et al. (2002), Engen-Skaugen et al. (2005) and Roald et al. (2006).

Sælthun et al. (1990) concluded that correct modelling of evapotranspiration is important when it comes to estimating the future water balance (Fossdal and Sælthun 1993). The annual evapotranspiration increase was 40–55 mm in mountainous areas, 45–100 mm in transitional areas and 50 to 110 mm in lowland areas. The corresponding increase in annual runoff for mountainous areas was more than 750 mm. In lowland and forested inland basins, annual runoff was shown to decrease in response to increased evapotranspiration. The wettest scenario resulted in increased runoff over all of Norway, up to 15% on the west coast.

Sælthun et al. (1998) drew similar conclusions. Evapotranspiration was shown to increase due to increased summer temperature and longer snow free periods. Annual evapotranspiration would increase between 100 and 200 mm over 100 years, and precipitation would increase between 15 and 20% for the same period. An evapotranspiration increase of 100 mm would counterbalance the precipitation increase in areas where present annual precipitation is less than 700 mm. The annual runoff would therefore increase in western areas and decrease in inland areas. Results from Roald et al. (2002) showed that runoff would increase over almost all of Norway, following the same pattern as the increase in precipitation.

The scenarios in Sælthun et al. (1990) and Sælthun et al. (1998) showed a drastic change in the seasonal distribution of runoff, with increases in winter, reduced spring flood peaks with earlier occurrence and decreases in summer. The changes were mostly controlled by the effect of temperature on snow processes. The seasonal distribution would not change much in coastal regions that do not have stable snow cover under the present climate. The largest changes were shown for the lower elevations of regions that now have a stable snow cover during winter. Roald et al. (2002) showed that summer runoff would decrease and autumn runoff would increase, especially on the west coast.

Sælthun et al. (1990) concluded that melting of Norwegian glaciers would increase and the summer discharge in glacier basins would therefore increase. Most of the glaciers would also experience a negative mass balance, resulting in reduced volume. The long-term effect would be reduced summer runoff in basins that have glaciers today. However, high altitude glaciers in maritime climates with high precipitation might maintain their volume and even grow. In Roald et al. (2002), simulations suggested that glaciers would accumulate and the effect on runoff would be negative, as opposed to a state of equilibrium.

Poland

Kaczmarek et al. (1997) used data from several GCMs with their hydrological model CLIRUN (Kaczmarek 1996; Kaczmarek 1993) for studying three middle-size catchments in Poland. These were followed up by additional studies with updated models (Kaczmarek 2003; Kaczmarek 2004). De Roo and Schmuck (2002) report on studies using different incremental scenarios. The early studies by Kaczmarek focused on the Warta basin, which is the largest tributary to the Oder River. De Roo and Schmuck analysed the entire Oder basin. Later studies by Kaczmarek covered other regions of Poland.

Kaczmarek et al. (1997) noted that current (i.e. 1997) climate models did not offer the degree of watershed specific information required for hydrological modelling. Moreover, the results for river flow showed great differences depending on the

different models used (Kaczmarek 1996). Gutry-Korycka (1999) also noted that the information from GCMs was not sufficient for definite projections of the influence of warming on river flow in the second half of the 21st century. Similarly, results on hydrological drought frequency differed considerably between the models, both in magnitude and direction (Kaczmarek and Jurak 2003).

De Roo and Schmuck (2002) used the LISFLOOD Model in their studies together with seven different incremental scenarios. They looked at, 1) annual precipitation increases of 15% and 22%, 2) annual precipitation decreases of 10% and 15%, 3) an average annual temperature increase and decrease of 1 °C and 4) a combined 15% increase in precipitation and 1 °C increase in temperature. They reported that a 15% increase in precipitation showed a sharp increase in maximum discharge of 600–900 $m^3 s^{-1}$ at all major gauge locations. A decrease in precipitation by 10% resulted in a decrease of peak discharge of 430–560 $m^3 s^{-1}$. A precipitation decrease by 15% led to a decrease of peak discharge of 590–810 $m^3 s^{-1}$.

Kaczmarek (2003) studied the influence of climate change on the water balance in Poland for the period 2030-2050 using the CLIRUN3 hydrological model and two anthropogenic climate change scenarios: GFDL (warm and dry) and GISS (warm and wet). They projected a decrease in river flow and soil moisture in summer and autumn. The flood season would also shift from March–April to January–February, in accordance with results from the EU project "Impact of Climate Change on Water Resources in Europe" (from the 4th Framework Programme).

Kaczmarek (2004) stated that although it is certain that a warmer climate will accelerate the hydrological cycle, less is known about impacts at river basin levels. In the maritime parts of Europe, he reports a tendency toward increasing streamflow during winter. Furthermore, a reduction during low flow periods is expected, which could lead to increased drought frequency and, in most catchments, increased flood frequency. For Poland itself, projected flow characteristics vary between models and scenarios.

Russia

Two studies were reported in Meteorology and Hydrology (Kondratyev and Bovykin 2003; Meleshko et al. 2004), one study in Water Resources (Grigoryev and Trapeznikov 2002), and one study in an INTAS Report (Kondratyev 2001). The study performed by Meleshko et al. (2004) covers the entire Baltic Sea Basin and is summarised in Sect. 3.7.4. Kondratyev and Bovykin (2003) used climate scenarios from ECHAM4/OPYC3 calculated for the Lake Ladoga drainage basin (258,000 km^2) for the period 2001–2100 (Arpe et al. 2000; Golitsyn et al. 2002). They coupled this to a model of hydrological regimes and nutrient fluxes for the system catchment and lake. This was applied for the much smaller Lake Krasnoye and its drainage basin (168 km^2) with the help of regression equations (Kondratyev et al. 1998; Kondratyev and Bovykin 2000). For Kondratyev (2001), eight different incremental scenarios were used instead.

According to Kondratyev and Bovykin (2003), a moderate increase in river discharge was projected for Lake Krasnoye. Snow water equivalent was shown to decrease by 25–28%. Soil moisture in the watershed would increase by 7–8% in autumn and winter, and decrease by 10–18% in summer. Spring floods would start earlier. The lake level would be characterised by earlier spring maximums and a 10 cm lower water level in summer, as compared to the 1964–1984 reference period.

Results from Kondratyev (2001) summarised characteristics of annual runoff, maximum water discharge in the tributaries, soil moisture in autumn, and numerous nutrient transport variables for the Lake Krasnoye catchment. Their findings showed mean annual runoff changes from −26% to +35%, maximum runoff changes from −59% to +66% and autumn soil moisture changes from −26% to +14%.

Grigoryev and Trapeznikov (2002) used probabilistic incremental scenarios for Lake Ladoga. They applied a transfer function model with climate characteristics as input and water level in the lake as output. According to their probabilistic climate scenario, the water level in Lake Ladoga would decrease by 50 cm.

Sweden

Sweden also participated in the Nordic research programme on Climate Change and Energy Production (CCEP; Sælthun et al. 1998) during 1991–1996 (see also Finland and Norway). This resulted, among others, in a comprehensive study of evapotranspiration effects (Lindström et al. 1994). Sensitivity studies of climate change effects on hydrology were conducted in an early study of effects on river regulation (Carlsson and

Sanner 1996). From 1997 to 2003, hydrological impacts studies concerning anthropogenic climate change were mainly produced within the Swedish Regional Climate Modelling Programme (SWECLIM; Bergström et al. 2001; Gardelin et al. 2002a; Gardelin et al. 2002b; Graham et al. 2001; Andréasson et al. 2002; Andréasson et al. 2004). Most recently, hydrological impact studies were conducted within the EU PRUDENCE project (Graham et al. 2007a).

As described under Finland, the CCEP research programme used an anthropogenic climate change scenario based on statistically downscaled information. The anthropogenic climate change scenarios from SWECLIM came primarily from RCM modelling. Most simulations were based on three different GCMs, HadCM2, HadAM3H and ECHAM4/OPYC3, downscaled with the Rossby Centre regional climate models RCA (Rummukainen et al. 2001; Jones et al. 2004) and RCAO (Döscher et al. 2002). Some use of statistically downscaled scenarios was also made (Bergström et al. 2003). Earlier SWECLIM simulations were based on business as usual (BaU) emissions scenarios (Houghton et al. 1992), while more recent simulations used the SRES (A2 and B2) scenarios (Nakićenović et al. 2000).

The HBV hydrological model was used in the Swedish studies (Bergström et al. 2001; Graham et al. 2001). Particular effort was placed on developing appropriate representation of evapotranspiration processes and on the interface used for transferring anthropogenic climate change information from climate models to hydrological models. Most studies to date used the delta change approach for transferring the signal of anthropogenic climate change to hydrological models. The PRUDENCE studies also investigated the use of precipitation scaling.

Six test basins representing different climate and hydrological regimes in Sweden were initially chosen for impacts analysis within both CCEP and SWECLIM. They were later supplemented by two additional basins, the Lule River Basin, representing a high degree of river regulation, and Lake Vänern, the basin containing Sweden's largest lake. Limited analyses to address soil frost and groundwater dynamics were also made in the Svartberget experimental forest site in northern Sweden. In the last year of SWECLIM, a hydrological model was developed to conduct hydrological change studies over all of Sweden using some 1000 subbasins.

Results from the HBV model using eight different regional climate simulations from RCA1 and four simulations from RCAO were reported by Andréasson et al. (2004). A general tendency is the shift in the runoff regime towards decreasing spring flood peaks and increasing autumn and winter flows. Mean annual change in runoff from the simulations shows increasing runoff in northern basins and decreasing runoff in southern basins. In the northernmost basin (Suorva) there is little impact on the magnitude of spring runoff as snow accumulation is less affected in this region. However, the timing of snowmelt is affected in all basins. Summer flows are severely reduced in the two southernmost basins, Blankaström and Torsebro.

The more recent RCAO scenario results generally show higher runoff during winter and lower spring runoff than results from the earlier RCA1 scenarios. The relative range of changed runoff between different simulations is larger towards the south of the country. This may be explained partly by increasing rates of projected evapotranspiration further south and associated uncertainty in modelling changes to future evapotranspiration. For a majority of the basins, the RCA1-HadCM2 simulations show greater impact on runoff than for RCA1-ECHAM4/OPYC3 simulations. Regarding RCAO simulations, impacts driven by ECHAM/OPYC3 are generally larger than those driven by HadAM3H.

Attempts to make some assessment of extreme flows were included in Bergström et al. (2001), Gardelin et al. (2002a) and Andréasson et al. (2004). These papers present changes in 100-year flood events obtained from hydrological modelling and frequency analysis. They report a decrease in the frequency of high spring floods and an increase in the frequency of flooding events for autumn and winter in many basins. However, such conclusions are subject to great uncertainty as the delta change approach used for these studies does not provide good representation of changes in variability coming from the climate models.

3.7.4 Baltic Sea Basinwide Hydrological Assessment

Studies addressing the hydrological response to anthropogenic climate change specifically for the Baltic Sea Basin are not numerous. On a global scale, IPCC (2001b) presented hydrological modelling results for all continents. On a Euro-

pean scale, Arnell (1999), Strzepek and Yates (1997), Lehner et al. (2001) and Meleshko et al. (2004) presented hydrological modelling results that include the Baltic Sea Basin. On regional scales, Graham (1999b) presented early results that specifically address the Baltic Sea Basin. These were updated to include improved methods and newer RCM scenarios in Graham (2004) and to include an ensemble of RCM models in Graham et al. (2007b). Finally, both Hagemann and Jacob (2007) and Graham et al. (2007b) present results for the Baltic Sea Basin using runoff routing methods. A summary of results from these studies follows below. All used the delta change approach, unless otherwise noted.

3.7.4.1 *Projected Changes in Runoff*

Included in the global scale results presented by the IPCC are maps showing change in annual runoff at the end of the 21st century from macroscale hydrological modelling. Results using two different GCM simulations (HadCM2, HadCM3) are shown there in mm yr^{-1} (IPCC 2001b, Fig. TS-3). Although the two simulations show contradictory trends for other regions around the globe, results for the Baltic Sea Basin are qualitatively similar. The trend shown is for increased annual runoff in the north of the basin and decreased runoff in the south. Magnitudes range from up to +150 mm yr^{-1} in the north to −150 mm yr^{-1} in the south. For comparison, the observed total mean annual runoff to the Baltic Sea is some 280 mm yr^{-1} (Bergström and Carlsson 1994). Close examination of the IPCC maps, however, reveals that the location where projected runoff change goes from positive to negative varies considerably between the two simulations. For instance, in Finland for simulations using HadCM2 a positive change in runoff is shown, while for simulations using HadCM3 much of the country is shown with a negative change.

More detail is found in Arnell (1999), where the results from macroscale hydrological modelling using four different GCM simulations (based on HadCM2 and CCC) are shown. In this case, the projected future climate is the middle of the 21st century, the 2050s. Here again, an increase in runoff is simulated for the northern areas of the Baltic Sea Basin and a decrease is simulated for the southern areas. Results are expressed in terms of percent change in annual runoff and range from some +50% to −25% for the Baltic Sea Basin. Although Arnell (1999) comments that there are large areas of agreement over Europe between the simulations, he specifically notes that discrepancies are high in the eastern Baltic region. Results for this area show a reduction of runoff by up to 20% in one simulation and an increase of over 25% in another simulation. Arnell (1999) also notes that by the 2050s snow cover at the end of March will have disappeared across eastern Poland, Belarus, Ukraine and the Baltic sea coast. This is broadly comparable to more recent findings from RCMs (see Sect. 3.5.2.4).

Meleshko et al. (2004) used results from seven GCMs (CGCM2, CSIRO-Mk2, CSM1.4, ECHAM4/OPYC3, GFDL-R30-c, HadCM3 and PCM). They applied a simple balance equation to define annual discharge for large river basins from GCM inputs of precipitation and evapotranspiration. This was done for the entire Baltic Sea Basin. Projections using the ensemble of seven GCMs showed an overall increase in total river runoff to the Baltic Sea of 1.9% for the period 2041–2060 and 5.7% for the period 2080–2099.

Graham (1999b) presented results using the HBV-Baltic hydrological model (Graham 1999a) together with climate model simulations from the RCA Model (Rummukainen et al. 1998). HBV-Baltic is a large-scale hydrological modelling application that covers the total Baltic Sea Basin up to its outflow into Öresund and the Danish Belts, as shown in Fig. 3.32. Three RCM simulations representing "business as usual" GHG emissions scenarios with forcing from two different GCM simulations (HadCM2, ECHAM4/OPYC3) were presented. Two of these simulations used a horizontal resolution of 88 km and were referred to as RCA88-H and RCA88-E for HadCM2 and ECHAM4/OPYC3 forcing, respectively. The effects from the RCA88-E scenario simulations were quite different to those from RCA88-H, particularly in the southern Baltic river basins. Total river discharge to the Baltic Sea decreased considerably for the RCA88-E simulation but increased somewhat for the RCA88-H simulation. These early simulations were based on 10-year time periods for the present compared to 10-year time periods for the future, which are relatively short in terms of representing interannual variability.

In Graham (2004) and Graham et al. (2007b), a number of additional hydrological response simulations were carried out using HBV-Baltic. These used 30-year time periods to represent both the future climate and the control climate (present

Fig. 3.32. Basin boundaries for HBV-Baltic. The five main Baltic Sea drainage basins are shown with thick lines (adapted from Graham 1999a)

climate). Graham et al. (2007b) used many of the RCM simulations from PRUDENCE (Christensen et al. 2007; see Sect. 3.5.1.2). This showed the ensemble of RCMs driven by the same GCM with the same GHG emissions scenario to result in a range of potential outcomes that follow similar mean trends. Based on the SRES-A2 emissions scenario (see Annex 6), Fig. 3.33 shows results of river discharge summarised as total inflows to the five main subregional Baltic Sea drainage basins and for the total Baltic Sea Basin. Results using nine RCM simulations with global forcing from HadAM3H (referred to as the common PRUDENCE experiment in Sect. 3.5.2) are shown in the left plot of the figure. Results using 2 RCM simulations with global forcing from ECHAM4/OPYC3 are shown in the right plot of the figure.

General trends in the north show increases in wintertime river flow coupled with somewhat lower and earlier springtime peak flows. This reflects the substantial changes that warmer temperatures will inflict on the snow regime in the north. Trends in the south show more pronounced effects on summertime river flow. River flow to the Gulf of Finland exhibits a combination of these effects, depending on which simulations one examines, even though these flows are highly dictated by the outflow from Lake Ladoga. River flow to the total Baltic Sea Basin is an integration of the combined effects to the five main sub-drainage basins.

The range of outcomes helps to characterise the uncertainty contributed from using different RCMs. As shown in Fig. 3.33 for RCMs driven by HadAM3H, this range is fairly narrow for much of the year. However, during late summer and autumn months larger deviations occur, which is most obvious in the plot for the total Baltic Sea Basin. Although it is not easily seen from the plots, much of this deviation originates from the Gulf of Finland and other eastern drainage basins.

According to Kjellström and Ruosteenoja (2007), the climate change signal for precipitation in this area is affected by different approaches in the RCMs for representing feedback from the

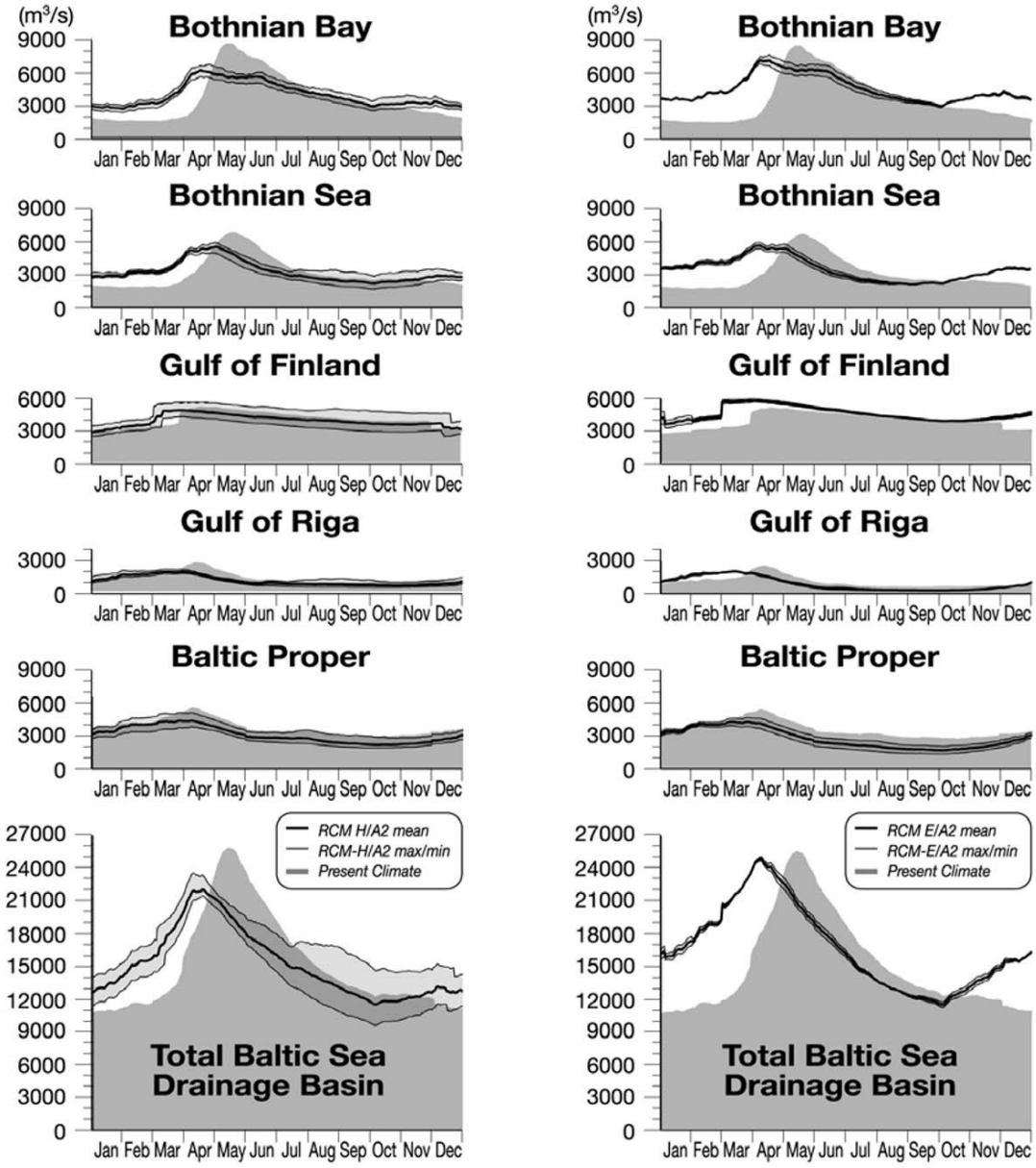

Fig. 3.33. Mean river discharge from HBV-Baltic using the delta change approach for RCM-A2 scenarios at ~ 50 km resolution, driven by global forcing from HadAM3H (*left*) and ECHAM4/OPYC3 (*right*). The plots summarise results using nine different RCMs with HadAM3H forcing and two RCMs with ECHAM4/OPYC3. The scenarios represent future climate for the period 2071–2100 compared to the control period 1961–1990 (adapted from Graham et al. 2007b)

Baltic Sea itself. In particular, anomalously high sea surface temperatures can have an effect (SSTs; see also Sect. 3.5.2.2). One of the two models that shows the greatest increase in river flow from the eastern side of the Baltic sea Basin is also the model that Kjellström and Ruosteenoja (2007) show to produce the greatest precipitation change in that region due to anomalous SSTs.

Effects on modelled river discharge from using different GCMs to drive the RCMs are seen by comparing the left and right plots in Fig. 3.33, although not as many simulations were available using ECHAM4/OPYC3. According to these results, forcing with ECHAM4/OPYC3 produced a considerably different river discharge response than simulations with forcing from HadAM3H.

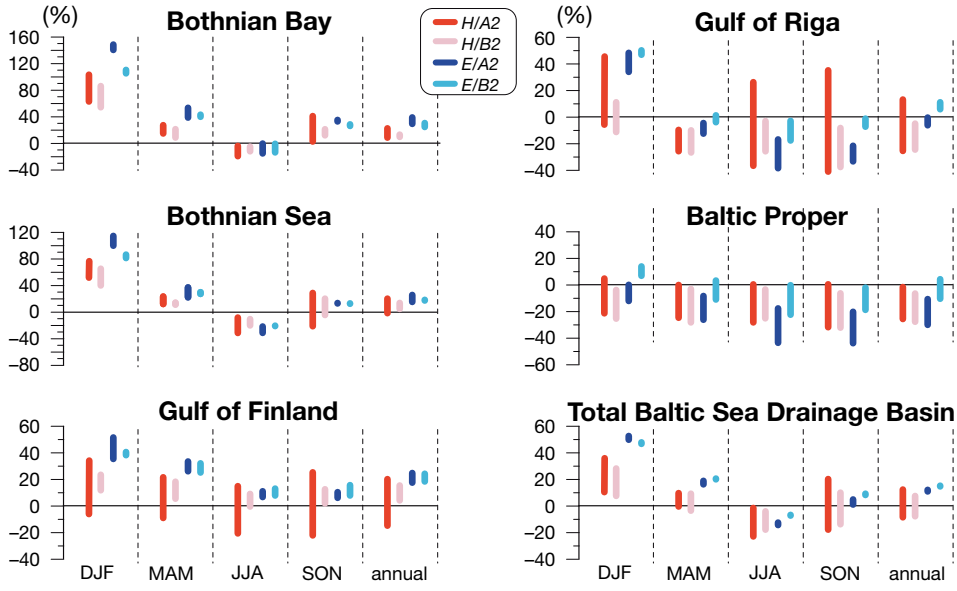

Fig. 3.34. Modelled percent volume change in river discharge from HBV-Baltic simulations using RCM scenarios for the period 2071–2100 compared to the control period 1961–1990. This is summarised by season for the five main Baltic Sea drainage basins (Fig. 3.32); December, January, February (DJF); March, April, May (MAM); June, July, August (JJA), and September, October, November (SON). Each bar represents the range of results between the simulations performed for SRES-A2 forced by HadAM3H (H/A2, 9 simulations), SRES-B2 forced by HadAM3H (H/B2, 3 simulations), SRES-A2 forced by ECHAM4/OPYC3 (E/A2, 2 simulations), and SRES-B2 forced by ECHAM4/OPYC3 (E/B2, 2 simulations) (created with results from Graham 2004 and Graham et al. 2007b)

River discharge in general tends to be higher for the ECHAM4/OPYC3 driven simulations. Such differences were also reported by Graham (2004), where simulations from the SRES-B2 scenarios were presented as well. There it was observed that the GCM model used for boundary conditions has as much impact on total river flow as the emissions scenarios used.

Changes in river flow to the Baltic Sea are further summarised in Fig. 3.34 as percent volume change per season. This figure includes results based on RCMs using two different GHG emissions scenarios (SRES-A2, SRES-B2) and two different GCMs (HadAM3H, ECHAM4/OPYC3). The length of each bar in the figure shows the range of results for each case, although the number of simulations varies between the cases (see figure caption for detail). Qualitatively, there are overall similarities between the different simulations. In many instances, the results tend to fall within the same sign (positive or negative) for the given seasons. However, the degree of similarity varies among the different subregions. The considerable differences obtained by using different GCMs are also apparent in these plots (e.g. compare H/A2 results to E/A2 results). This figure also shows that the largest range of uncertainty with respect to the relative change in volume occurs in the Gulf of Riga drainage basin, as evidenced by numerous long bars.

Two runoff routing schemes have been applied to the Baltic Sea Basin to date. These are the RCroute scheme (Graham 2002; Graham et al. 2007b) and the HD Model (Hagemann and Dümenil 1999; Graham et al. 2007b; Hagemann and Jacob 2007). Both of these were used to produce routed river flow directly from RCM results. As stated above, hydrological response studies from river routing techniques are highly influenced by RCM biases. Therefore they are best used when converted to percent change in river discharge, as done in the reported literature. It was reported that despite large differences in individual RCM simulations, the overall signal of the ensemble mean response was in agreement between RCroute and the HD Model (Graham et al. 2007b). These were also qualitatively in agreement with the various results using HBV-Baltic as presented above.

However, choosing a single RCM from this group of results as a basis for further impact studies would result in quite different answers depending on the RCM used.

There is a notable difference between the two river routing approaches in that RCroute uses runoff generation directly from the RCMs and the HD Model performs its own re-partitioning of RCM precipitation into runoff and evapotranspiration (Hagemann and Jacob 2007). This is a likely explanation to why results from the HD Model show a narrower range of uncertainty around the mean than those from RCroute, as it effectively filters out some of the biases in precipitation partitioning in the RCMs.

3.7.4.2 *Projected Changes in Evapotranspiration*

Although evapotranspiration is a critical component of the water balance, comprehensive anthropogenic climate change effects on this variable are little reported for the Baltic Sea Basin. One reason for this is that there is a large amount of uncertainty associated with evapotranspiration and projected future climates (Bergström et al. 2001).

Hydrological studies typically include calculation of their own estimates of evapotranspiration, both for the present climate and for future climates. This has shown to produce reasonable estimates for present climates as calibration can be performed against observations of river flow. However, using the same calibrated evapotranspiration parameterisations for the future can be suspect, particularly for temperature based methods.

For this reason, delta change techniques have come into use for estimating evapotranspiration as well (Andréasson et al. 2004; Lenderink et al. 2007). There are various ways to perform such estimates, but a main objective is that the annual percent change in evapotranspiration matches the annual percent change as simulated by climate models, while preserving the water balance in the hydrological simulations. This approach was applied by Graham (2004); estimates of future change in evapotranspiration from four simulations for the Baltic Sea Basin are presented from that work in Table 3.3.

3.7.5 Synthesis of Projected Future Hydrological Changes

Many different studies using numerous models and approaches to evaluating projections of hydrological change within the Baltic Sea Basin are summarised above. The studies were conducted on a broad range of scales, using different levels of detail and different future scenario simulations. Although it is difficult to assemble such an array of results into definite conclusions, there are common signals and similarities shown. A fundamental conclusion is that the assumed projected future anthropogenic climate changes provide the greatest source of uncertainty for projected future hydrological changes.

Some robust findings are that snow and cold weather processes were shown to be sensitive to anthropogenic climate change throughout the Baltic Sea Basin. Warmer temperatures will impact greatly on snowpack volumes and duration, resulting in considerable impact to timing of runoff. Simultaneous increases and/or decreases in precipitation will strongly affect corresponding runoff volumes. However, the response of evapotranspiration is a key process in determining how runoff volumes will change and how groundwater levels will in turn be affected.

Further conclusions are that there will be a north–south gradient in how projected future hydrological changes occur over the Baltic Sea Basin, and effects during cold months show larger relative change than for warm months. According to analyses using an ensemble of RCM anthropogenic climate change scenarios, the following concluding remarks were made by Graham et al. (2007b) for scenario simulations for the period 2071–2100 compared to control simulations for the period 1961–1990.

- On average for the total basin, summer river flows show a decrease of as much as 22%, while winter flows show an increase of up to 54%.
- On the large scale, annual river flows show an increase in the northernmost catchments of the Baltic Sea Basin, while the southernmost catchments show a decrease.
- The occurrence of medium to high river flow events shows a higher frequency.
- High flow events show no pronounced increase in magnitude on the large scale.
- The greatest range of variation in flow due to different RCMs occurs during summer to autumn.

The authors point out, however, that there are deficiencies in the methods used for performing hydrological response studies. Although the delta change approach may provide usable estimates of mean changes, representation of changes to ex-

Table 3.3. Mean annual evapotranspiration change in percent estimated from four anthropogenic climate change scenarios simulated with the RCAO Model. This is the difference between the scenario period 2071–2100 and the control period 1961–1990. These are summarised for the five main Baltic Sea drainage basins (Fig. 3.32) and the total Baltic Sea Basin. H/A2, H/B2, E/A2 and E/B2 are simulation descriptors for the HadAM3H and ECHAM4/OPYC3 GCMs with SRES-A2 and SRES-B2 scenarios, respectively (adapted from Graham 2004)

	Bothnian Bay Basin	Bothnian Sea Basin	Gulf of Finland Basin	Gulf of Riga Basin	Baltic Proper Basin	Total Baltic Sea Basin
RCAO-H/A2	23%	19%	19%	15%	11%	16%
RCAO-H/B2	13%	11%	12%	10%	6%	10%
RCAO-E/A2	20%	24%	22%	19%	15%	19%
RCAO-E/B2	15%	17%	17%	16%	13%	15%

treme events is inadequate. Using methods incorporating a precipitation bias correction approach with RCM simulations versus the delta approach resulted in higher peak flows for the projected future climate. However, there are considerable differences in the performance between different RCMs, not only with regard to precipitation, but also temperature (see Sect. 3.5). Such differences can vary regionally as well. It is difficult to establish uniform procedures for scaling such critical variables and the question also arises as to how much scaling is reasonable without adversely affecting the original anthropogenic climate change signal. Furthermore, river flow routing of RCM-generated runoff can be used to analyse both model performance and scenario trends, but regard must be given to the precipitation biases that most RCMs show.

3.8 Projections of Future Changes in the Baltic Sea

3.8.1 Oceanographic Models and Anthropogenic Climate Change

The Baltic Sea is located in the transition zone between continental and maritime climate regimes. Under present climate conditions (see e.g. Annex 1.1 and Sect. 2.3), about half of the Baltic Sea is ice-covered in winter. Baltic Sea salinity is controlled by river runoff, net precipitation, and water exchange with the North Sea. Regional sea surface temperature varies with season but is also affected by the ocean circulation. The region is also characterised by land uplift and subsidence, which exert long-term effects on the coastal geometry. Anthropogenic climate change will likely affect regional sea ice and water temperature, as well as sea level and, possibly, salinity and oxygen conditions in the Baltic Sea deeps.

These aspects have been studied thoroughly using four regional coupled atmosphere–ocean modelling projections (Döscher and Meier 2004; Meier et al. 2004a) based on HadAM3H and ECHAM4/OPYC3 GCM driven simulations from RCAO, each forced by both B2 and A2 emission scenarios (cf. Table 3.1). In addition, so-called delta-change experiments have been performed (Meier 2006). In these, the 30-year monthly mean changes of the forcing functions for the Baltic Sea model RCO were calculated from the time slice experiments. These changes were added to reconstructed atmospheric surface fields and runoff for the period 1902–1998 (Kauker and Meier 2003). The results of both RCAO and RCO are compared with other studies on anthropogenic climate change in the Baltic Sea.

3.8.2 Projected Changes in Sea Ice

Since anthropogenic climate change might affect the ice season in the Baltic Sea considerably, the Baltic Sea ice in changing climate has been investigated in several studies (e.g. Tinz 1996, 1998; Haapala and Leppäranta 1997; Omstedt et al. 2000; Haapala et al. 2001; Meier 2002b, 2006; Meier et al. 2004a). These authors have applied different methods, based upon either statistical or dynamical downscaling of GCM results. The models used vary in complexity.

The main conclusion from these studies is that the projected decrease of ice cover over the next 100 years is dramatic, independent of the applied models or scenarios. For instance, Haapala et al. (2001) applied two different coupled ice–ocean models for the Baltic Sea using the same atmospheric forcing. They found that overall the simulated changes of quantities such as ice extent and ice thickness, as well as the interannual variations of these variables, were fairly similar in both mod-

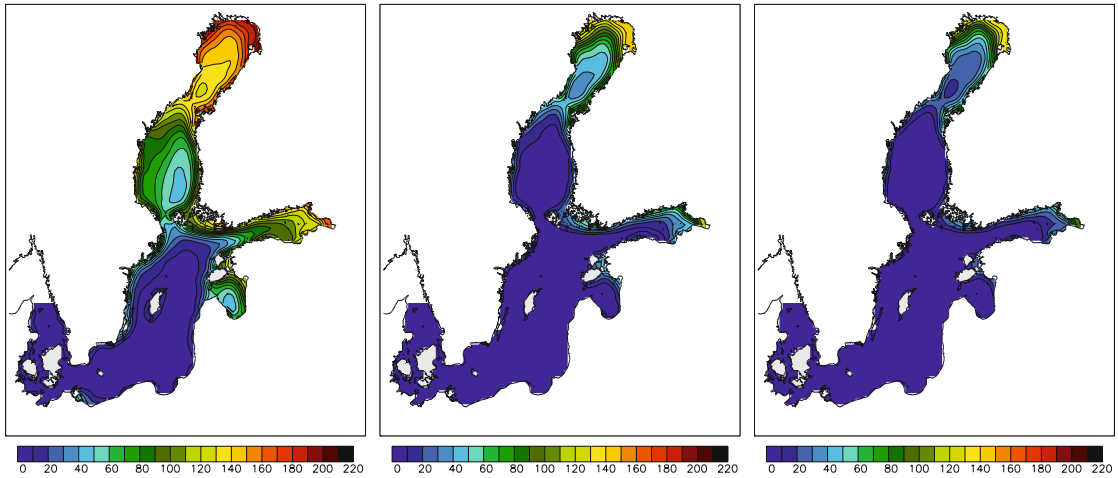

Fig. 3.35. Mean number of ice days averaged for regional downscaling simulations of HadAM3H and ECHAM4/OPYC3: control (*left panel*), B2 scenario (*middle panel*), and A2 scenario (*right panel*) (adapted from Meier et al. 2004a)

els. However, looking in more detail, differences were also reported, such as the spatial distributions of ice thickness.

RCAO results suggest that the Baltic Sea ice extent may decrease by 57 or 71% towards the end of the 21st century in the B2 and A2 scenarios, respectively (Meier et al. 2004a). The Bothnian Sea, large areas of the Gulf of Finland and Gulf of Riga, and the outer parts of the south-western archipelago of Finland would become ice-free in the mean. The length of the ice season would decrease by 1–2 months in the northern parts and 2–3 months in the central parts of the Baltic Sea (Fig. 3.35).

None of the simulated winters in 2071–2100 are completely ice-free due to a non-linear sensitivity of the simulated sea ice cover on the winter mean air temperature (Fig. 3.36). Severe ice winters are projected to be more sensitive to anthropogenic climate change than mild ice winters. These results are in accordance with earlier studies based on uncoupled ice-ocean modelling (Meier 2002b).

However, based upon the variability of the entire 20th century, an ice-free winter was found assuming changes of atmospheric surface variables corresponding to an A2 scenario (Meier 2006). Using the process-oriented PROBE-Baltic model and results from the first simulations with the RCA model, Omstedt et al. (2000) found that the scenario simulation indicates a maximum ice extent close to the observed long-term minimum and that there is no ice during 3 out of 10 winters. Miętus et al. (2004) also report that the ice season is likely to become shorter due to higher sea water temperature.

In addition to scenarios, sensitivity studies were performed (e.g. Omstedt and Nyberg 1996; Omstedt et al. 1997; Meier 2002b, 2006). These studies show that the summer heat content may affect only the subsequent ice season. The time scale of the upper layer heat content amounts to a few months at the maximum. The sensitivity of ice cover and ice thickness to changes in salinity is relatively small.

3.8.3 Projected Changes in Sea Surface Temperature and Surface Heat Fluxes

The ensemble average annual mean sea surface temperature (SST) increases by 2.9 °C from 1961–1990 to 2071–2100. The ensemble consists of the four RCAO scenario simulations described by Räisänen et al. (2004). The SST increase is strongest in May and June (Fig. 3.37), and in the southern and central Baltic Sea (Döscher and Meier 2004). Details of the spatial SST patterns in the scenarios can partly be explained by sea ice reduction. In the northern basins the future year-to-year variability of mean SST was projected to increase because of melting ice. Results based on coupled and uncoupled ocean simulations are rather similar, as seen for example in Fig. 3.37 (Meier 2006).

All RCAO scenarios showed changes in the seasonal cycle of atmosphere–to–ocean heat transfer (Döscher and Meier 2004). There is a reduced heat

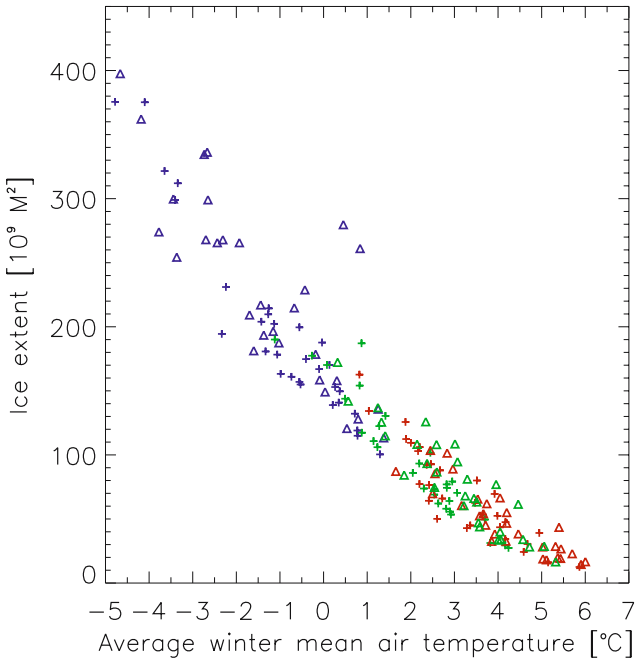

Fig. 3.36. Scatterplot of annual maximum ice extent in the Baltic Sea and winter mean (December through February) air temperature at Stockholm: RCAO-H (*plus signs*), RCAO-E (*triangles*), control (*blue*), B2 (*green*), and A2 (*red*). RCAO-H and RCAO-E denote simulations using RCAO with lateral boundary data from HadAM3H and ECHAM4/OPYC3, respectively (from Meier et al. 2004a)

loss in autumn, increased heat uptake in spring, and reduced heat uptake in summer. The overall heat budget change is characterised by increased solar radiation (due to reduced cloudiness and reduced surface albedo in winter), which is balanced by changes in the remaining heat flux components, i.e. net longwave radiation (out of the ocean) is increased, sensible heat flux (out of the ocean) is reduced, and latent heat flux (out of the ocean) is increased.

To date, dynamical downscaling experiments of Baltic Sea climate were only performed for limited periods. As the time slices were too short to properly spin up initial stratification for future climate, Meier (2002a) investigated the uncertainty of SST scenarios caused by the unknown future salinity, comparing scenarios with and without spin-up. He found that area mean SST changes do not differ much and that horizontal anomaly patterns are similar. However, some local differences were not negligible. The largest positive and negative differences were found in winter and summer, respectively, both in the Bothnian Bay.

Sensitivity studies showed that the heat content of the Baltic Sea is much more sensitive to changes in the wind forcing than the heat content of the North Sea (Schrum and Backhaus 1999). However, the opposite is true for the heat flux from the water to the atmosphere during autumn, because advective and atmospheric heat flux changes are working in the same direction in the Baltic Sea but in opposite directions in the North Sea.

3.8.4 Projected Changes in Sea Level and Wind Waves

In the following, scenarios of mean sea level and storm surges are discussed separately, because many studies focus only on mean sea level changes.

Sea level change is not expected to be geographically uniform in the Baltic Sea, so information about its distribution is needed for the assessments of the impact on coastal regions. It is therefore important to analyse the long-term trend in changes of sea level, to study the variability of annual mean sea level in regions of interest, and to assess the importance of the corresponding meteorological and oceanographic parameters, especially wind distributions, as well as air and water temperatures.

Since the end of the 19$^{\text{th}}$ century a possibly anthropogenic climate change related eustatic sea

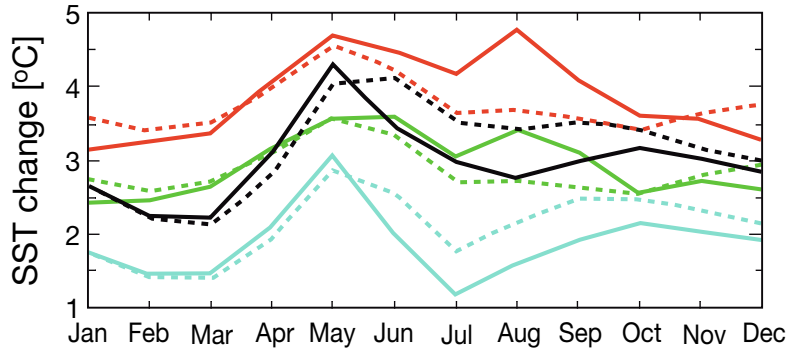

Fig. 3.37. Mean annual cycle of monthly sea surface temperature change: RCAO-H/B2 (*blue solid line*), RCAO-H/A2 (*black solid line*), RCAO-E/B2 (*green solid line*), and RCAO-E/A2 (*red solid line*). Dashed lines denote the corresponding RCO scenarios (adapted from Meier 2006)

level rise of about 1 mm yr^{-1} has been observed at the Swedish station Stockholm (Ekman 1988). Other long-term sea level records indicate similar trends (Church et al. 2001; Sect. 2.3.2).

Utilising different methods, several studies suggest an accelerated sea level rise by the end of the 21st century. For instance, using a statistical downscaling method Heyen et al. (1996) found a slight increase of Baltic sea level anomalies in winter when air pressure from a GCM greenhouse experiment is downscaled. It was found that a global mean sea level rise of 50 cm from 1990 to 2080 would lead to a sea level rise of 33–46 cm in Danish waters (Fenger et al. 2001).

It can be expected that by the year 2100 many regions currently experiencing a relative fall in sea level will instead have a rising relative sea level (Fenger et al. 2001). Johansson et al. (2004) calculated mean sea level scenarios for the 21st century at the Finnish coast. They considered land uplift, the projected global average sea level rise and the projected trends of the leading sea level pressure component in GCM scenarios. The latter was used to estimate changes of the water balance associated with changes of the NAO.

Johansson et al. (2004) concluded that the past trend of decreasing mean sea level in the Gulf of Finland (Sect. 2.3.2) will not continue in the future because the accelerated global average sea level rise will balance the land uplift. Indeed, land uplift and the global average sea level rise, according to Church et al. (2001), seem to be the dominant contributions to the future changes of mean sea level in the Baltic Sea (Meier et al. 2004b).

Model studies concerning future sea levels have been carried out as well. The local hydrodynamically driven sea level change component in the semi-enclosed sub-basins of the Estonian coastal sea due to changes in wind climate was analysed on the basis of sensitivity and scenario runs of a 2D hydrodynamic model (Suursaar et al. 2006). It was demonstrated that every change in long-term wind regime (e.g. in average wind speed, variability or directional distribution) has an effect on the established sea level regime; the effect is different along the coastline, and it depends on coastline configuration. Following the observed trend towards an increase in atmospheric westerlies, the hydrodynamic model simulations predicted an increase of up to 5–6 cm in annual means in some windward bays of the Gulf of Riga, if the average wind speed increases by 1–2 m s^{-1}. This local sea level rise component could be up to 9–11 cm in winter months, while in summer a sea level rise is unlikely. Further enhancement of the seasonal signal in sea level variations in the form of lower return periods for extreme sea level events is anticipated.

In dynamical downscaling experiments for the entire Baltic Sea performed at the Rossby Centre using either HadCM2 or ECHAM4/OPYC3, increased winter mean sea levels were found mainly in the gulfs (Meier 2001; Meier et al. 2004b). These changes follow approximately the wind speed changes averaged over the Baltic Sea surface (see e.g. Räisänen et al. 2004).

However, compared to land uplift and the global average sea level rise, wind induced seasonal sea level changes may be smaller. The downscaling experiments indicate that in the future climate the risk of coastal inundation may be largest in the eastern and southern parts of the Baltic Sea

(Meier et al. 2004b). This agrees with Miętus et al. (2004), who project a Baltic sea level rise of 33–125 cm in the 21st century (75 cm on average) at the Polish coast due to global sea level rise (Church et al. 2001) and changes in atmospheric circulation patterns.

In the scenarios there is no overall agreement whether the intensity or frequency of storm surges will increase in future climate in addition to the mean sea level rise. Using statistical downscaling, Baerens and Hupfer (1999) found that storm surges at the German Baltic Sea coast will not change significantly.

However, regional wind changes could have additional impact on surge heights (Meier 2006). For instance, the 100-year surge in the Gulf of Riga could change from the present 2 m to a future 1.9–3.3 m relative to the mean sea level for the period 1903–1998 (Fig. 3.38). The future range comes from using different scenarios. Although modelled wind speed changes are rather uniform with similar percent changes in mean and extreme wind speeds (Räisänen et al. 2004), extreme sea levels will increase significantly more than the mean sea level (Meier et al. 2004b; Meier 2006).

Miętus (1999) studied an ECHAM3 time-slice experiment using statistical downscaling (under doubled CO_2-concentration as compared to the late 1980s) and found no statistically significant changes in mean wave height but an increase in wave height range (see also Miętus 2000). Increased wind speed variability and increased occurrence of strong and very strong winds were also projected. More frequent north-western and south-western wind may increase the amount of water in the Baltic Sea at the Polish coast and change the gradient of the water surface. This would also lead to a sea level rise of about 0.07–0.09 cm year^{-1} at the Polish coast as well as to increased wave amplitudes and higher levels of storm surges. Increased sea level variability is projected, most notably at the eastern part of the coast. Another approach, using ECHAM1-LSG and transfer functions and a CO_2-trebling scenario for the late 2060s, also shows a clear increase in sea level (Miętus 1999).

Several studies have focused on the assessment of the impact of rising mean sea level and increased storm surge frequency on coastal processes like erosion and sediment transport. For instance, Orviku et al. (2003) concluded that the most marked coastal changes in Estonia result from a combination of strong storms, high sea levels induced by storm surges, ice free seas and unfrozen sediments, all of which enhance erosion and transport of sediments above the mean sea level and inland relative to the mean coastline. Kont et al. (2003) selected seven case study areas characterising all shore types of Estonia for sea level rise vulnerability and adaptation assessment. According to their scenarios the longest coastline section recession (6.4 km) would occur on the western coast of the Estonian mainland. Meier et al. (2006a) combined the results of calculated sea level changes in the Baltic Sea with scenarios of global average sea level rise, land uplift and digital elevation models to estimate flood prone areas in future climate. Regional and local maps of flood prone areas can serve as decision support for spatial planning. The planning of cities located at the eastern and south-eastern coasts of the Baltic proper, the Gulf of Riga and the Gulf of Finland would be especially affected.

Using surface winds from the Rossby Centre scenarios and a simplified wave model, scenario simulations of the wave climate have been performed (Meier et al. 2006a). Meier et al. (2006a) found that the annual mean significant wave height and the 90th percentile may increase by about 0–0.4 and 0–0.5 m, respectively. In all scenarios performed, the largest increases were found in the Gulf of Bothnia and in the eastern Gotland Sea when lateral boundary data from ECHAM4/OPYC3 were applied.

3.8.5 Projected Changes in Salinity and Vertical Overturning Circulation

The long spin-up time and the positive bias of precipitation and runoff in many control simulations of state-of-the-art regional climate models (cf. Sects. 3.5 and 3.7) make it difficult to perform projections for salinity. In several studies, future stratification was spun up in long simulations. Omstedt et al. (2000) and Meier (2002a) carried out 100-year long scenario simulations using the repeated atmospheric forcing of a time slice experiment.

Assuming that the variability of the 20th century will not change, 100-year long delta-change experiments were performed by Meier (2006). Thereby, the negative impact of the positive bias of the freshwater inflow is avoided. However, it was assumed there that the hydrological changes are large compared to the model biases, which is actually not the case.

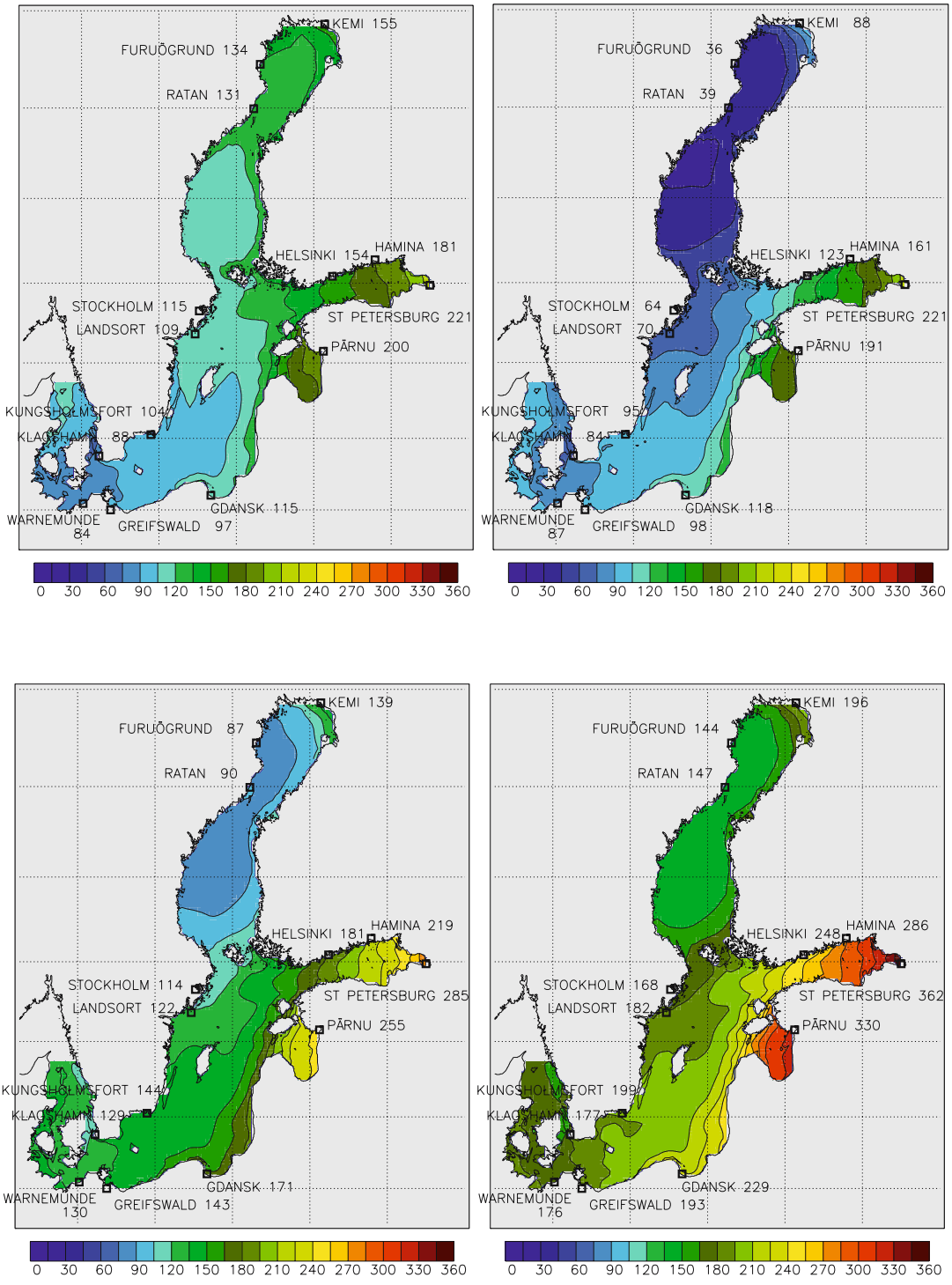

Fig. 3.38. 100-year surge (*in cm*) of the hindcast experiment using RCO (*upper left panel*) relative to the mean sea level for the period 1903–1998 and 3 selected regional scenarios of the 100-year surge (*in cm*): "lower case" scenario (RCO-H/B2) with a global average sea level rise of 9 cm (*upper right panel*), "ensemble average" scenario with a global average sea level rise of 48 cm (*lower left panel*), and "higher case" scenario (RCO-E/A2) with a global average sea level rise of 88 cm (*lower right panel*) (from Meier 2006)

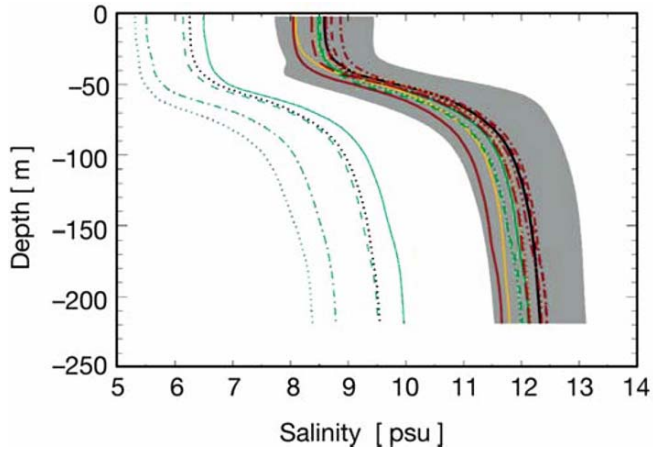

Fig. 3.39. Median profiles of salinity at Gotland Deep for 16 future climate projections from RCO for the period 2071–2100 (*colored lines*) and for the present climate for the period 1961–1990 (*black solid line, shaded areas indicate the ±2 standard deviation band calculated from two-daily values for 1903–1998*). The projections include A2 and B2 emissions scenarios from 7 different RCMs driven by 5 GCMs. Effects of both wind and freshwater inflow changes are included. A detailed discussion of salinity biases of the RCO model is given by Meier (2006) (from Meier et al. 2006b)

In projections performed at the Rossby Centre (Räisänen et al. 2004) the total mean annual river flow to the Baltic Sea changes between −2 and +15% of present-day flow (Graham 2004). In some of the scenarios, the monthly mean wind speed over sea increases, especially in winter and spring, up to 30%. Both increased freshwater inflow and increased mean wind speeds could cause the Baltic Sea to drift into a new state with significantly lower salinity (Fig. 3.39).

However, even with the highest projected freshwater inflow, the Baltic Sea will not be transformed into a freshwater sea, because the relationship between freshwater supply and average salinity of the final steady-state is non-linear (Meier and Kauker 2003b). A pronounced halocline would still be expected to remain and separate the upper and lower layers in the Baltic Proper, limiting the impact of direct wind-induced mixing to the surface layer. Although salinity in the entire Baltic Sea might be significantly lower at the end of the 21st century, stability and deep water ventilation will very likely change only slightly (Fig. 3.40) because only the changing wind-induced mixing alters vertical and horizontal gradients of density on time scales longer than 20 years (Meier 2006).

Sixteen salinity projections were performed by Meier et al. (2006b) using seven RCMs, five driving global models and two emissions scenarios (Fig. 3.39). These results show mean salinity change by the end of the 21st century (2071–2100) to range between +4 and −45%, although the positive change is not statistically significant. This substantial range in results is mainly due to differences in precipitation and wind speed changes in the Baltic Sea Basin from the different simulations. However, several of the scenario simulations suggest that future salinity will be considerably lower compared to the simulated variability of present climate. Salinity changes will have large impacts on species distributions, growth and reproduction of organisms (see Chap. 5).

Based upon model simulations, the sensitivity of the average steady-state salinity to the external forcing (e.g. freshwater supply, wind speed and amplitude of the sea level in Kattegat) has been estimated in several studies (e.g. Stigebrandt 1983; Gustafsson 1997; 2000b, 2004; Schrum 2001; Meier and Kauker 2003b; Rodhe and Winsor 2002, 2003; Stigebrandt and Gustafsson 2003; Meier 2005).

It was found that the sensitivity of the steady-state salinity to the freshwater supply is non-linear. In different model approaches the results agree rather well. For instance, the sensitivity of the three-dimensional general circulation model RCO (Meier and Kauker 2003b) is only slightly higher than the sensitivity of the process oriented model by Stigebrandt (1983). Even with 100% increased freshwater supply the Baltic Sea cannot be classified as a freshwater sea. Further, the sensitivity in different sub-basins was stud-

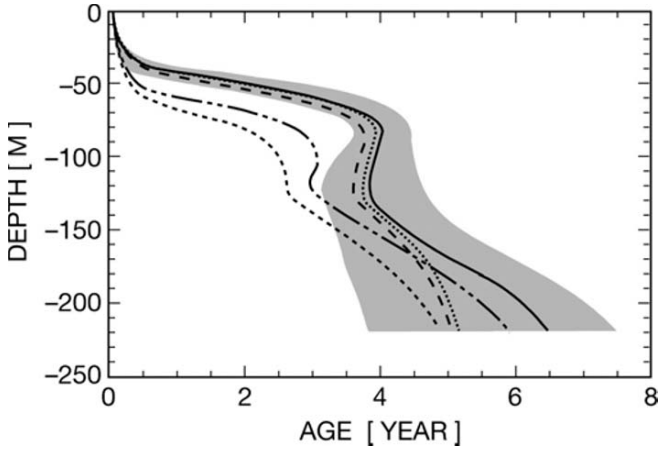

Fig. 3.40. Median profiles of age at Gotland Deep: RCO hindcast simulation for 1961–1990 (*black solid line, the shaded area indicates the range between the first and third quartiles*) and four scenario simulations for 2071–2100 (*dotted line:* RCO-H/B2, *dashed line:* RCO-H/A2, *dash-dotted line:* RCO-E/B2, *long-dashed line:* RCO-E/A2) (adapted from Meier 2006). The age is the time elapsed since a particle left the sea surface and is a measure of deep water renewal

ied when the changing freshwater supply is non-uniform (Stigebrandt and Gustafsson 2003). In contrast to these investigations, Rodhe and Winsor (2002, 2003) found a much larger sensitivity to freshwater inflow. An explanation could be that in the empirical model of Rodhe and Winsor (2002) the freshwater content anomaly depends only on the freshwater supply and not on the wind forcing, as found by Meier and Kauker (2003a).

Meier (2005) investigated not only the sensitivity of modelled salinity but also the sensitivity of modelled age to freshwater supply, wind speed and amplitude of the sea level in Kattegat (Fig. 3.40). In steady-state the average salinity of the Baltic Sea is most sensitive to perturbations of freshwater inflow. Increases in freshwater inflow and wind speed both result in decreased salinity, whereas increases in the Kattegat sea level results in increased salinity. The average age is most sensitive to perturbations of the wind speed. Especially, decreased wind speed causes significantly increased age of the deep water. On the other hand, the impact of changing freshwater or sea level in Kattegat on the average age is comparatively small, suggesting invariance of stability and ventilation in the steady-state. Immediately after the onset of increased freshwater inflow, the saltwater inflow into the Baltic Sea drops significantly due to increased recirculation (Meier 2005). After the typical response time scale, the vertical overturning circulation partially recovers.

3.9 Future Development in Projecting Anthropogenic Climate Changes

Global climate models play a central role in projecting future anthropogenic climate change, both by providing estimates of change on large horizontal scales and by providing the large-scale information needed by various downscaling methods. Further improvement of these models is therefore essential. This concerns especially the parameterisation of sub-grid scale phenomena (such as cloud processes, radiative transfer, convection, small-scale mixing in the atmosphere and the ocean, as well as the exchange of heat, water and momentum between the atmosphere and the other components of the climate system) which are crucially important for the response of climate to external forcing. Success in improving global climate models will require huge efforts from the international community, focusing not only on modelling per se but also on collecting and making widely available detailed observations that will help to guide the development of the models.

Model improvements are also needed for regional climate models. Even if the horizontal resolution is better in those models than in the global climate models, they still have the problem of parameterisation of sub-grid scale processes. It is likely that in the next five to ten years horizontal resolutions of only a few kilometres will become common. Even at such finer scales, many phenomena remain unresolved, including individ-

ual clouds. Reanalysis-driven experiments with regional climate models can be compared to high-resolution gridded datasets. Since the horizontal resolution in the models is likely to improve, the observational datasets also need to be represented on finer grids. In this way errors and systematic biases can be identified, leading to further improvements in model formulation. Furthermore, global climate models can benefit from improved parameterisations in regional climate models since the horizontal resolution in the global models will, in a few years time, be close to that of today's regional models.

Climate models should evolve to also include other processes than those of the more "traditional" physical climate system. Complex interaction and feedback processes involving the biogeochemical cycles makes it necessary to introduce other model components to the climate models. Examples of such components are, among others: fully coupled models of atmospheric chemistry, aerosol models, interactive vegetation models, models describing the carbon cycle, and models including marine chemistry.

Despite the efforts put into improving climate models, it is likely that the projections from different models will continue to differ for many years to come, particularly on regional scales. Therefore, it is also important to ask how to best deal with these differences. Is it reasonable to assume that all models give equally likely projections, or should the projections be weighted according to model quality (e.g. in simulating present-day climate)? First steps toward the latter direction have been taken (e.g. Giorgi and Mearns 2002, 2003; Murphy et al. 2004), but as yet there is only limited understanding of which aspects of the present-day climate simulation matter most for simulation of projected anthropogenic climate changes. On the other hand, it is also important to evaluate the possibility that the behaviour of the real climate system might fall outside the range of conventional model results (e.g. Allen and Ingram 2002; Stainforth et al. 2005).

Both statistical and dynamical downscaling have proved to have added value for assessing regional climate in comparison with global models, although they may show different results. Comparison of future scenarios downscaled by the two approaches may form a basis for assessing uncertainties associated with the downscaling. The two approaches have different advantages and disadvantages due the nature of the methods used. While the dynamical approach may have problems with biases, the statistical approach basically avoids this problem as it is a data-based method. However, being physically based, dynamical methods realistically simulate non-linear effects and other dynamical features, whereas statistical methods often lack the full range of the true variability. Therefore, choice of the approach to be used depends mainly on the questions to be addressed. One important advantage of the statistical approach is that it can deal with local scales, including site scale. In the interim before the resolution of RCMs is considerably improved, it provides an alternative way to create the local anthropogenic climate change scenarios needed for many impact studies.

Hydrological studies have shown that biases in precipitation from climate models make it difficult to directly use meteorological outputs in hydrological and water resources oriented applications. Evapotranspiration is also a source of much uncertainty, both in climate models and hydrological models. The combination of biases in meteorological variables and the need for high resolution has to date precluded using the actual hydrological components from climate models for detailed assessment of hydrological impacts. Continued work to improve the hydrological processes in both global and climate models, including river routing techniques, is needed.

Such development, together with finer resolution, as mentioned above, would serve to enhance the quality and utility of climate model simulations, particularly if it leads to better representation of extreme hydrological events. Recognising that biases may be around for some time to come, hydrological development should also focus on improved methods to filter out biases without misrepresenting the anthropogenic climate change signal coming from climate models.

Regarding ocean processes, the shortcomings of global models are limiting for many variables. For instance, sea level scenarios for the Baltic Sea remain rather uncertain due to the large uncertainty of the global average sea level rise. In addition, overestimation of precipitation by regional climate models considerably affects salinity in the Baltic Sea. Salinity is not only biased by the erroneous freshwater surplus; mixing also has a considerable impact.

As mixing is approximately proportional to the third power of the wind speed, any wind speed biases strongly impact on Baltic Sea cli-

mate. Consequently, mixing and other variables, such as sea level extremes, are typically underestimated as RCMs commonly underestimate high wind speeds.

To improve scenarios for the Baltic Sea, the horizontal resolution of ocean models should be increased such that mesoscale processes are included. Description of important processes like saltwater plume dynamics, entrainment and interleaving needs to be improved as well. Thus, further work to improve Baltic Sea models should focus on advanced mixing parameterisations (e.g. including Langmuir circulation and breaking of internal waves) and the coupling between ocean and state–of–the–art wave models.

3.10 Summary of Future Anthropogenic Climate Change Projections

Increasing greenhouse gas (GHG) concentrations are expected to lead to a substantial warming of the global climate during this century. Cubasch et al. (2001) estimated the annual globally averaged warming from 1990 to 2100 to be in the range of 1.4 to 5.8 °C. This range in temperature change takes into account differences between climate models and a range of anthropogenic emissions scenarios, but it excludes other uncertainties (for example, in the carbon cycle) and should not be interpreted as giving the absolute lowest and highest possible changes in the global mean temperature during the period considered.

Projected future warming in the Baltic Sea Basin generally exceeds the global mean warming in GCM (global climate model) simulations. Looking at the annual mean from an ensemble of 20 GCM simulations, regional warming over the Baltic Sea Basin would be some 50% higher than global mean warming. In the northern areas of the basin, the largest warming is generally simulated in winter; further south the seasonal cycle of warming is less clear.

However, the relative uncertainty in the regional warming is larger than that in the global mean warming. Taking the northern areas of the basin as an example, the warming from late 20th century to late 21st century could range from as low as 1 °C in summer (lowest scenario for summer) to as high as 10 °C in winter (highest scenario for winter). The simulated warming would generally be accompanied by an increase in precipitation in the Baltic Sea Basin, except in the southernmost areas in summer. The uncertainty for precipitation change is, however, larger than that for temperature change, and the coarse resolution of GCMs does not resolve small-scale variations of precipitation change that are induced by the regional topography and land cover.

A more geographically detailed assessment of future anthropogenic climate change in the Baltic Sea Basin requires the use of statistical or dynamical downscaling methods. Yet, as only a limited number of GCM simulations have been downscaled by RCMs (regional climate models) or statistical downscaling methods, the range of results derived from such downscaling experiments does not fully reflect the range of uncertainties in the GCM projections. Accepting this, the range of results from available downscaling studies is presented below as it gives an indication of plausible future changes. All values refer to changes projected for the late 21st century, represented here as differences in climate between the years 1961–1990 and 2071–2100. All references to "northern" and "southern" areas of the Baltic Sea Basin are defined by the subregions shown in Fig. 3.12.

Consistent with GCM studies, all available downscaling studies also indicate increases in temperature during all seasons for every subregion of the Baltic Sea Basin. Combined results show a projected warming of the mean annual temperature by some 3 to 5 °C for the total basin. Seasonally, the largest part of this warming would occur in the northern areas of the Baltic Sea Basin during winter months and in the southern areas of the Baltic Sea Basin during summer months. Corresponding changes in temperatures would be 4 to 6 °C in winter and 3 to 5 °C in summer, as estimated from a matrix of regional climate model experiments.

As noted above, these ranges most probably underestimate the real uncertainty. The diurnal temperature range – the difference between daily maximum and minimum temperature – would decrease, most strongly in autumn and winter months. Such levels of warming would lead to a lengthening of the growing season, defined here as the continuous period when daily mean temperature exceeds 5 °C. Taking an example from one RCM indicates that the growing season length could increase by as much as 20 to 50 days for northern areas and 30 to 90 days for southern areas by the late 21st century. The range depends on the range of different emissions scenarios used.

Projected changes in precipitation from downscaling studies also depend both on differences in

GHG emissions scenarios and differences between climate models. Moreover, precipitation results are more sensitive than temperature results to the statistical uncertainty in determining climatological means from a limited number of simulated years, particularly at regional scales. Seasonally, winters are projected to become wetter in most of the Baltic Sea Basin and summers to become drier in southern areas for many scenarios. Northern areas could generally expect winter precipitation increases of some 25 to 75%, while the projected summer changes lie between −5 and 35%. Southern areas could expect increases ranging from some 20 to 70% during winter, while summer changes would be negative, showing decreases of as much as 45%.

Taken together, these changes lead to a projected increase in annual precipitation for the entire basin. In broad terms, these results are consistent with GCM studies of precipitation change, although the projected summer decrease in the southern areas of the basin tends to be larger and extend further north in the available RCM studies than in most reported GCMs. This difference reflects the fact that the few GCM simulations that have been downscaled by RCMs also show this pattern of summer precipitation change.

Projected changes in wind differ widely between various climate models. Differences in the circulation patterns of the driving GCMs are particularly important for the modelled outcome of this variable. From the RCM results presented here, only those driven by the ECHAM4/OPYC3 GCM show statistically significant changes for projected future climate scenarios. For mean daily wind speed over land areas, this would amount to a mean increase of some 8% on an annual basis and a maximum mean seasonal increase of up to 12% during winter. The corresponding mean seasonal increase over the Baltic Sea in winter, when decrease in ice cover enhances near-surface winds, would be up to 18%. For RCMs driven by the HadAM3H GCM, the changes are small and not statistically significant. Modelled changes in extreme wind generally follow the same pattern as for the mean wind; however, the spatial resolution of both GCMs and RCMs is far too coarse to accurately represent the fine scales of extreme wind.

As the downscaled projections for wind differ widely, there is no robust signal seen in the RCM results. Looking at projected changes in large-scale atmospheric circulation from numerous GCMs, they indicate that an increase in windiness for the Baltic Sea Basin would be somewhat more likely than a decrease. However, the magnitude of such a change is still highly uncertain and it may take a long time before projected GHG-induced changes in windiness, if ever, emerge from background natural variability. It can be noted, moreover, that ECHAM4/OPYC3 is one of the GCMs that gives higher values of change in large-scale wind.

Hydrological studies using climate change projections show that increases in mean annual river flow from the northernmost catchments would occur together with decreases in the southernmost catchments. Seasonally, summer river flows would tend to decrease, while winter flows would tend to increase, by as much as 50%. The southernmost catchments would be affected by the combination of both decreased summer precipitation and increased evapotranspiration. Oceanographic studies show that mean annual sea surface temperatures could increase by some 2 to 4 °C by the end of the 21st century. Ice extent in the sea would then decrease by some 50 to 80%. The average salinity of the Baltic Sea could range between present day values and decreases of as much as 45%. However, it should be noted that these oceanographic findings, with the exception of salinity, are based upon only four regional scenario simulations using two emissions scenarios and two global models.

3.11 References

Achberger C (2004) Recent and future regional climate variations in Sweden in relation to large-scale circulation. Earth Sciences Centre, A92. Göteborg University

Achberger C, Linderson ML, Chen D (2003) Performance of the Rossby Centre regional Atmospheric model in Southern Sweden: Comparison of simulated and observed precipitation. Theor App Climatol 76:219–234

Achberger C, Chen D, Alexandersson H (2006) The surface winds of Sweden during 1999–2000. Int J Climatol 26:159–178

Alexandersson H, Tuomenvirta H, Schmith T, Iden K (2000) Trends of storms in NW Europe derived from an updated pressure data set. Clim Res 14:71–73

Allen MR, Ingram WJ (2002) Constraints on future changes in climate and the hydrologic cycle. Nature 419:224–232

Andersen HE, Kronvang B, Larsen SE, Hoffmann CC, Jensen TS, Rasmussen EK (2006) Climate-change impacts on hydrology and nutrients in a Danish lowland river basin. Sci Total Env 365: 223–237

Andréasson J, Gardelin M, Bergström S (2002) Modelling hydrological impacts of climate change in the Lake Vänern region in Sweden. Vatten 58:25–32

Andréasson J, Bergström S, Carlsson B, Graham LP, Lindström G (2004) Hydrological change – climate change impact simulations for Sweden. Ambio 33:228–234

Arnell NW (1998) Climate change and water resources in Britain. Climatic Change 39:83–110

Arnell NW (1999) The effect of climate change on hydrological regimes in Europe: A continental perspective. Glob Env Change 9:5–23

Arnell NW, Hudson DA, Jones RG (2003) Climate change scenarios from a regional climate model: Estimating change in runoff in southern Africa. J Geophy Res 108:4519, doi: 10.1029/2002JD002782

Arpe K, Bengtsson L, Golitsyn GS (2000) Analysis of changes in hydrological regime on the Lake Ladoga watershed and in the discharge of the Neva River in 20$^{\text{th}}$ and 21$^{\text{st}}$ centuries using a global climate model. Russ Meteorol Hydrol 12:5–13

Baerens C, Hupfer P (1999) Extremwasserstände an der deutschen Ostseeküste nach Beobachtungen und in einem Treibhausgasszenario (Extreme water levels at the German Baltic Sea coast according to observations and a greenhouse gas scenario). Die Küste 61:47–72 (in German)

Barthelet P, Terray L, Valcke S (1998) Transient CO_2 experiment using the ARPEGE/OPAICE non flux corrected coupled model. Geophys Res Lett 25:2277–2280

Benestad RE (2002a) Empirically downscaled multimodel ensemble temperature and precipitation scenarios for Norway. J Clim 15:3008–3027

Benestad RE (2002b) Empirically downscaled climate scenarios for northern Europe. Clim Res 21: 105–125

Benestad RE (2004) Tentative probabilistic temperature scenarios for northern Europe. Tellus A 56: 89–101

Beniston M, Stephenson DB, Christensen OB, Ferro CAT, Frei C, Goyette S, Halsnæs K, Holt T, Jylhä K, Koffi B, Palutikof J, Schöll R, Semmler T, Woth K (2007) Future extreme events in european climate: An exploration of regional climate model projections. Climatic Change 81:71–95

Bergström S (1976) Development and application of a conceptual runoff model for Scandinavian catchments. Doctoral thesis, Department of Water Resources Engineering, Institute of Technology, Lund University

Bergström S (1995) The HBV Model In: Singh VP (ed) Computer Models of Watershed Hydrology. Water Resources Publications, Highlands Ranch Colorado

Bergström S, Carlsson B (1994) River runoff to the Baltic Sea: 1950–1990. Ambio 23:280–287

Bergström S, Carlsson B, Gardelin M, Lindström G, Pettersson A, Rummukainen M (2001) Climate change impacts on runoff in Sweden – assessments by global climate models dynamical downscaling and hydrological modelling. Clim Res 16:101–112

Bergström S, Andréasson J, Beldring S, Carlsson B, Graham LP, Jónsdóttir JF, Engeland K, Turunen MA, Vehviläinen B, Førland E J (2003) Climate Change Impacts on Hydropower in the

Nordic Countries – State of the art and discussion of principles. CWE Report no 1, CWE Hydrological Models Group, Rejkjavik, Iceland
Bertrand C, Van Ypersele JP, Berger A (2002) Are natural climate forcings able to counteract the projected anthropogenic global warming? Climatic Change 55:413–427
Bjørge D, Haugen JE, Nordeng TE (2000) Future climate in Norway. DNMI Research Report no 103
Blenckner T, Chen D (2003) Comparison of the impact of regional and North Atlantic atmospheric circulation on an aquatic ecosystem. Clim Res 23:131–136
Boer GJ, Yu B (2003) Climate sensitivity and response. Clim Dyn 20:415–429
Boville BA, Gent PR (1998) The NCAR climate system model version One. J Clim 11:1115–1130
Braconnot P, Marti O, Joussaume S (1997) Adjustment and feedbacks in a global coupled ocean–atmosphere model. Clim Dyn 13:507–519
Busuioc A, Chen D, Hellström C (2001a) Temporal and spatial variability of precipitation in Sweden and its link with the large scale atmospheric circulation. Tellus 53A,3:348–367
Busuioc A, Chen D, Hellström C (2001b) Performance of statistical downscaling models in GCM validation and regional climate estimates: Application for Swedish precipitation. Int J Climatol 21: 557–578
Butina M, Melnikova G, Stikute I (1998a) Potential impact of climate change on the hydrological regime in Latvia. In: Raschke E, Isemer HJ (eds) Conference Proceedings of the Second Study Conference on BALTEX, International BALTEX Secretariat Publication No 11
Butina M, Melnikova G, Stikute I (1998b) Potential impact of climate change on the hydrological regime in Latvia. In: Lemmelä R, Helenius N (eds) Proceedings of the Second International Conference on Climate and Water. Espoo, Finland 17–20 August 1998, 3:1610–1617
Carlsson B, Sanner H (1996) Modelling influence of river regulation on runoff to the Gulf of Bothnia. Nord Hydrol 27:337–350
Chen D (2000) A monthly circulation climatology for Sweden and its application to a winter temperature case study. Int J Climatol 20:1067–1076
Chen D, Achberger C (2006) Past and future atmospheric circulation over the Baltic region based on observation reanalysis and GCM simulations. Research Report C74 Earth Sciences Centre Göteborg University, Sweden
Chen D, Hellström C (1999) The influence of the North Atlantic Oscillation on the regional temperature variability in Sweden: Spatial and temporal variations. Tellus 51A,4:505–516
Chen D, Li X (2004) Scale dependent relationship between maximum ice extent in the Baltic Sea and atmospheric circulation. Glob Planet Change 41:275–283
Chen D, Omstedt A (2005) Climate-induced variability of sea level in Stockholm: Influence of air temperature and atmospheric circulation. Adv Atmos Sci 20,5:655–664
Chen D, Achberger C, Räisänen J, Hellström C (2006) Using statistical downscaling to quantify the GCM-related uncertainty in regional climate change scenarios: A case study of Swedish precipitation. Adv Atmos Sci 23,1:54–60
Christensen JH, Christensen OB (2003) Severe summertime flooding in Europe. Nature 421:805–806
Christensen JH, Machenhauer B, Jones RG, Schär C, Ruti PM, Castro M, Visconti G (1997) Validation of present-day regional climate simulations over Europe: LAM simulations with observed boundary conditions. Clim Dyn 13:489–506
Christensen JH, Räisänen J, Iversen T, Bjørge D, Christensen OB, Rummukainen M (2001) A synthesis of regional climate change simulations – a Scandinavian perspective. Geophys Res Lett 28: 1003–1006
Christensen JH, Carter TR, Giorgi F (2002) Prudence employs new methods to assess European climate change. EOS 83:147
Christensen JH, Carter TR, Rummukainen M (2007) Evaluating the performance and utility of regional climate models: The PRUDENCE project. Climatic Change 81:1–6
Christensen OB, Christensen JH (2004) Intensification of extreme European summer precipitation in a warmer climate. Glob Planet Change 44:107–117
Christensen OB, Christensen JH, Machenhauer B, Botzet M (1998) Very-high-resolution regional climate simulations over Scandinavia present climate. J Clim 11:3204–3229

Christensen OB, Christensen JH, Botzet M (2002) Heavy precipitation occurrence in Scandinavia investigated with a regional climate model. In: Beniston M (ed) Climatic Change: Implications for the hydrological cycle and for water management. Kluwer

Church JA, Gregory JM, Huybrechts P, Kuhn M, Lambeck K, Nhuan MT, Qin D, Woodworth PL (2001) Changes in sea level. In: IPCC Climate Change 2001: The scientific basis contribution of working group I to the Third Assessment Report of the Intergovernmental Panel on Climate Change. Cambridge University Press, Cambridge New York

Cubasch U, Meehl GA, Boer GJ, Stouffer RJ, Dix M, Noda A, Senior CA, Raper S, Yap KS (2001) Projections of future climate change. In: IPCC Climate Change 2001: The scientific basis contribution of working group I to the Third Assessment Report of the Intergovernmental Panel on Climate Change. Cambridge University Press, Cambridge New York

De Castro M, Gallardo C, Jylhä K, Tuomenvirta H (2007) The use of a climate-type classification for assessing climate change effects in Europe from an ensemble of nine regional climate models. Clim Change 81:329–341

De Roo A, Schmuck G (2002) Assessment of the effects of engineering, land use and climate scenarios on flood risk in the Oder catchment. European Commission, Joint Research Centre, Institute for Environment and Sustainability

Déqué M, Rowell DP, Lüthi D, Giorgi F, Christensen JH, Rockel B, Jacob D, Kjellström E, De Castro M, Van Den Hurk B (2007) An intercomparison of regional climate simulations for Europe: Assessing uncertainties in model projections. Climatic Change 81:53–70

Déqué M, Marquet P, Jones RG (1998) Simulation of climate change over Europe using a global variable resolution general circulation model. Clim Dyn 14:173–189

Diansky NA, Volodin EM (2002) Simulation of present-day climate with a coupled atmosphere–ocean general circulation model. Izvestia Atmos Ocean Phys 38:732–747

Döscher R, Meier HEM (2004) Simulated sea surface temperature and heat fluxes in different climates of the Baltic Sea. Ambio 33:242–248

Döscher R, Willén U, Jones C, Rutgersson A, Meier HEM, Hansson U, Graham LP (2002) The development of the regional coupled ocean–atmosphere model RCAO. Boreal Env Res 7:183–192

Ekman M (1988) The world's longest continued series of sea level observations. Pure Appl Geophys 127:73–77

Emori S, Nozawa T, Abe-Ouchi A, Numaguti A, Kimoto M, Nakajima T (1999) Coupled ocean–atmosphere model experiments of future climate change with an explicit representation of sulfate aerosol scattering. J Met Soc Jpn 77:1299–1307

Engen-Skaugen T, Roald LA, Beldring S, Førland EJ, Tveito OE, Engeland K, Benestad R (2005) Climate change impacts on water balance in Norway. Research Report No 1/2005 Climate Norwegian Meteorological Institute Oslo

Fenger J, Buch E, Jacobsen PR (2001) Monitoring and impacts of sea level rise at Danish coasts and near shore infrastructures. In: Jørgensen AM, Fenger J, Halsnæs K (eds) Climate change research – Danish Contributions. Danish Climate Centre Copenhagen, pp. 237–254

Ferro CAT (2004) Attributing variation in a regional climate change modelling experiment. PRUDENCE working note available at http://prudence.dmi.dk/public/publications/analysis_of_variance.pdf

Ferro CAT, Hannachi A, Stephenson DB (2005) Simple techniques for describing changes in probability distributions of weather and climate. J Clim 18:4344–4354

Flato GM, Boer GJ (2001) Warming asymmetry in climate change experiments. Geophys Res Lett 28: 195–198

Flato GM, Boer GJ, Lee WG, McFarlane NA, Ramsden D, Reader MC, Weaver AJ (2000) The Canadian centre for climate modelling and analysis global coupled model and its climate. Clim Dyn 16: 451–467

Forster PM, De F, Blackburn M, Glover R, Shine KP (2000) An examination of climate sensitivity for idealised climate change experiments in an intermediate general circulation model. Clim Dyn 16: 833–849

Fossdal ML, Sælthun NR (1993) Energy planning models – climate change. Report from a Nordic expert meeting. NVE-report 08/1993 Norwegian Water Resources and Energy Administration, Oslo

Frei C, Christensen JH, Déqué M, Jacob D, Jones RG, Vidale PL (2003) Daily precipitation statistics in regional climate models: Evaluation and intercomparison for the European Alps. J Geophys Res 108,D3, 4124 doi: 101029/2002JD002287

Gardelin M, Andreasson J, Carlsson B, Lindström G, Bergström S (2002a) Modelling av effekter av klimatförändringar på tillrinningen till vattenkraftsystemet (Modelling of effects of climate change on inflow to the hydropower system). Elforsk Report 02:27 Elforsk Stockholm (in Swedish)

Gardelin M, Bergström S, Carlsson B, Graham LP, Lindström G (2002b) Climate change and water resources in Sweden – analysis of uncertainties. In: Beniston M (ed) Climatic Change: Implications for the Hydrological Cycle and for Water Management. Advances in Global Change Research. Kluwer, Dordrecht

Gellens D, Roulin E (1998) Streamflow response of Belgian catchments to IPCC climate change scenarios. J Hydrol 210:242–258

Gillett NP, Zwiers FW, Weaver AJ, Stott PA (2003) Detection of human influence on sea-level pressure. Nature 422:292–294

Giorgi F, Marinucci M (1991) Validation of a regional atmospheric model over Europe: Sensitivity of wintertime and summertime simulations to selected physics parameterizations and lower boundary conditions. Q J Roy Met Soc 117:1171–1206

Giorgi F, Mearns LO (2002) Calculation of average uncertainty range and reliability of regional climate changes from AOGCM simulations via the "reliability ensemble averaging" (REA) method. J Clim 15:1141–1158

Giorgi F, Mearns LO (2003) Probability of regional climate change based on the Reliability Ensemble Averaging (REA) method. Geophys Res Lett 30 12 1629 (doi:101029/2003GL017130)

Giorgi F, Marinucci M, Visconti G (1990) Use of a limited area model nested in a general circulation model for regional climate simulation over Europe. J Geophys Res 95:18413–18431

Giorgi F, Marinucci M, Visconti G (1992) A $2 \times CO_2$ climate change scenario over Europe generated using a limited area model nested in a general circulation model 2 Climate change scenario. J Geophys Res 97:10011–10028

Giorgi F, Hewitson B, Christensen J, Hulme M, von Storch H, Whetton P, Jones R, Mearns L, Fu C (2001) Regional climate information – evaluation and projections. In: IPCC Climate Change 2001: The Scientific Basis Contribution of Working Group I to the Third Assessment Report of the Intergovernmental Panel on Climate Change. Cambridge University Press, Cambridge New York

Giorgi F, Bi XQ, Pal J (2004a) Mean interannual variability and trends in a regional climate change experiment over Europe I: Present-day climate (1961–1990). Clim Dyn 22:733–756

Giorgi F, Bi XQ, Pal J (2004b) Mean interannual variability and trends in a regional climate change experiment over Europe II: Climate change scenarios (2071–2100). Clim Dyn 23:839–858

Golitsyn GS, Efimova LK, Mokhov II (2002) Izmenenija temperatury i osadkov v bassejne Ladozhskogo ozera po raschetam klimaticheskoj modeli obshchej cirkuljacii v XIX–XXI vekah (Changes of temperature and precipitation on the Lake Ladoga watershed in 19^{th} – 21^{st} centuries simulated by a general circulation model). Izvestia RGO 134,6:80–87 (in Russian)

Gordon C, Cooper C, Senior CA, Banks H, Gregory JM, Johns TC, Mitchell JFB, Wood RA (2000) The simulation of SST, sea ice extents and ocean heat transports in a version of the Hadley Centre coupled model without flux adjustments. Clim Dyn 16:147–166

Grabs WE, Daamen K, Gellens D, Grabs W, Kwadijk JCJ, Lang H, Middlekoop H, Parmet BWAH, Schädler B, Schulla J, Wilke K (1997) Impact of Climate Change on Hydrological Regimes and Water Resources Management in the Rhine Basin. CHR-Report no I–16, International Commision for the Hydrology of the Rhine Basin (CHR) Lelystad

Graham LP (1999a) Modeling runoff to the Baltic Sea. Ambio 28:328–334

Graham, LP (2004) Climate change effects on river flow to the Baltic Sea. Ambio 33:235–241

Graham LP (1999b) Modeling the large-scale hydrologic response to climate change in the Baltic Basin. In: Elíasson J (ed) Proceedings from the Northern Research Basins 12^{th} International Symposium and Workshop, Reykjavík Iceland 23–27 August, pp. 99–110

Graham LP (2002) A simple runoff routing routine for the Rossby Centre Regional Climate Model. In: Killingtveit A (ed) Proceedings from XXII Nordic Hydrological Conference, Røros Norway 4–7 August, Nordic Hydrological Programme Report 47:573–580

Graham LP, Rummukainen M, Gardelin M, Bergström S (2001) Modelling Climate Change Impacts on Water Resources in the Swedish Regional Climate Modelling Programme. In: Brunet M, López D (eds) Detecting and Modelling Regional Climate Change and Associated Impacts. Springer, Berlin Heidelberg New York, pp. 567–580

Graham LP, Andréasson J, Carlsson B (2007a) Assessing climate change impacts on hydrology from an ensemble of regional climate models, model scales and linking methods – a case study on the Lule River Basin. Climatic Change 81:293–307

Graham LP, Hagemann S, Jaun S, Beniston M (2007b) On interpreting hydrological change from regional climate models. Climatic Change 81:97–122

Gregory JM, Mitchell JFB, Brady AJ (1997) Summer drought in northern midlatitudes in a time-dependent CO_2 climate experiment. J Clim 10:662–686

Grigoryev AS, Trapeznikov JA (2002) The water level in the Ladoga Lake in the conditions of potential climate change. Water Resource 29:174–178 (in Russian)

Gustafsson BG (1997) Interaction between Baltic Sea and North Sea. Dt Hydrogr Z 49:163–181

Gustafsson BG (2000) Time-dependent modeling of the Baltic entrance area. 2. Water and salt exchange of the Baltic Sea. Estuaries 23:253–266

Gustafsson BG (2004) Sensitivity of Baltic Sea salinity to large perturbations in climate. Clim Res 27:237–251

Gutry-Korycka M (1999) Ekstremalne stany systemu hydrologicznego w perspektywie ocieplenia klimatu (fakty czy hipotezy). In: Komitet Narodowy PAN IGBP Global Change 1999 Zmiany i zmienność klimatu Polski – ich wpływ na gospodarkę ekosystemy i człowieka (Changes and variability of Poland's climate – their influence on economy, ecosystems and people). Łódź Conference proceedings (in Polish)

Haapala J, Leppäranta M (1997) The Baltic Sea ice season in changing climate. Boreal Env Res 2: 93–108

Haapala J, Meier HEM, Rinne J (2001) Numerical investigations of future ice conditions in the Baltic Sea. Ambio 30:237–244

Hagemann S, Dümenil L (1999) Application of a global discharge model to atmospheric model simulations in the BALTEX region. Nordic Hydrology 30:209–230

Hagemann S, Jacob D (2007) Gradient in the climate change signal of European discharge predicted by a multi-model ensemble. Climatic Change 81:309–327

Hagemann S, Machenhauer B, Christensen OB, Déqué M, Jacob D, Jones R, Vidale PL (2002) Intercomparison of water and energy budgets simulated by regional climate models applied over Europe. Max-Planck-Institute for Meteorology Rep 338. Hamburg, Germany

Hagemann S, Machenhauer B, Jones R, Christensen OB, Déqué M, Jacob D, Vidale PL (2004) Evaluation of water and energy budgets in regional climate models applied over Europe. Clim Dyn 23:547–567

Hall MM, Bryden HL (1982) Direct estimates and mechanisms of ocean heat transport. Deep-Sea Res 29:339–359

Hamlet AF, Lettenmaier D (1999) Effects of climate change on hydrology and water resources in the Columbia River Basin. J Am Water Resour Assoc 35:1597–1623

Hanssen-Bauer I, Tveito OE, Førland EJ (2000) Temperature scenarios for Norway: Empirical Downscaling from the ECHAM4/OPYC3 GSDIO integration. DNMI Report no 24/00 KLIMA Norwegian Meteorological Institure Oslo Norway

Hanssen-Bauer I, Tveito OE, Førland EJ (2001) Precipitation scenarios for Norway Empirical downscaling from ECHAM4/OPYC3 DNMI Report no 10/01 KLIMA Norwegian Meteorological Institute Oslo Norway

Hanssen-Bauer I, Førland E, Haugen JE, Tveito OE (2003) Temperature and precipitation scenarios for Norway: Comparison of results from dynamical and empirical downscaling. Clim Res 25:15–27

Hanssen-Bauer I, Achberger C, Benestad R, Chen D, Førland E (2005) Empirical–statistical downscaling of climate scenarios over Scandinavia: A review. Clim Res 29:255–268

Harvey LDD (2004) Characterizing the annual-mean climatic effect of anthropogenic CO_2 and aerosol emissions in eight coupled atmosphere–ocean GCMs. Clim Dyn 23:569–599

Hay LE, Wilby RL, Leavesley GH (2000) A comparison of delta change and downscaled GCM scenarios for three mountainous basins in the United States. J Am Water Res Ass 36:387–398

Hegerl GC, Zwiers FV, Stott P, Kharin VV (2004) Detectability of anthropogenic changes in annual temperature and precipitation extremes. J Clim 17:3683–3700

Heino R, Kitaev L (2003) INTAS project (2002–2005): Snow cover changes over Northern Eurasia during the last century: Circulation consideration and hydrological consequences (SCCONE). BALTEX Newsletter 5: 8–9

Hellström C, Chen D, Achberger C, Räisänen J (2001) A Comparison of climate change scenarios for Sweden based on statistical and dynamical downscaling of monthly precipitation. Clim Res 19:45–55

Henderson-Sellers A, Hansen AM (1995) Climate Change Atlas. Atmospheric and Oceanographic Sciences Library 17. Kluwer

Hennessy KJ, Gregory JM, Mitchell JFB (1997) Changes in daily precipitation under enhanced greenhouse conditions. Clim Dyn 13:667–680

Heyen H, Zorita E, von Storch H (1996) Statistical downscaling of monthly mean North Atlantic airpressure to sea level anomalies in the Baltic Sea. Tellus 48A:312–323

Hirst A, O'Farrell SP, Gordon HP (2000) Comparison of a coupled ocean–atmosphere model with and without oceanic eddy-induced advection Part I: Ocean spinup and control integrations. J Clim 13: 139–163

Hoerling MP, Hurrell JW, Xu T, Bates GT, Phillips A (2004) Twentieth century North Atlantic climate change Part II: Understanding the effect of Indian Ocean warming. Clim Dyn 23:391–405

Houghton JT, Callendar BA, Varney SK (eds) (1992) Climate Change 1992 – The Supplementary Report to the IPCC Scientific Assessment. Intergovernmental Panel on Climate Change. Cambridge University Press

Huffman GJ, Adler RF, Arkin A, Chang A, Ferraro R, Gruber A, Janowiak J, Joyce RJ, Mc Nab A, Rudolf B, Schneider U, Xie P (1997) The Global Precipitation Climatology Project (GPCP) combined precipitation data set. Bull Am Met Soc 78:5–20

Hulme M, Barrow EM, Arnell NW, Harrison PA, Johns TC, Downing TE (1999) Relative impacts of human-induced climate change and natural variability. Nature 397:688–691

Huntingford C, Cox PM (2000) An analogue model to derive additional climate change scenarios from existing GCM simulations. Clim Dyn 16:575–586

Hurrell JW, Van Loon H (1997) Decadal variations in climate associated with the North Atlantic Oscillation. Climatic Change 36:301–326

Hurrell JW, Kushnir Y, Ottersen G, Visbeck M (eds) (2003) The North Atlantic Oscillation: Climate Significance and Environmental Impact. Geophys Monogr Series 134

Hurrell JW, Hoerling MP, Phillips A, Xu T (2004) Twentieth century North Atlantic climate change Part I: Assessing determinism. Clim Dyn 23:371–389

Huybrechts P, De Wolde J (1999) The dynamic response of the Greenland and Antarctic ice sheets to multiple-century climatic warming. J Clim 12:2169–2188

ILMAVA Project (2002) Effect of Climate Change on Energy Resources in Finland Final report on the Ilmava Project within the Climtech Programme. Tammelin B, Forsius J, Jylhä J, Järvinen P, Koskela J, Tuomenvirta H, Turunen MA, Vehviläinen B, Venäläinen A, Finnish Meteorological Institute Helsinki (in Finnish)

IPCC (2001a) Climate Change 2001: The scientific basis contribution of Working Group I to the Third Assessment Report of the Intergovernmental Panel on Climate Change. Cambridge University Press, Cambridge New York

IPCC (2001b) Climate Change 2001: Impacts, adaptation and vulnerability. Contribution of Working Group II to the Third Assessment Report of the Intergovernmental Panel on Climate Change. Cambridge University Press, Cambridge New York

Jacob D, Van Den Hurk B, Andrae U, Elgered G, Fortelius C, Graham LP, Jackson S, Karstens U, Köpken C, Lindau R, Podzun R, Rockel B, Rubel F, Sass B, Smith R, Yang X (2001) A comprehensive model inter-comparison study investigating the water budget during the BALTEX-PIDCAP period. Meteorol Atmos Phys 77:19–43

Jansons V, Butina M (1998) Potential impacts of climate change on nutrient loads from small catchments. In: Lemmelä R, Helenius N (eds) Proceedings of the Second International Conference on Climate and Water, Espoo Finland 17–20 August 1998, 2

Järvet A (1998) An assessment of the climate change impact on groundwater regime. In: Kallaste T, Kuldna P (eds) Climate Change Studies in Estonia, Ministry of Environment Republic of Estonia, SEI Tallinn

Johansson MM, Kahma KK, Boman H, Launiainen J (2004) Scenarios for sea level on the Finnish coast. Boreal Env Res 9:153–166

Johns TC, Carnell RE, Crossley JF, Gregory JM, Mitchell JFB, Senior CA, Tett SFB, Wood RA (1997) The second Hadley Centre Coupled ocean–atmosphere GCM: Model description spinup and validation. Clim Dy 13:103–134

Jones CG, Ullerstig A (2002) The representation of precipitation in the RCA2 model (Rossby Centre Atmosphere Model Version 2). SWECLIM Newsletter 12:27–39

Jones CG, Willén U, Ullerstig A, Hansson U (2004) The Rossby Centre Regional Atmospheric Climate Model – Part I: Model climatology and performance for the present climate over Europe. Ambio 33:199–210

Jones RG, Murphy JM, Noguer M (1995) Simulation of climate-change over Europe using a nested regional climate model, 1. Assessment of control climate including sensitivity to location of lateral boundaries. Q J Roy Met Soc 121:1413–1449

Jones RG, Murphy JM, Noguer M, Keen AB (1997) Simulation of climate change over Europe using a nested regional climate model, 2. Comparison of driving and regional model responses to a doubling of carbon dioxide. Q J Roy Met Soc 123:265–292

Joshi M, Shine K, Ponater M, Stuber N, Sausen R, Li L (2003) A comparison of climate response to different radiative forcings in three general circulation models: Towards an improved metric of climate change. Clim Dyn 20:843–854

Jylhä K, Tuomenvirta H, Ruosteenoja K (2004) Climate change projections for Finland during the 21st century. Boreal Env Res 9:127–152

Jylhä K, Fronzek S, Tuomenvirta H, Carter TR, Ruosteenoja K (2007) Changes in frost and snow in Europe and Baltic sea ice by the end of the 21st century. Climatic Change (in press)

Järvet A, Jaagus J, Roosaare J, Tamm T, Vallner L (2000) Impact of climate change on water balance elements in Estonia. Estonia Geographical Studies 8:35–55

Kaas E, Frich P (1995) Diurnal temperature range and cloud cover in the Nordic countries: Observed trends and estimates for the future. Atmos Res 37:211–228

Kaczmarek Z (1993) Water balance model for climate impact analysis. Acta Geophys Pol 41:423–437

Kaczmarek Z (1996) Wpływ klimatu na bilans wody (Impact of climate on water balance). In: Kaczmarek Z (ed) Wpływ niestacjonarności i globalnych procesów geofizycznych na zasoby wodne Polski Oficyna (The impact of nonlinearity and global geophysical processes on water resources in Poland). Wydawnicza Politechniki Warszawskiej Warszawa, 33–53 (in Polish)

Kaczmarek Z (2003) Wpływ klimatu na gospodarkę wodną (Impact of climate on water management). In: Komitet Prognoz "Polska 2000 Plus" (ed) Czy Polsce grożą katastrofy klimatyczne? IGBP PAN Warszawa, 32–52 (in Polish)

Kaczmarek Z (2004) Climate change and European water resources. In: Liszewska M (ed) Potential climate changes and sustainable water management. Publ Inst Geophys Pol Acad Sc 377:33–38

Kaczmarek Z, Jurak D (2003) Assessment and prediction of hydrological droughts. Glob Change 10: 79–95

Kaczmarek Z, Napiórkowski J, Strzepek KM (1996) Climate change impacts on the water supply system in the Warta River Catchment Poland. Int J Water Resour Dev 12:165–180

Kaczmarek Z, Napiórkowski J, Jurak D (1997) Impact of climate change on water resources in Poland. Publ Inst Geophys Pol Acad Sc E-1

Kalinin M (2004) Climate and Water Resources of Belarus. In: Isemer HJ (ed) Conference Proceedings of the Fourth Study Conference on BALTEX, International BALTEX Secretariat Publication No 29

Kallaste T, Kuldna P (1998) Climate Change Studies in Estonia. Ministry of Environment Republic of Estonia SEI Tallinn

Kalnay E, Kanamitsu M, Kistler R, Collins W, Deaven D, Gandin L, Iredell M, Saha S, White G, Woollen J, Chelliah M, Zhu Y, Ebisuzaki W, Higgins W, Janowiak J, Mo KC, Ropelweski C, Wand J, Leetma A, Reynolds R, Jenne R, Joseph D (1996) The NCEP/NCAR 40 reanalysis project. Bull Am Met Soc 77:437–471

Kauker F, Meier HEM (2003) Modeling decadal variability of the Baltic Sea Part 1: Reconstructing atmospheric surface data for the period 1902–1998. J Geophys Res 108(C8) 3267 doi:101029/2003JC001797

Keevallik S (1998) Climate change scenarios for Estonia. In: Tarand A, Kallaste T (eds) Country case study on climate change impacts and adaptation assessments in the Republic of Estonia. Ministry of Environment Republic of Estonia SEI Tallinn

Kilsby CG, O'Connell PE, Fallows CS, Hashemi AM (1999) Generation of precipitation scenarios for assessing climate change impacts on river basin hydrology. In: Balabanis P, Bronstert A, Casale R, Samuels P (eds) Proceedings from Ribamod – River Basin Modelling Management and Flood Mitigation Concerted Action – Final Workshop Wallingford United Kingdom 26–27 February 1998. Office for Official Publications of the European Communities

Kistler R, Kalnay E, Collins W, Saha S, White G, Woollen J, Chelliah M, Ebisuzaki W, Kanamitsu M, Kousky V, Van Den Dool H, Jenne R, Fiorino M (2001) The NCEP/NCAR 50-year reanalysis: Monthly means CD-ROM and documentation. Bull Am Met Soc 82:247–268

Kjellström E (2004) Recent and future signatures of climate change in Europe. Ambio 33:193–198

Kjellström E, Ruosteenoja K (2007) Present-day and future precipitation in the Baltic Sea region as simulated in a suite of regional climate models. Climatic Change 81:281–291

Kjellström E, Döscher R, Meier HEM (2005) Atmospheric response to different sea surface temperatures in the Baltic Sea: Coupled versus uncoupled regional climate model experiments. Nord Hydrol 36:397–409

Kjellström E, Bärring L, Jacob D, Jones R, Lenderink G, Schär C (2007) Modelling daily temperature extremes: Recent climate and future changes over Europe. Climatic Change 81:249–265

Knutson TR, Delworth TL, Dixon KW, Stouffer RJ (1999) Model assessment of regional surface temperature trends (1949–1997). J Geophys Res 104:30981–30996

Kondratyev S (2001) Final Report of the Institute of Limnology RAS to the Project "The Impact of long-term changes in the weather on the dynamics of lakes in the United Kingdom Finland and Russia", No 96–1749

Kondratyev S, Bovykin I (2000) Hydrologic response of small lake and its drainage basin to precipitation and air temperature changes. Proc of Univ of Joensuu Karelian Inst 129:423–427

Kondratyev S, Bovykin V (2003) The effect of possible climatic changes on the hydrological regime of a catchment – lake system (in Russian). Sov Meteorol Hydrol 10:86–96

Kondratyev S, Gronskaya T, Wirkkala RS, Bovykin I, Yefremova L, Ignatieva N, Raspletina G, Chernykh O, Gayenko M, Markova E, Aksenchuk I (1998) Lake Ladoga and its drainage basin: GIS development and application. Univ of Joensuu Karelian Inst Working Papers 5:109–118

Kont A, Jaagus J, Aunap R (2003) Climate change scenarios and the effect of sea-level rise for Estonia. Glob Planet Change 36:1–15

Latif M, Roeckner E, Mikolajewicz U, Voss R (2000) Tropical stabilisation of the thermohaline circulation in a greenhouse warming simulation. J Clim 13:1809–1813

Leckebusch G, Ulbrich U (2004) On the relationship between cyclones and extreme windstorm events over Europe under climate change. Glob Planet Change 44:181–193

Legates DR, Wilmott CJ (1990) Mean seasonal and spatial variability in gauge-corrected global precipitation. Int J Climatol 10:111–127

Lehner B, Henrichs T, Döll P, Alcamo J (2001) EuroWasser – Model-based assessment of European water resources and hydrology in the face of global change. Kassel World Water Series 5. Center for Environmental Systems Research, University of Kassel, Germany

Lenderink G, Buishand A, Van Deursen W (2007) Estimates of future discharges of the river Rhine using two scenario methodologies: Direct versus delta approach. Hydrol Earth Sys Sci 33:1145–1159

Lettenmaier DP, Wood AW, Palmer RN, Wood EF, Stakhiv EZ (1999) Water resources implications of global warming: A US regional perspective. Climatic Change 43:537–579

Linderson ML, Achberger C, Chen D (2004) Statistical downscaling and scenario construction of precipitation in Scania southern Sweden. Nord Hydrol 35:261–278

Lindström G, Gardelin M, Persson M (1994) Conceptual Modelling of Evapotranspiration for Simulations of Climate Change Effects. SMHI Reports Hydrology No 10, Swedish Meteorological and Hydrological Institute, Norrköping, Sweden

Lohmann D, Nolte-Holube R, Raschke E (1996) A large-scale horizontal routing model to be coupled to land surface parameterization schemes. Tellus 48A:708–721

Manabe S, Stouffer RJ, Spelman MJ, Bryan K (1991) Transient responses of a coupled ocean–atmosphere model to gradual changes of atmospheric CO_2 Part I: Annual mean response. J Clim 4: 785–818

McAvaney BJ, Covey C, Joussaume S, Kattsov V, Kitoh A, Ogana W, Pittman AJ, Weaver AJ, Wood RA, Zhao ZC (2001) Model evaluation. In: IPCC: Climate change 2001: The scientific basis. Contribution of Working Group I to the Third Assessment Report of the Intergovernmental Panel on Climate Change. Cambridge University Press, Cambridge New York

Meehl GA, Boer GJ, Covey C, Latif M, Stouffer RJ (2000) The Coupled Model Intercomparison Project (CMIP). Bull Am Met Soc 81:313–318

Meier HEM (2001) The first Rossby Centre regional climate scenario for the Baltic Sea using a 3D coupled ice–ocean model. Reports Meteorology and Climatology No95, SMHI Norrköping Sweden

Meier HEM (2002a) Regional ocean climate simulations with a 3D ice-ocean model for the Baltic Sea Part 1: Model experiments and results for temperature and salinity. Clim Dyn 19:237–253

Meier HEM (2002b) Regional ocean climate simulations with a 3D ice-ocean model for the Baltic Sea Part 2: Results for sea ice. Clim Dyn 19:255–266

Meier HEM (2005) Modeling the age of Baltic Sea water masses: Quantification and steady state sensitivity experiments. J Geophys Res 110 C02006 doi:101029/2004JC002607

Meier HEM (2006) Baltic Sea climate in the late twenty-first century: A dynamical downscaling approach using two global models and two emissions scenarios. Clim Dyn 27:39–68 DOI 101007/s00382–006–0124–x

Meier HEM, Kauker F (2003a) Modeling decadal variability of the Baltic Sea Part 2: Role of freshwater inflow and large-scale atmospheric circulation for salinity. J Geophys Res 108,C11, 3368 doi: 101029/2003JC001799

Meier HEM, Kauker F (2003b) Sensitivity of the Baltic Sea salinity to the freshwater supply. Clim Res 24:231–242

Meier HEM, Döscher R, Halkka A (2004a) Simulated distributions of Baltic sea-ice in warming climate and consequences for the winter habitat of the Baltic ringed seal. Ambio 33:249–256

Meier HEM, Broman B, Kjellström E (2004b) Simulated sea level in past and future climates of the Baltic Sea. Clim Res 27:59–75

Meier HEM, Broman B, Kallio H, Kjellström E (2006a) Projections of future surface winds sea levels and wind waves in the late 21st century and their application for impact studies of flood prone areas in the Baltic Sea region. In: Schmidt-Thome P (ed) Special Paper 41, Geological Survey of Finland Helsinki Finland

Meier HEM, Kjellström E, Graham LP (2006b) Estimating uncertainties of projected Baltic Sea salinity in the late 21st century. Geophys Res Lett 33, L15705 doi:101029/2006GL026488

Meleshko VP, Kattsov VM, Govorkova VA, Malevsky-Malevich SP, Nadyozhina ED, Sporyshev PV (2004) Anthropogenic climate change in XXI century in Northern Eurasia. Sov Meteorol Hydrol 7: 5–26 (in Russian)

Middelkoop H, Daamen K, Gellens D, Grabs W, Kwadijk JCJ, Lang H, Parmet BWAH, Schädler B, Schulla J, Wilke K (2001) Impact of climate change on hydrological regimes and water resources management in the Rhine Basin. Clim Change 49:105–128

Miętus M (1999) Rola regionalnej cyrkulacji atmosferycznej w kształtowaniu warunków klimatycznych i oceanograficznych w polskiej strefie brzegowej Morza Bałtyckiego (The influence of regional atmospheric circulation on climate and oceanographic conditions in the Polish coastal zone). Instytut Meteorologii i Gospodarki Wodnej Warszawa (in Polish with English Summary)

Miętus M (2000) Climatic and oceanographic conditions in the southern Baltic area under an increasing CO_2 concentration. Geogr Polon 73:89–97

Miętus M, Filipiak J, Owczarek M (2004) Klimat wybrzeża południowego Bałtyku Stan obecny i perspektywy zmian (Climate at the seashore of the southern Baltic Sea. Present conditions and future changes). In: Cyberski J (ed) Środowisko polskiej strefy południowego Bałtyku – stan obecny i przewidywane zmiany w przededniu integracji europejskiej. Wydawnictwo Gdańskie Gdańsk, pp. 11–44 (in Polish)

Ministry of Environmental Protection and Regional Development (2001) The Third National Communication of the Republic of Latvia under the United Nations Framework Convention on Climate Change

Ministry of the Environment (2003) Lithuania's Second National Communication under the Framework Convention on Climate Change

Mitchell JFB, Manabe S, Meleshko V, Tokioka T (1990) Equilibrium climate change – and its implications for the future In: Houghton JT et al. (eds) Climate Change. The IPCC Scientific Assessment. Cambridge University Press, Cambridge New York, pp. 131–172

Mitchell JFB, Johns TC, Eagles M, Ingram WJ, Davis RA (1999) Towards the construction of climate change scenarios. Climatic Change 41:547–581

Mitchell JFB, Karoly DJ, Hegerl GC, Zwiers FW, Allen MR, Marengo J (2001) Detection of climate change and attribution of causes. In: IPCC Climate Change 2001: The Scientific Basis Contribution of Working Group I to the Third Assessment Report of the Intergovernmental Panel on Climate Change. Cambridge University Press, Cambridge New York

Mitchell TD (2003) Pattern scaling: An examination of the accuracy of the technique for describing future climate. Clim Change 60:217–242

Moberg A, Jones P (2004) Regional climate model simulations of daily maximum and minimum near-surface temperatures across Europe compared with observed station data 1961–1990. Clim Dyn 23: 695–715

Moberg A, Sonechkin DM, Holmgren K, Datsenko NM, Karlén W (2005) Highly variable Northern Hemisphere temperatures reconstructed from low- and high-resolution proxy data. Nature 433: 613–617

Munich Re Group (1999) Topics 2000 Natural catastrophes – the current position. Münchener Rückversicherungs-Gesellschaft, pp. 66, www.munichre.com

Murphy J (1999) An evaluation of statistical and dynamical techniques for downscaling local climate. J Clim 12:2256–2284

Murphy J (2000) Predictions of climate change over Europe using statistical and dynamical downscaling techniques. Int J Climatol 20:489–501

Murphy JM, Mitchell JFB (1994) Transient response of the Hadley Centre coupled ocean–atmosphere model to increasing carbon dioxide Part I Control climate and flux correction. J Clim 8:36–47

Murphy JM, Sexton DMH, Barnett DN, Jones GS, Webb MJ, Collins M, Stainforth DA (2004) Quantification of modelling uncertainties in a large ensemble of climate change simulations. Nature 430:768–772

Nakićenović N, Alcamo J, Davis G, De Vries B, Fenhann J, Gaffin S, Gregory K, Grübler A, Jung TY, Kram T, La Rovere EL, Michaelis L, Mori S, Morita T, Pepper W, Pitcher H, Price L, Riahi K, Roehrl A, Rogner HH, Sankovski A, Schlesinger M, Shukla P, Smith S, Swart R, Van Rooijen S, Victor N, Dadi Z (2000) Emission scenarios A Special Report of Working Group III of the Intergovernmental Panel on Climate Change. Cambridge University Press, Cambridge New York

New M, Hulme M, Jones P (1999) Representing twentieth-century space-time climate variability, Part I: Development of a 1961–90 mean monthly terrestrial climatology. J Clim 12:829–856

Nozawa T, Emori S, Takemura T, Nakajima T, Numaguti A, Abe-Ouchi A, Kimoto M (2000) Coupled ocean–atmosphere model experiments of future climate change based on IPCC SRES scenarios. Preprints 11th Symposium on Global Change Studies. 9–14 January 2000 Long Beach USA

Numaguti A (1999) Origin and recycling processes of precipitating water over the Eurasian continent: Experiments using an atmospheric general circulation model. J Geophys Res 104:1957–1972

Omstedt A, Chen D (2001) Influence of atmospheric circulation on the maximum ice extent in the Baltic Sea. J Geophys Res 106,C3:4493–4500

Omstedt A, Nyberg L (1996) Response of Baltic Sea ice to seasonal interannual forcing and to climate change. Tellus 48A:644–662

Omstedt A, Gustafsson B, Rodhe J, Walin G (2000) Use of Baltic Sea modelling to investigate the water cycle and the heat balance in GCM and regional climate models. Clim Res 15:95–108

Omstedt A, Meuller L, Nyberg L (1997) Interannual seasonal and regional variations of precipitation and evaporation over the Baltic Sea. Ambio 26:484–492

Orviku K, Jaagus J, Kont A, Ratas U, Rivis R (2003) Increasing activity of coastal processes associated with climate change in Estonia. J Coastal Res 19:364–375

Osborn TJ (2004) Simulating the winter North Atlantic Oscillation: The roles of internal variability and greenhouse gas forcing. Clim Dyn 22:605–623

Osborn TJ, Briffa KR, Tett SFB, Jones PD, Trigo RM (1999) Evaluation of the North Atlantic Oscillation as simulated by a coupled climate model. Clim Dyn 15:685–702

Power SB, Colman RA, McAvaney BJ, Dahni RR, Moore AM, Smith NR (1993) The BMRC coupled atmosphere/ocean/sea-ice model. BMRC Research Report No 37, Bureau of Meteorology Research Centre Melbourne Australia

Prentice IC, Farquhar GD, Fasham MJR, Goulden ML, Heimann M, Jaramillo VJ, Kheshgi HS, Le Quéré C, Scholes RJ, Wallace DWR (2001) The carbon cycle and atmospheric carbon dioxide. In: IPCC Climate Change 2001: The Scientific Basis Contribution of Working Group I to the Third Assessment Report of the Intergovernmental Panel on Climate Change: Cambridge University Press, Cambridge New York

Pryor SC, Barthelmie RJ (2003) Long-term trends in near-surface flow over the Baltic. Int J Climatol 23,3:271–289

Pryor SC, Barthelmie RJ (2004) Use of RCM simulations to assess the impact of climate change on wind energy availability. Risø-R-1477(EN) Risø National Laboratory Roskilde Denmark

Pryor SC, Barthelmie RJ and JT Schoof (2005a) The Impact of non-stationarities in the climate system on the definition of a normal wind year: A case study from the Baltic. Int J Climatol 25,6: 735–752

Pryor SC, Barthelmie RJ, Kjellström E (2005b) Analyses of the potential climate change impact on wind energy resources in northern Europe using output from a Regional Climate Model. Clim Dyn 25,7–8:815–835

Raab B, Vedin H (1995) Climate Lakes and Rivers. National Atlas of Sweden, vol. 14. SNA Publishing Box 45209 S–10430, Stockholm, Sweden

Rauthe M, Paeth H (2004) Relative importance of Northern Hemisphere circulation modes in predicting regional climate change. J Clim 17:4180–4189

Rimkus E (2001) Prognosis of maximum snow water equivalent changes in Lithuania. In: Meywerk J (ed) Conference Proceedings of the Third Study Conference on BALTEX, International BALTEX Secretariat Publication No 20

Rind D, Healy R, Parkinson C, Martinson D (1995) The role of sea ice in $2 \times CO_2$ climate sensitivity Part I: The total influence of sea ice thickness and extent. J Clim 8:449–463

Roald LA, Beldring S, Væringstad T, Engeset R, Skaugen TE, Førland E (2002) Scenarios of annual and seasonal runoff for Norway based on climate scenarios for 2030–2049. Norwegian Water Resources and Energy Directorate Consultancy Report A 10, Norwegian Meteorological Institute Report no 19/02 KLIMA

Roald LA, Beldring S, Skaugen TE, Førland EJ, Benestad R (2006) Climate change impacts in streamflow in Norway. NVE Consultancy-report A 1-2006 Norwegian Water Resources and Energy Directorate Oslo

Rockel B, Woth K (2007) Extremes of near-surface wind speed over Europe and their future changes as estimated from an ensemble of RCM simulations. Climatic Change 81:267–280

Rodhe J, Winsor P (2002) On the influence of the freshwater supply on the Baltic Sea mean salinity. Tellus 54A:175–186

Rodhe J, Winsor P (2003) Corrigendum: On the influence of the freshwater supply on the Baltic Sea mean salinity. Tellus 55A:455–456

Roeckner E, Bengtsson L, Feichter J, Lelieveld J, Rodhe H (1999) Transient climate change simulations with a coupled atmosphere–ocean GCM including the tropospheric sulfur cycle. J Clim 12: 3004–3032

Roosaare J (1998) Local-scale spatial interpretation of climate change impact on river runoff in Estonia. In: Lemmelä R, Helenius N (eds) Proceedings of the Second International Conference on Climate and Water Espoo Finland 17–20 August 1998, 1

Rubel F, Hantel M (2001) BALTEX 1/6-degree daily precipitation climatology 1996–1998. Meteorol Atmos Phys 77:155–166

Rummukainen M, Räisänen J, Ullerstig A, Bringfelt B, Hansson U, Graham LP, Willén U (1998) RCA – Rossby Centre regional atmospheric climate model: Model description and results from the first multi-year simulation. Reports Meteorology and Climatology 83, Swedish Meteorological and Hydrological Institute, Norrköping Sweden

Rummukainen M, Bergström S, Källén E, Moen L, Rodhe J, Tjernström M (2000) SWECLIM: The first three years. Reports Meteorology and Climatology 94, Swedish Meteorological and Hydrological Institute Norrköping Sweden

Rummukainen M, Räisänen J, Bringfelt B, Ullerstig A, Omstedt A, Willén U, Hansson U, Jones C (2001) A regional climate model for northern Europe: Model description and results from the downscaling of two GCM control simulations. Clim Dyn 17:339–359

Rummukainen M, Räisänen J, Bjørge D, Christensen JH, Christensen OB, Iversen T, Jylhä K, Ólafsson H, Tuomenvirta H (2003) Regional climate scenarios for use in Nordic water resources studies. Nord Hydrol 34:399–412

Rummukainen M, Bergström S, Persson G, Rodhe J, Tjernström M (2004) The Swedish Regional Climate Modelling Programme SWECLIM: A review. Ambio 4–5:176–182

Ruosteenoja K, Tuomenvirta H, Jylhä K (2007) GCM-based regional temperature and precipitation change estimates for Europe under four SRES scenarios applying a super-ensemble pattern-scaling method. Climatic Change 81:193–208

Russell GL, Rind D (1999) Response to CO_2 transient increase in the GISS coupled model Regional coolings in a warmer climate. J Clim 12:531–539

Russell GL, Miller JR, Rind D, Ruedy RA, Schmidt G, Sheth S (2000) Comparison of model and observed regional temperature changes during the past 40 years. J Geophys Res 105:14891–14898

Räisänen J (1994) A comparison of the results of seven GCM experiments in northern Europe. Geophysica 11:3–30

Räisänen J (2000) CO_2-induced climate change in northern Europe: Comparison of 12 CMIP2 experiments. Reports Meteorology and Climatology 87, Swedish Meteorological and Hydrological Institute, Norrköping Sweden

Räisänen J (2001a) CO_2-induced climate change in CMIP2 experiments Quantification of agreement and role of internal variability. J Clim 14:2088–2104

Räisänen J (2001b) Hiilidioksidin lisääntymisen vaikutus Pohjois-Euroopan ilmastoon globaaleissa ilmastomalleissa (The impact of increasing carbon dioxide on the climate of northern Europe in global climate models). Terra 113:139–151 (in Finnish with English abstract, figure and table captions)

Räisänen J (2002) CO_2-induced changes in interannual temperature and precipitation variability in 19 CMIP2 experiments. J Clim 15:2395–2411

Räisänen J, Alexandersson H (2003) A probabilistic view on recent and near future climate change in Sweden. Tellus 55A:113–125

Räisänen J, Joelsson R (2001) Changes in average and extreme precipitation in two regional climate model experiments. Tellus 53A:547–566

Räisänen J, Döscher R (1999) Simulation of present-day climate in Northern Europe in the HadCM2 OAGCM. Reports Meteorology and Climatology 84, Swedish Meteorological and Hydrological Institute, Norrköping Sweden

Räisänen J, Rummukainen M, Ullerstig A, Bringfelt B, Hansson U, Willén U (1999) The First Rossby Centre Regional Climate Scenario: Dynamical Downscaling of CO_2-induced Climate Change in the HadCM2 GCM. Reports Meteorology and Climatology 85, Swedish Meteorological and Hydrological Institute, Norrköping Sweden

Räisänen J, Rummukainen M, Ullerstig A (2001) Downscaling of greenhouse gas induced climate change in two GCMs with the Rossby Centre regional climate model for northern Europe. Tellus 53A:168–191

Räisänen J, Hansson U, Ullerstig A, Döscher R, Graham LP, Jones C, Meier M, Samuelsson P, Willén U (2003) GCM driven simulations of recent and future climate with the Rossby Centre coupled atmosphere – Baltic Sea regional climate model RCAO SMHI Reports Meteorology and Climatology 101, SMHI SE 60176 Norrköping, Sweden

Räisänen J, Hansson U, Ullerstig A, Döscher R, Graham LP, Jones C, Meier M, Samuelsson P, Willén U (2004) European climate in the late 21st century: Regional simulations with two driving global models and two forcing scenarios. Clim Dyn 22:13–31

Sælthun NR (1996) The "Nordic" HBV model – version developed for the project Climate change and Energy Production. NVE publication no 7/1996 Norwegian Water Resources and Energy Administration Oslo

Sælthun NR, Bogen J, Hartman Flood M, Laumann T, Roald LA, Tvede AM, Wold B (1990) Climate change impacts on Norwegian water resources. NVE publication V42 Norwegian Water Resources and Energy Administration Oslo

Sælthun NR, Aittoniemi P, Bergström S, Einarsson K, Jóhannesson T, Lindström G, Ohlsson PE, Thomsen T, Vehviläinen B, Aamodt KO (1998) Climate Change Impacts on Runoff and Hydropower in the Nordic Countries. TemaNord 1998:522 Nordic Council of Ministers Copenhagen

Sælthun NR, Bergström S, Einarsson K, Jóhannesson T, Lindström G, Thomsen T, Vehviläinen B (1999) Potential Impacts of climate change on floods in Nordic hydrological regimes. In: Balabanis P, Bronstert A, Casale R, P Samuels (eds) Proceedings from Ribamod – River Basin Modelling Management and Flood Mitigation. Wallingford United Kingdom 26–27 February 1998. Office for Official Publications of the European Communities

Scaife AM, Knight JR, Vallis GK, Folland CK (2005) A stratospheric influence on the winter NAO and North Atlantic surface climate. Geophys Res Lett 32 L18715

Schaeffer M, Selten FM, Opsteegh JD, Goosse H (2004) The influence of ocean convection patterns on high-latitude climate projections. J Clim 17:4316–4329

Scharling M (2000) Klimagrid – Danmark normaler 1961–90 måneds- og årsværdier Nedbør 10×10 20×20 & 40×40 km temperatur og potentiel fordampning 20×20 & 40×40 km (Climate grid Denmark. Climate normals 1961–90, monthly and annual values. Precipitation 10×10 20×20 & 40×40 km. Temperature and potential evaporation 20×20 & 40×40 km). Danish Meteorological Institute Technical Report 00-11 (in Danish)

Schrum C (2001) Regionalization of climate change for the North Sea and Baltic Sea. Clim Res 18: 31–37

Schrum C, Backhaus JO (1999) Sensitivity of atmosphere–ocean heat exchange and heat content in the North Sea and the Baltic Sea. Tellus 51A:526–549

Schär C, Vidale PL, Lüthi D, Frei C, Häberli C, Liniger MA, Appenzeller C (2004) The role of increasing temperature variability for European summer heat waves. Nature 427:332–336

Selten FM, Branstator GW, Dijkstra HA, Kliphuis M (2004) Tropical origins for recent and future Northern Hemisphere climate change. Geophys Res Lett 31 L21205 (doi: 101029/2004GL020739)

Semmler T, Jacob D (2004) Modeling extreme precipitation events – a climate change simulation for Europe. Glob Planet Change 44:119–127

Shindell DT, Schmidt GA, Miller RL, Rind D (2001) Northern Hemispheric climate response to greenhouse gas ozone solar and volcanic forcing. J Geophys Res 106:7193–7210

Shindell DT, Miller RL, Smith GA, Pandolfo L (1999) Simulation of recent northern winter climate trends by greenhouse-gas forcing. Nature 399:452–455

SILMU (1996) The Finnish Research Programme on Climate Change. Final Report (Roos J ed) Edita Helsinki

Skaugen TE, Tveito OE (2002) Heating degree-days – Present conditions and scenario for the period 2021–2050. DNMI Report no 01/02 KLIMA Norwegian Meteorological Institute Oslo Norway

Skaugen TE, Astrup M, Roald LA, Førland EJ (2002) Scenarios of extreme precipitation of duration 1 and 5 days for Norway caused by climate change. Norwegian Water Resources and Energy Directorate Consultancy Report A 7

Stainforth DA, Alna T, Christensen C, Collins M, Fauli N, Frame DJ, Kettleborough JA, Knight S, Martin A, Murphy JM, Pianl C, Sexton D, Smith LA, Spicer RA, Thorpe AJ, Allen MR (2005) Uncertainty in the predictions of the climate response to rising levels of greenhouse gases. Nature 433:403–406

Stephenson DB, Pavan V (2003) The North Atlantic Oscillation in coupled climate models: A CMIP1 evaluation. Clim Dyn 20:381–399

Stephenson DB, Pavan V, Collins M, Junge MM, Quadrelli R and Participating CMIP2 Modelling Groups (2006) North Atlantic Oscillation response to transient greenhouse gas forcing and the impact on European winter climate: A CMIP2 multi-model assessment. Clim Dyn 27:401–420

Stigebrandt A (1983) A model for the exchange of water and salt between the Baltic and the Skagerrak. J Phys Oceanogr 13:411–427

Stigebrandt A, Gustafsson BG (2003) Response of the Baltic Sea to climate change – Theory and observations. J Sea Res 49:243–256

Stocker TF, Schmittner A (1997) Influence of CO_2 emission rates on the stability of the thermohaline circulation. Nature 388:862–865

Stouffer RJ, Manabe S (2003) Equilibrium response of thermohaline circulation to large changes in atmospheric CO_2 concentration. Clim Dyn 20:759–773

Strzepek KM, Yates DN (1997) Climate change impacts on the hydrologic resources of Europe: A simplified continental scale anlaysis. Climatic Change 36:79–92

Suursaar Ü, Jaagus J, Kullas T (2006) Past and future changes in sea level near the Estonian coast in relation to changes in wind climate. Boreal Env Res 11:123–142

Tarand A, Kallaste T (eds) (1998) Country Case Study on Climate Change Impacts and Adaptation Assessments in the Republic of Estonia Ministry of Environment Republic of Estonia. SEI Tallinn

Thodsen H (2007) The influence of climate change on stream flow in Danish rivers. J Hydrol 333: 226–238

Thodsen H, Erichensen A, Lumborg U, Edelvang K (2005) Effekt af afstrømnings ændringer som følge af klima ændringer på salinitet og næringsstofforhold i Odense Fjord (The effect of climate change induced changes of river flow on salinity and nutrient conditions in the Odense fjord (in Danish)) Abstracts from Det 13 Danske Havforskermøde Copenhagen

Thompson SL, Pollard D (1995) A global climate model (GENESIS) with a land-surface-transfer scheme (LSX) Part 1: Present-day climate. J Clim 8:732–761

Tinz B (1996) On the relation between annual maximum extent of ice cover in the Baltic Sea level pressure as well as air temperature field. Geophysica 32:319–341

Tinz B (1998) Sea ice winter severity in the German Baltic in a greenhouse gas experiment. Deutsch Hydr Z 50:33–45

Tokioka T, Noda A, Kitoh A, Nikaidou Y, Nakagawa S, Motoi T, Yukimoto S, Takata K (1995) A transient CO_2 experiment with the MRI CGCM Quick Report. J Meteorol Soc Jpn 73:817–826

Tuomenvirta H, Heino R (1996) Climatic changes in Finland – recent findings. Geophysica 32:61–75

Tuomenvirta H, Uusitalo K, Vehviläinen B, Carter T (2000) Ilmastonmuutos mitoitussade ja patoturvallisuus: Arvio sadannan ja sen ääriarvojen sekä lämpötilan muutoksista Suomessa vuoteen 2100 (Climate change, design, precipitation and dam safety: Estimation of the changes of extreme precipitation and temperature in Finland until 2100). Ilmatieteenlaitoksen raportteja 2000:4 Helsinki (in Finnish)

Uppala SM, Kållberg PW, Simmons AJ, Andrae U, Da Costa Bechtold V, Fiorino M, Gibson JK, Haseler J, Hernandez A, Kelly GA, Li X, Onogi K, Saarinen S, Sokka N, Allan RP, Andersson E, Arpe K, Balmaseda MA, Beljaars ACM, Van De Berg L, Bidlot J, Bormann N, Caires S, Chevallier F, Dethof A, Dragosavac M, Fisher M, Fuentes M, Hagemann S, Hólm E, Hoskins BJ, Isaksen L, Janssen PAEM, Jenne R, McNally AP, Mahfouf JF, Morcrette JJ, Rayner NA, Saunders RW, Simon P, Sterl A, Trenberth KE, Untch A, Vasiljevic D, Viterbo P, Woollen J (2005) The ERA-40 Reanalysis. Q J Roy Met Soc 131:2961–3012 doi:101256/qj04176

Varis O, Kajander T, Lemmelä R (2004) Climate and water: From climate models to water resources management and vice versa. Climatic Change 66:321–344

Vehviläinen B (1994) The watershed simulation and forecasting system in the National Board of Waters and the Environment. Publications of Water and Environment Research Institute 17 Helsinki

Vehviläinen B, Huttunen M (1997) Climate change and water resources in Finland. Boreal Env Res 2: 3–18

Vidale PL, Lüthi C, Frei C, Seneviratne S, Schär C (2003) Predictability and uncertainty in a regional climate model. J Geophys Res 108(D18) 4586 doi:101029/2002JD002810

Vidale PL, Lüthi C, Wegmann R, Schär C (2007) European climate variability in a heterogeneous multi-model ensemble. Climatic Change 81:209–232

Volodin EM, Galin VY (1999) Interpretation of winter warming on Northern Hemisphere continents in 1977–94. J Clim 12:2947–2955

Voss R, Sausen R, Cubasch U (1998) Periodically synchronously coupled integrations with the atmosphere–ocean general circulation model ECHAM3/LSG. Clim Dyn 14:249–266

Washington WM, Meehl GA (1989) Climatic sensitivity due to increased CO_2: Experiments with a coupled atmosphere and ocean general circulation model. Clim Dyn 4:1–38

Washington WM, Weatherly JW, Meehl GA, Semtner AJ Jr, Bettge TW, Craig AP, Strand WG Jr, Arblaster J, Wayland VB, James VB R, Zhang Y (2000) Parallel climate model (PCM) control and transient simulations. Clim Dyn 16:755–774

Weaver AJ, Eby M, Fanning AF, Wiebe EC (1998) Simulated influence of carbon dioxide orbital forcing and ice sheets on the climate of the Last Glacial Maximum. Nature 394:847–853

Wetherald RT, Manabe S (1995) The mechanisms of summer dryness induced by greenhouse warming. J Clim 8:3096–3108

Wigley TML, Raper SCB (1987) Thermal expansion of sea water associated with global warming. Nature 330:127–131

Wigley TML, Raper SCB (1992a) Implications for climate and sea level rise of revised IPCC emissions scenarios. Nature 357:293–300

Wigley TML, Raper SCB (1992b) Implications of revised IPCC emissions scenarios. Nature 357:127–131

Wigley TML, Raper SCB (2001) Interpretation of high projections for global-mean warming. Science 293:451–455

World Bank (2002) Republic of Belarus Ministry of Natural Resources and Environmental Protection: Assessment of potential impact of climatic changes in the Republic of Belarus and vulnerability and adaptation of social and economic systems to climate change. Minsk

Xie P, Arkin PA (1997) Global precipitation: A 17-year monthly analysis based on gauge observations, satellite estimates, and numerical model outputs. Bull Am Met Soc 78:2539–2558

Yukimoto S, Endoh M, Kitamura Y, Kitoh A, Motoi T, Noda A (2000) ENSO-like interdecadal variability in the Pacific Ocean as simulated in a coupled GCM. J Geophys Res 105:13945–13963

Zhang X, Shi G, Liu H, Yu Y (eds) (2000) IAP global ocean–atmosphere–land system model. Science Press Beijing China

Zorita E, von Storch H (1997) A survey of statistical downscaling techniques. GKSS 97/E/20

Zwiers FW, Kharin VV (1998) Changes in the extremes of the climate simulated by CCC GCM2 under CO_2 doubling. J Clim 11:2200–2222